MICROSTRUCTURE, MECHANICAL AND THERMAL CHARACTERISTICS OF FOAMED GEOPOLYMER CONCRETE USING FLY ASH AND PALM OIL FUEL ASH AS BINDERS

MICHAEL LIU YONG JING

DISSERTATION SUBMITTED IN FULFILMENT
OF THE REQUIREMENT FOR THE DEGREE OF
MASTER OF ENGINEERING SCIENCE

DEPARTMENT OF CIVIL ENGINEERING
FACULTY OF ENGINEERING
UNIVERSITY OF MALAYA
KUALA LUMPUR

2013

UNIVERSITI MALAYA

ORIGINAL LITERARY WORK DECLARATION

Name of Candidate : **MICHAEL LIU YONG JING**

I.C/Passport No :

Registration/Matric No : **KGA 120017**

Name of Degree : **MASTER OF ENGINEERING SCIENCE**

Title of Project Paper/Research Report/Dissertation/Thesis ("this Work"):

MICROSTRUCTURE, MECHANICAL AND THERMAL CHARACTERISTICS OF FOAMED GEOPOLYMER CONCRETE USING FLY ASH AND PALM OIL FUEL ASH AS BINDERS

Field of Study : **CIVIL ENGINEERING**

I do solemnly and sincerely declare that:

(1) I am the sole author/writer of this Work;
(2) This Work is original;
(3) Any use of any work in which copyright exists was done by way of fair dealing and for permitted purposes and any excerpt or extract from, or reference to or reproduction of any copyright work has been disclosed expressly and sufficiently and the title of the Work and its authorship have been acknowledged in this Work;
(4) I do not have any actual knowledge nor do I ought reasonably to know that the making of this work constitutes an infringement of any copyright work;
(5) I hereby assign all and every rights in the copyright to this Work to the University of Malaya ("UM"), who henceforth shall be owner of the copyright in this Work and that any reproduction or use in any form or by any means whatsoever is prohibited without the written consent of UM having been first had and obtained;
(6) I am fully aware that if in the course of making this Work I have infringed any copyright whether intentionally or otherwise, I may be subject to legal action or any other action as may be determined by UM.

Candidate's Signature Date

Subscribed and solemnly declared before,

Witness's Signature Date

Name :
Designation:

ABSTRACT

The use of cement is still needed within the manufacture of concrete even though the current concrete are of composite materials. This phenomenon has led to the huge release of carbon dioxide (CO_2) into the atmosphere and initiated the global warming. Other than the manufacturing sector, the energy sector such as power plants generate large amount of noxious gases as well. The enhancement of energy efficacy of buildings could be achieved by reducing the heat loss in buildings that would lessen the amount of energy used and thus, scale down the consumption of fossil fuels by power plants. In addition, the cumulative agricultural wastes (i.e. oil palm shell (OPS), empty fruit bunches, palm oil fuel ash (POFA), and palm oil clinker) in Malaysia has become a significant factor towards the land and air pollutions especially in the proximity of the palm oil factories, which led to the disorder in environmental sustainability.

A more resource- and energy-efficient construction industry would preserve the environment. In this research work, the geopolymer technology is introduced in the production of concrete to omit the use of cement, which also utilized the OPS as lightweight coarse aggregate and the binders consist of POFA and fly ash (FA). Additionally, foam is added to enhance the thermal insulation characteristic. The concrete termed as oil palm shell foamed geopolymer concrete (OPSFGC). Thus far, there is no literature available on this type of concrete. The objective of this research was to explore the possibility of the OPSFGC as structural and insulating material. Hence, this research investigated the physical properties of the OPS, mechanical and transport properties and thermal behaviour of the OPSFGC. The in-depth study on the microstructure of OPSFGC and its paste were analysed as well.

Three OPSFGC mixtures with target densities of 1300, 1500 and 1700 kg/m^3 were prepared using artificial foaming agent; a control mix without foam (OPSNFGC) and conventional materials – block and brick – were used for comparison. It is found that OPSFGC and OPSNFGC are characterized as lightweight concrete (LWC). The mechanical properties of OPSFGC and OPSNFGC, such as compressive, splitting tensile and flexural strengths, generally reduced with the reduction in the density; the modulus of elasticity (MOE) also followed a similar trend. Moreover, a high early strength (3-day compressive strength) can be achieved of up to 90% when compared with the 28-day compressive strength, however, rate of strength gain was only about 11.3% after 7-day.

Furthermore, the OPSFGC17 and OPSNFGC exhibited 'fair' quality concrete with UPV values of more than 3 km/s. In accordance with RILEM (1983), OPSFGC13 and OPSFGC15 can be categorized as structural and insulating concrete – Class-II with strength and thermal conductivity of 8 and 13 MPa, and 0.47 and 0.50 W/mK, correspondingly. Whilst the OPSFGC17 and OPSNFGC produced a higher compressive strength of about 26 and 30 MPa, respectively fall under the structural grade LWC. Last but not least, the microstructure analysis showed the morphology and mineralogy of the specimens, which validated the obtained results and discussion.

ABSTRAK

Penggunaan simen masih diperlukan dalam pembuatan konkrit walaupun dengan penggunaan konkrit komposit. Fenomena ini telah menyebabkan pelepasan karbon dioksida (CO_2) secara berleluasa ke atmosfera dan mengakibatkan pemanasan global. Selain daripada sektor perkilangan, sektor tenaga seperti loji janakuasa turut menghasilkan sejumlah besar gas-gas toksik. Peningkatan keberkesanan tenaga bangunan boleh dicapai dengan mengurangkan kehilangan haba dalam bangunan yang akan mengurangkan jumlah tenaga yang digunakan dan secara sedemikian, ia turut mengurangkan penggunaan bahan api fosil oleh loji janakuasa. Di samping itu, sisa-sisa pertanian yang terkumpul (iaitu, cangkang kelapa sawit (OPS), tandan buah kosong, abu kelapa sawit terbakar (POFA) dan klinker kelapa sawit) di Malaysia telah menjadi salah satu faktor yang penting terhadap pencemaran tanah dan udara terutamanya di tempat yang berdekatan dengan kilang kelapa sawit yang membawa kepada gangguan dalam kelestarian alam sekitar.

Kecekapan dalam penggunaan sumber serta tenaga dalam industri pembinaan akan lebih memelihara alam sekitar. Dalam kerja-kerja penyelidikan ini, teknologi 'geopolymer' diperkenalkan dalam penghasilan konkrit dengan mengabaikan penggunaan simen, dan memanfaatkan OPS sebagai agregat kasar ringan serta penggunaan bahan pengikat yang terdiri daripada POFA dan abu terbang (FA). Selain itu, buih ditambah untuk meningkatkan penebatan haba. Konkrit ini dikenali sebagai konkrit 'geopolimer' berbusa dengan cangkang kelapa sawit (OPSFGC). Setakat ini, tiada penerbitan yang dijumpai berkaitan dengan konkrit jenis ini. Kajian ini bertujuan untuk meneroka kesesuaian OPSFGC sebagai bahan struktur yang bersifat penebat. Maka, kajian ini menyiasat ciri-ciri fizikal, mekanikal dan kebolehtelapan serta kekonduksian

haba OPSFGC tersebut. Selain daripada itu, penyelidikan secara mendalam pada struktur dalaman OPSFGC turut dianalisis juga.

Tiga jenis OPSFGC yang berketumpatan 1300, 1500 dan 1700 kg/m^3 telah disediakan dengan menggunakan larutan berbuih buatan; satu jenis konkrit ‘geopolymer’ tanpa buih sebagai kawalan (OPSNFGC) dan bahan-bahan konvensional seperti blok dan bata digunakan sebagai perbandingan. Ia didapati bahawa OPSFGC dan OPSNFGC mempunyai ciri-ciri sebagai konkrit ringan (LWC). Ciri-ciri mekanikal OPSFGC dan OPSNFGC, seperti kekuatan mampatan, tegangan dan lenturan, secara amnya dikurangkan dengan pengurangan ketumpatan; modulus keanjalan (MOE) turut mengikuti trend yang serupa. Tambahan pula, kekuatan awal yang tinggi (kekuatan kemampatan pada hari ke-3) dapat dicapai hingga 90% berbanding dengan kekuatan kemampatan pada hari ke-28, namun, kadar kenaikan kekuatan kemampatan hanya sekitar 11.3 % selepas hari ke-7.

Di samping itu, OPSFGC17 dan OPSNFGC dipamerkan sebagai konkrit berkualiti 'memuaskan' dengan nilai-nilai UPV yang lebih daripada 3 km/s. Selaras dengan RILEM (1983), OPSFGC13 dan OPSFGC15 boleh dikategorikan sebagai konkrit jenis struktur dan penebat - kelas - II dengan kekuatan dan kekonduksian haba, dari 8 dan 13 MPa, dan 0.47 dan 0.50 W/mK, masing-masing. Manakala, OPSFGC17 dan OPSNFGC menghasilkan kekuatan kemampatan yang lebih tinggi sekitar 26 dan 30 MPa, masing-masing jatuh dikategorikan sebagai kelas konkrit ringan jenis struktur. Akhirnya, analisis struktur dalaman menunjukkan morfologi dan mineralogi spesimen yang mengesahkan keputusan yang diperolehi serta perbincangan tersebut.

ACKNOWLEDGEMENT

I would like to convey appreciation to those who have assisted and supported in the completion of this study directly or indirectly. Foremost, I would like to express my deepest gratitude to my respected supervisor, Dr. U. Johnson Alengaram for his excellent guidance and patience and supported me throughout the research study. I also acknowledge with immense gratefulness the precious time he had spent in supervising my study, patiently corrected my writing and financially supported my research without asking for any returns. He has been encouraging and inspiring me to explore new ideas and to aim high. His patience and forgiveness towards my ignorance and mistakes have moulded me to become a better individual. It is a privilege to become your student. I am also greatly indebted to my co-supervisor, Prof. Ir. Dr. Mohd Zamin bin Jumaat for his invaluable advice, ideas, supports, accessibility and also constructive suggestions during the course of this research study.

Furthermore, I would like to thank to my colleagues, especially Mr. Mo Kim Hung for his willingness in the assistance in the laboratory works and giving his best suggestions and insights to improve this research study. Also, I am grateful to Mr. Yap Soon Poh for his advice and ideas to accomplish this thesis. The extra hours and technical supports provided by the laboratory staffs, Mr. Sreedharan and Mr. Mansor are acknowledged. Additionally, thanks to Mr. Rajakumaran for being helpful in the laboratory works particularly in the preparation of materials and geopolymer concrete. The scholarship granted by the University of Malaya is greatly appreciated.

Lastly, I would like to thank my mother and brother for giving endless supports, love and patience. Thanks to my father and sister for being understanding and caring at all times. There is nothing I value more than the closeness of family. I am beholden to Jesus Christ for listening to my prayers and blessed the family and people everywhere.

TABLE OF CONTENTS

LIST OF TABLES

LIST OF FIGURES

Page

LIST OF SYMBOLS AND ABBREVIATIONS

Symbols	Descriptions
ΔT	Temperature difference between hot and cold plates
$\Delta\varepsilon$	Difference in strains
$\Delta\sigma$	Difference in stresses
A	Cross-sectional area of the test specimen
$A1$	Mass of oven-dried oil palm shell in air
$A2$	Mass of oven-dried mining sand
b	Average width of the test specimen
$B1$	Mass of saturated surface dry oil palm shell in air
$B2$	Mass of pycnometer filled with water, to calibration mark
$C1$	Apparent mass of the saturated oil palm shell in water
$C2$	Mass of pycnometer filled with mining sand and water to calibration mark
D	Density of the fresh specimen
d	Diameter or average depth of the test specimen
E_s	Static modulus of elasticity of the test specimen
F	Maximum load at failure
f_c	Compressive strength of the test specimen
f_r	Flexural strength of the test specimen
f_t	Splitting tensile strength of the test specimen
i	Cumulative volume of water absorbed at time t
k	Thermal conductivity
l	Length of the test specimen
L	Distance between centres of the transducer faces

m_1	Mass of empty container
m_2	Container completely filled with compacted fresh specimen
P	Maximum applied load indicated by the testing machine
S	Sorptivity coefficient
$S2$	Mass of saturated surface dry mining sand
T	Transit time
t	Recorded time
t_k	Thickness of the test specimen
V	Volume of the container
V	Pulse velocity
W_b	Buoyant mass of the saturated specimen in water
W_d	Oven-dry mass of the test specimen in air
W_s	Saturated surface dry mass of the test specimen in air
Φ	Heat flow

Abbreviations	**Descriptions**
Al	Aluminium
Al_2O_3	Alumina
Ca	Calcium
$Ca(OH)_2$	Calcium hydroxide
CaO	Calcium oxide
CM	Cementitious material
CO_2	Carbon dioxide
CSH	Calcium silicate hydrates
EDX	Energy dispersive X-ray
EFB	Empty fruit bunches

FA	Fly ash
FC	Foamed concrete
Fe_2O_3	Ferric oxide
FESEM	Field emission scanning electron microscope
FGC	Foamed geopolymer concrete
FTIR	Fourier transform infrared spectroscopy
GGBS	Ground granulated blast slag
H_2O	Water
ITZ	Interfacial transition zone
K_2SiO_3	Potassium silicate
KOH	Potassium hydroxide
LOI	Loss on ignition
LWA	Lightweight aggregate
LWAC	Lightweight aggregate concrete
LWC	Lightweight concrete
MK	Metakaolin
MOE	Modulus of elasticity
Na	Sodium
Na_2SiO_3	Sodium silicate
NaOH	Sodium hydroxide
NWC	Normal weight concrete
ODD	Oven-dry density
OPC	Ordinary Portland cement
OPS	Oil palm shell
OPSC	Oil palm shell concrete
OPSFGC	Oil palm shell foamed geopolymer concrete

OPSFRC	Oil palm shell fibre-reinforced concrete
OPSGC	Oil palm shell geopolymer concrete
OPSNFGC	Oil palm shell non-foamed geopolymer concrete
PCE	Polycarboxylate ether
PFG	POFA-FA geopolymer
POFA	Palm oil fuel ash
PUNDIT	Portable ultrasonic non-destructive digital indicating tester
PVA	Polyvinyl alcohol
RCA	Recycled aggregate
RHA	Rice hush ash
SBU	Secondary building unit
SF	Silica fume
SG	Specific gravity
Si	Silicon
SiO_2	Silica or quartz
SO_3	Sulphuric anhydride
SP	Superplasticizer
SSD	Saturated surface dry
UPV	Ultrasonic pulse velocity
XRD	X-ray diffraction
XRF	X-ray fluorescence

CHAPTER ONE

INTRODUCTION

1.1 Research background

The requirement of sustainable development is not a trend but rather a strategy that will last and has become more relevant because of the occurrence of global warming attributed to the polluted air that we are breathing (Aïtcin, 2000). Associated with the ordinary Portland cement (OPC), concrete is reasoned as one of the most widely used construction materials that incur major environmental issues. The production of cement is one of the main contributors towards the global warming caused by the emission of carbon dioxide (CO_2). Davidovits (1994b) reported that the production of 1 ton of cement generates 0.55 tons of CO_2 and involves the combustion of carbon-fuel to yield an additional 0.40 tons of CO_2; accounted as 1 billion metric tons world production of cement produces 1 billion metric tons of CO_2. Chances for ecosystems to adapt naturally are diminishing as the climate is changing and the earth is warming up due to the human-induced global warming.

There are many efforts been put on to reduce the environment impact by replacing the usage of the cement with the other pozzolanic materials such as palm oil fuel ash (POFA), rice hush ash (RHA), fly ash (FA), metakaolin (MK) and ground granulated blast slag (GGBS). Davidovits (1999) was the pioneer in introducing binders other than cement that could be produced by the reaction between alkaline liquids and source materials that are rich in silica and alumina, commonly known as geopolymerization. The material has been termed ‘geopolymer’. The geopolymerization process is aided by heat

curing and drying (Hardjito et al., 2004). The use of geopolymer technology not only substantially reduces the CO_2 emissions by the cement industry, but also utilizes the waste materials such as FA (Hardjito et al., 2004).

Other than being environmentally sustainable, construction materials that are light, durable and economic are more preferable for the future needs. Lightweight concrete (LWC) is defined as concrete having an oven dried density (ODD) between 800 and 2000 kg/m^3, compared with the normal weight concrete (NWC), which has an ODD of more than 2000 kg/m^3 (BS EN 206-1: 2000). There are three types of LWC, which are commonly used in construction, namely no-fines concrete, lightweight aggregate concrete (LWAC) and foamed concrete (FC). The usage of LWC is beneficial in reduction of size of structural members and foundation, handling of larger precast units, enhances the thermal and sound insulation properties, and economical. Furthermore, the use of LWC is important in producing earthquake resistant building since the mass of structures or building is proportional to the earthquake forces (Kılıç et al., 2003).

Other than cement, production of concrete also be made up of sand and aggregate, where quarrying operations are energy intensive and able to release high level of waste (Ahmari et al., 2012). Besides environmental awareness to ensure a sustainable environment, an alternative material in construction industry is rather preferred towards a greener development. Being the second largest palm oil producer, Malaysia contributes large quantities of wastes such as empty fruit bunches (EFB), palm oil clinkers, oil palm shells (OPS) and POFA (Alengaram et al., 2013); where these unutilized wastes would cause land and air pollutions prior to the palm oil factories. Researchers have incorporated OPS as lightweight aggregate (LWA) to produce a LWC and replacing POFA in OPC to improve the environmental sustainability. A low-cost house is constructed by using OPS

as the LWA to build the walls and structural members which includes footings, beams and lintels (Teo et al., 2007).

The need to optimize the energy behaviour of the buildings has been required in the scientific and government policies. A more energy efficient building is now more focused in urban environmental issue that can reduce the amount of carbon dioxide and sulphur dioxide emitted into the atmosphere by reducing the quantities of fossil fuels (Papadopoulos & Giama, 2007). According to Mahlia et al. (2007), a proper insulation material with the capacity to achieve acceptable comfort for the building occupants while reducing the cooling load is necessary as it would generate huge energy and cost savings as well as reduce environmental emissions from the power plants.

1.2 Problem statement

As the construction industry is considered to be one of the fastest growing industries, the environmental issue has become worse towards depletion of the ozone layer. The usage of concrete increases with the growth of the construction industry. Thus, the production of the OPC also raises the greenhouse effect. The production of the geopolymer concrete can greatly reduce the greenhouse effect and also utilize the waste materials by palm oil mills and coal-fired power plants such as POFA and FA. The heat loss in the building also produces negative impact to the environmental sustainability by increasing the energy consumption, which leads to the reduction of fossil energy. Moreover, the disposal of OPS may contribute to the land pollution which would increase environmental hazard.

Previous researches have shown mostly the usage of FA as cementitious material (CM) in geopolymer concrete due to its vast of availability. Also, FC with incorporation

of OPS as LWA could achieved 58% higher thermal insulation when compared to the conventional brick (Alengaram et al., 2013). This finding suggests that there is a prospective way to enhance the energy efficiency of buildings as well as reducing the emission of CO_2 by omitting the usage of the OPC. A wide range of researches on the selection of materials, mechanical properties testing, thermal behaviour and the microstructure have to be carried out to obtain a cementitious-based construction that fulfils the above mentioned requirements product.

1.3 Research objectives

The objectives of the research can be summarised as given below:

i. To develop structural and non-structural grade of foamed and non-foamed geopolymer concrete using oil palm shell as lightweight aggregate and utilized fly ash and palm oil fuel ash as binders;

ii. To investigate the mechanical and transport properties of the oil palm shell foamed and non-foamed geopolymer concrete (OPSFGC and OPSNFGC);

iii. To determine the thermal conductivity of OPSFGC and OPSNFGC, in comparison with the conventional materials such as block and brick;

iv. To study the morphology and mineralogy of the geopolymer paste and OPSFGC with respect to the field emission scanning electron microscope, energy dispersive X-ray analysis, X-ray diffraction and Fourier transform infrared spectroscopy.

1.4 Scope of the research

The research make use of the locally available industrial by-products such as the low-calcium FA (ASTM Class-F) and POFA to produce geopolymer binders. Also, the OPS was used as LWA of the geopolymer concrete. The foaming agent is generated by the foam generator and induced into the geopolymer concrete to produce OPSFGC. Differ than the normal OPC concrete curing regime, the geopolymer concrete specimens were oven-cured at 65 ˚C for 48 hours. A mix design was developed to produce the OPSFGC with the target densities of 1300, 1500 and 1700 kg/m^3.

The tests on the material properties of OPS, POFA and FA were carried out and followed by the tests on the mechanical and transport properties of the OPSFGC at different densities including the OPSNFGC. The mechanical and transport properties include compressive strength, flexural strength, splitting tensile strength, modulus of elasticity (MOE), ultrasonic pulse velocity (UPV), porosity and sorptivity. Two panels of each densities were cast to determine their thermal conductivities and then compared with the conventional materials, i.e. concrete block and common burnt clay brick.

The microstructure analysis was performed to study the morphology between the OPSNFGC and different densities of OPSFGC, whereas the mineralogy of the POFA-FA geopolymer (PFG) paste was performed to understand the formation of the aluminosilicate gel. Geopolymer paste was used instead of geopolymer concrete in order to minimize the disruption of aggregate particles on the validity of geopolymer framework analysis (Kusbiantoro et al., 2012).

1.5 Significance of the research

The addition of foam gives great reduction to density in concrete, thus the concrete is categorized as LWC with a qualified density of below 2000 kg/m^3. The reduction of concrete density not only enhance its properties (e.g., workability, fire resistance, acoustic and thermal insulation), but also possesses strength of structural grade concrete. The thermal insulation properties of concrete would allow the reduction of the heat flow in a building, which will improve the energy efficiency of the building. Other than huge energy and cost savings, the reduction of power plant emissions could be achieved by using a proper insulation material that provides acceptable comfort for building occupants (Mahlia et al., 2007).

Other than addition of foam, the use of LWA also reduces the density of concrete. The use of agricultural waste – OPS as LWA in the concrete has been carried out extensively. In the recent research, the use of OPS as LWA has not only improved the environmental sustainability, but also able to manufacture a structural grade LWC. Shafigh et al. (2011a) reported that the use of crushed OPS as LWA could produce a grade 30 LWC with a 28-day compressive strength ranged from 34 to 53 MPa. Besides that, the use of POFA as CM also lessens the waste and environmental impacts. The replacement of POFA as CM is potentially suppressing the concrete expansion due to the sulphate attack (Awal & Hussin, 1997) and also enhance the compressive strength and permeability of the concrete (Chindaprasirt et al., 2007).

The research on the manufacture of geopolymer concrete has been done widely due to its enormous benefits that lead to the development of the environment sustainability. A wide-range of geopolymer binders have been used to develop the

geopolymer concrete. However, there is a limited literatures on the incorporation of foam in geopolymer concrete. Raden and Hamidah (2012) made an effort to utilize waste paper sludge ash as source material to develop foamed geopolymer concrete (FGC). The density and the compressive strength of FGC were found to be approximately 1800 kg/m^3 and 3 MPa, respectively. Abdullah et al. (2012) added pre-formed foam into 50-mm geopolymer paste and obtained 28-day compressive strength and density of 18 MPa and 1667 kg/m^3, correspondingly.

This research work will provide better understanding on the development of the structural and non-structural FGC integrated with the OPS as LWA and binder that consists POFA and FA. The use of agricultural wastes, namely POFA and OPS, is as part of the substantial waste reduction in Malaysia. Furthermore, the findings will include the strength development, transport properties, functional behaviour and the microstructure analysis of the OPSFGC.

1.6 Outline of the research approach

After thorough introduction of the background, objectives and research approach in the first chapter, the remainder of the chapters are arranged and described as the following:

Chapter 2 Literature review

This chapter discusses the literature reviews on the environmental sustainability and the construction of energy-efficient buildings. It also provides a brief literature reviews on the background and the properties of the LWC and FC. Other than that, this chapter reviews the background and the properties of geopolymer concrete. An appropriate literature review has been conducted on the utilization of palm oil wastes.

Chapter 3 Materials and experimental programme

In this chapter, the materials used in the development of OPSFGC were reported. Also, this chapter explains the mixture proportions, mixing procedures, curing method and testing procedures of the OPSFGC. The testing procedures include the fresh and hardened concrete properties such as workability, mechanical, transport and functional properties, and the microstructure analysis. These testing procedures are conducted in accordance to the relevant standards.

Chapter 4 Results and discussions

This chapter presents and discusses all the test results which have been carried out on the OPSFGC and OPSNFGC. The thermal conductivity test results were to compare with the conventional materials, block and brick. Also, the morphology of the geopolymer concrete and the mineralogy of the geopolymer paste at different curing period were discussed.

Chapter 5 Conclusions and recommendations

The summary and conclusions of the research work are highlighted in this chapter. Moreover, the recommendations for the future research works are listed in this chapter.

CHAPTER TWO

LITERATURE REVIEW

2.1 Concrete and environment

2.1.1. Environmental sustainability

Modern concretes are produced with composite materials in today's world, however cement is still an indispensable material in the concrete production (Aïtcin, 2000). Yet, concrete is the most important building material, where the worldwide concrete production is more than 10 billion tons each year (Meyer, 2009). Davidovits (1994b) reported that the production of 1 tonne of cement generates 0.55 tonnes of CO_2 and involves the ignition of carbon fuel to yield an additional 0.40 tons of CO_2; accounted as 1 billion metric tons world production of cement produces 1 billion metric tons of CO_2. Meanwhile, Malhotra (1999) stated that the cement industry is liable for about 7% of the worldwide generated CO_2. From here, it is known that the production of OPC emits a significant amount of CO_2, which would worsen the environmental sustainability by increasing the greenhouse gas emissions.

In order to reduce the negative impact on the environment, many researchers have put in effort by replacing the cement with the other pozzolanic materials such as POFA, RHA, FA, MK and GGBS to develop a more environment friendly concrete. Greening of the construction industry has to be started with the green materials, where the green construction will be more energy- and resource-efficient (Mehta, 2002). Other than creating a better environment, the replacement of OPC with the industrial by-products

even up to 70%) in concrete also enhance the energy efficiency and durability of concrete (Naik et al., 2003).

2.1.2. Energy-efficient construction

Energy efficiency is the utmost criteria in green building indices attributed to the sustainable development. A energy efficient design and construction has become urgent gradually as the cost of energy consumption is escalating and more awareness on the effects of global warming are raised (Ng & Low, 2010). The scientific and government policy has enforced the need for an optimization of the building's energy behaviour in order to lessen carbon footprint. Huge energy consumption leads to a diminishing of the available fossil fuels and pollutes the atmospheric environment.

When the usage of electricity in a building increases, the power station will be likely to generate more power by burning fossil fuels. The burning of the fossil fuels will eventually releases emissions of hazardous gases, which is probable to cause greenhouse effect and acid rain that will give a negative impact towards the environment. In Malaysia, the emissions from the electricity generation produced the largest emission as reported by Mahlia (2002). This phenomenon is harmful towards the quality of life in the country.

The construction of the buildings with a material of good thermal insulation characteristic is more advantageous compared to the conventional building materials. Thermally insulated buildings tend to benefited from the energy efficiency due to the reduction of the heating and cooling cost and therefore environmental pollution will be reduced (Saygılı & Baykal, 2011). Other than reducing the maintenance and energy cost,

the buildings that are constructed to be both durable an environmental friendly tend to have a better air quality that will boost the productivity (Naik, 2008).

2.2 Lightweight concrete

2.2.1. Background

Since the ancient Rome, the LWC has been a popular concrete to be used due to its low density and better thermal insulation characteristic (Chandra & Berntsson, 2002). In general, the LWC is used to reduce the dead load of a structure as well as increase the resistance caused by the seismic forces since the mass of structures or buildings is proportional to the seismic forces (Kılıç et al., 2003). According to BS EN 206-1 (2000), concrete having an ODD in the range of 800 to 2000 kg/m^3 can be classified as LWC.

The ACI 213R (2003) classified LWC into three categories according to the strength and density, where the low strength concrete corresponding to low density and is mostly used for insulating purposes; moderate strength is used for filling and block concrete; and the structural LWC is used for reinforced concrete. Besides having smaller size of foundations or structural members, the reduction in the total weight of structure is able to increase the productivity.

2.2.2. Types of lightweight concrete

It is known that the basic principle of Short and Kinniburgh (1978) in making concrete light is by including air in its composition. Generally, there are three of LWC as presented in Figure 2.1 and illustrated in Figure 2.2.

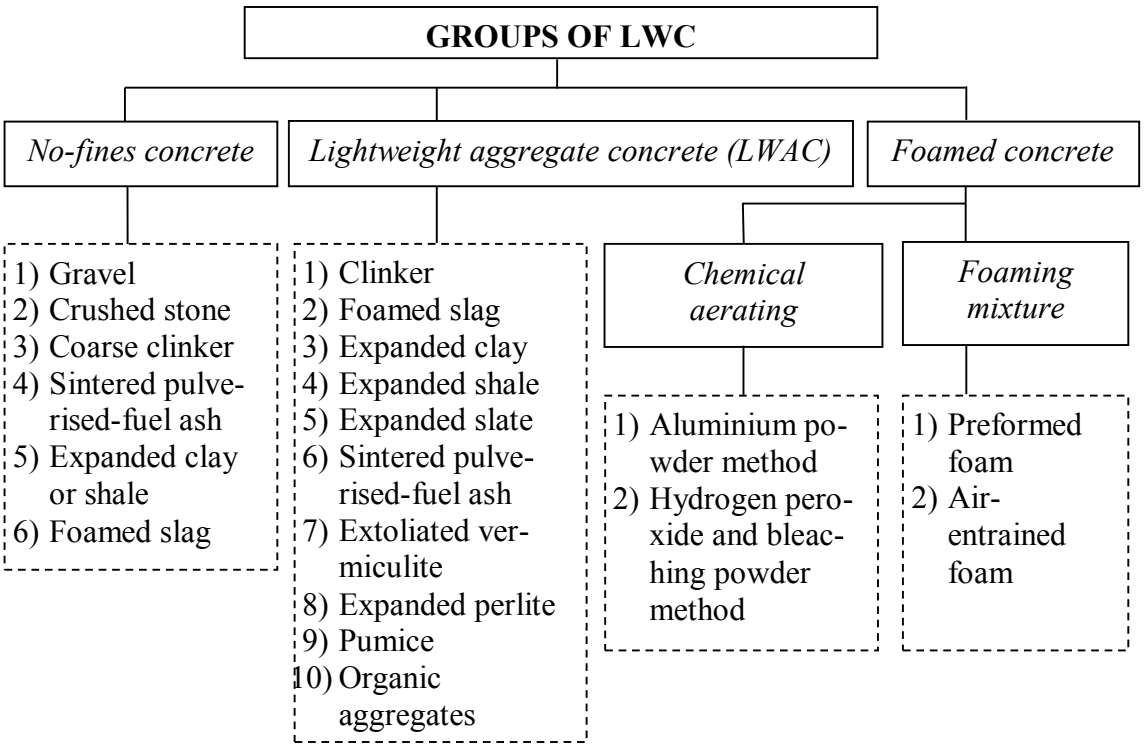

Figure 2.1: Group of LWC (Short & Kinniburgh, 1978)

No-fines concrete uses only single-size coarse aggregates, leaving voids between aggregates to produce a porous structure (Figure 2.2a) that make it lightweight. The types coarse aggregates can be either lightweight or normal-weight types with the sizes between 10 and 20 mm. The no-fines concrete has the ability to allow water permeates through it and this type of concrete is commonly used on walkway and residential street.

The production of LWAC is alike to the NWC but the coarse aggregates are being replaced with the LWA, either partially or completely (Figure 2.2b) to reduce the unit

weight of concrete. There are a number of types of LWA that has been used widely such as natural aggregates, manufactured aggretgates and industrial by-products. Usually aggregates occupy 70 to 80% by volume fraction of concrete, allowing aggregates exert a major influence on the MOE of concrete and expected to have impact on other properties as well (Mindess et al., 2003).

Despite that, a more environmental and economical benefits can be achieved if the waste produces are used to replace the aggregates (Bai et al., 2004), instead of using the natural resources that would affect the sustainable environment. The main idea of developing the foamed concrete (FC) is by introducing air bubbles into the cement paste or mortar matrix to form air voids within (Figure 2.2c), which is done either by chemical aeration or foaming mixture.

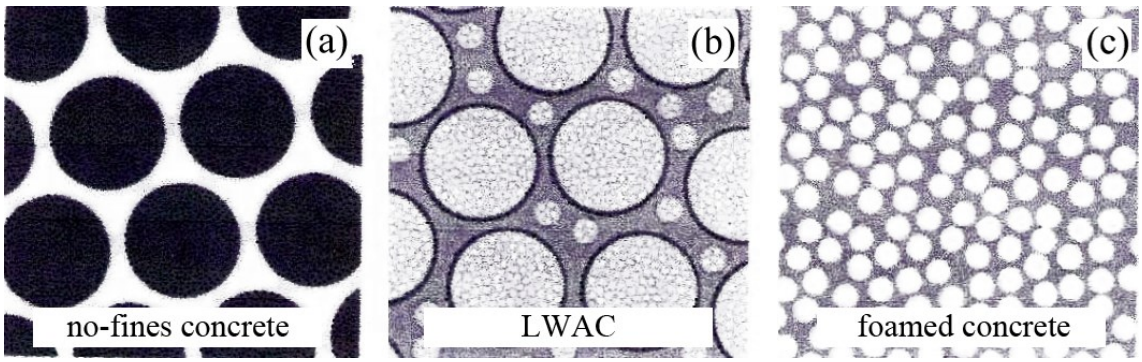

Figure 2.2: Illustrated diagram on basic form of LWC (Newman & Choo, 2003)

2.3 Foamed concrete

2.3.1. Background

FC is known as aerated or cellular in European countries, pore concrete in Russia and air entraining or gas concrete elsewhere. FC may not contain coarse and fine aggregates in order to acquire a great reduction of density, yet the pozzolanic materials are usually replace the fine aggregates. The production of FC is by mixing of materials such as cement, filler, water, superplasticizer (SP) and foaming agent under controlled conditions (Kearsley & Wainwright, 2002). The addition of the foam creates pores volume within the paste or mortar matrix without induce any chemical reaction with the cement.

According to Ramamurthy et al. (2009), there are many factors that influenced the stability and consistency of FC such as the types of foaming agent, formula and method of foam preparation for uniform air-voids distribution, material and mix design strategies. These significant factors affected the properties of FC with respect to its performance at fresh and hardened state. Although the strength of the FC is proportional with the density, FC possesses a superior properties compared to other types of concrete such as fire resistance, thermal conductivity and acoustic properties. In addition, the advantages of FC in environment and economy aspects includes the rapid construction rate, lower haulage and handling cost.

2.3.2. Lightweight aggregate foamed concrete

The term ‘foamed concrete’ has been misunderstood as majority of the FC does not contain any coarse aggregates hence it should be termed as ‘foamed mortar’ instead (Aldridge, 2000). Gelim and Ali (2011) distinguished FC as having an air content of more than 25%. The incorporation of foam into LWAC can be explored extensively using the locally available waste materials. The use of foam in LWAC not only reduces the self-weight of the concrete, yet a more environmental and economic FC can be produced. Also, the FC is included as structural element, non-structural partitions and thermal insulating materials (Narayanan & Ramamurthy, 2000).

2.3.3. Properties of foamed concrete

2.3.3.1. Density and strength

FC is best labelled as the low density and strength concrete, although the other properties gives greater interest to architects, engineers and builders. Nambiar and Ramamurthy (2006) stated that the foam volume governs the strength instead of the material properties when the concrete density is at lower range. The pores introduced in the concrete due to the addition of foam played an important role in the density reduction. Other than that, Hamidah et al. (2005) reported that the decrease of the ratio of sand to cement increases the density of the FC.

The strength of the concrete can be expressed as a function of the void content taken as the sum of the induced voids and the volume of evaporable water. Alengaram et al. (2013) proclaimed that the compressive strength of the FC is proportional with the density, where the agricultural by-product is being used as LWA. At a higher volume of

foam, the inclusion of bubbles seemed to produce larger voids that result in widespread of void size and lower mechanical strength (Nambiar & Ramamurthy, 2007a). Jones and McCarthy developed FC of 28-day compressive strength of about 30 MPa by incorporated FA in FC at the density range 1400 to 1600 kg/m^3 (Jones & McCarthy, 2005).

2.3.3.2. Transport properties

The transport property in porous materials is measureable as sorptivity that assessed the absorbance and transmittance of water by capillarity, which is based on the unsaturated flow theory (Wilson et al., 1991). Kearsley and Wainwright (2002) reported that the porosity of FC is greatly controlled by the dry density and not on the content and types of CM. Besides that, the size and distribution of the pores continuity and tortuosity of the pores also have considerable significance on the permeable porosity of concrete (McCarter et al., 1992).

Polat et al. (2010) showed a strong correlation on the inverse proportion of the sorptivity against the density of concrete. Also, Panesar (2013) reported that the sorptivity increases with an increase in foam volume. Tasdemir (2003) stated that the capillary sorptivity coefficient of concrete decreased with the increase in the compressive strength.

2.3.3.3. Thermal behaviour

Sengul et al. (2011) expressed that the thermal conductivity of a material is the total heat transferred through the surface of a unit thickness, for the reason of temperature changes prone to certain conditions. Saygılı and Baykal (2011) reported that the decrease in the

thermal conductivity is due to increase of void ratio that decreased the unit weight of concrete.

Since air exhibited lowest conductivity compared to the solid and liquid states due to its molecular structure (Ng & Low, 2010), it attributes to a lower thermal conductivity in porous concrete. Also, Ramamurthy et al. (2009) proclaimed that FC possesses superior thermal insulating characteristic owing to its cellular structure.

2.3.4. Microstructural behaviour of foamed concrete

The introduction of foam into concrete has a great influence on the physical properties that would reflect its structural behaviours. According to Visagie (2000), the air-voids structure may influence the physical properties of the FC, where the same porosity and density of FC can be achieved at both cases; FC with more tiny pores and FC with fewer large pores. Other than the pore sizes, the strength of the FC also depends on the pore distribution. Rickard (2012) reported that interconnected pore structure possesses lesser strength loss compared to an isolated pore structure.

The field emission scanning electron microscope (FESEM) has been a primary tool to investigate the morphology of concretes and cement pastes for many years, aided further by the energy dispersive X-ray analysis (EDX) to study their characteristics. The structure of FC is described by the microporous matrix and macropores, where the size of macropores is larger than 60 μm due to the aeration and micropores tend to materialize between the macropores (Alexanderson, 1979; Petrov & Schlegel, 1994).

The compressive strength of FC was said to be a function of porosity and age, where the porosity of FC is greatly controlled by the dry density and not on the content and type of CM (Kearsley & Wainwright, 2002). Moreover, a stable and spherical cell structure of FC is important for the optimum structural and functional properties (Prim & Wittmann, 1983). On the other hand, the significant drop in compressive strength is associated with the formation of the macropores in FC (Pospisil et al., 1992).

2.4 Geopolymer concrete

2.4.1. Background

Geopolymer was first introduced by Davidovits (1999) where cementless concrete can be produced by the reaction between the alkaline solutions and the source materials that are rich in silica and alumina, aided by heat curing and drying (Hardjito et al., 2004). Furthermore, Xu and van Deventer (2000) found that natural minerals that are rich in silica and alumina could be the source material for geopolymers, where the reaction mechanisms involved dissolution, gel formation, setting and hardening phases.

Duxson et al. (2007) illustrated the reaction mechanisms for geopolymerization that outline the processes from the transformation of solid aluminosilicate source to a synthetic alkali aluminosilicate (Figure 2.3). Further, the potential requirements for geopolymerization include fine grinding of raw materials and heat treatment.

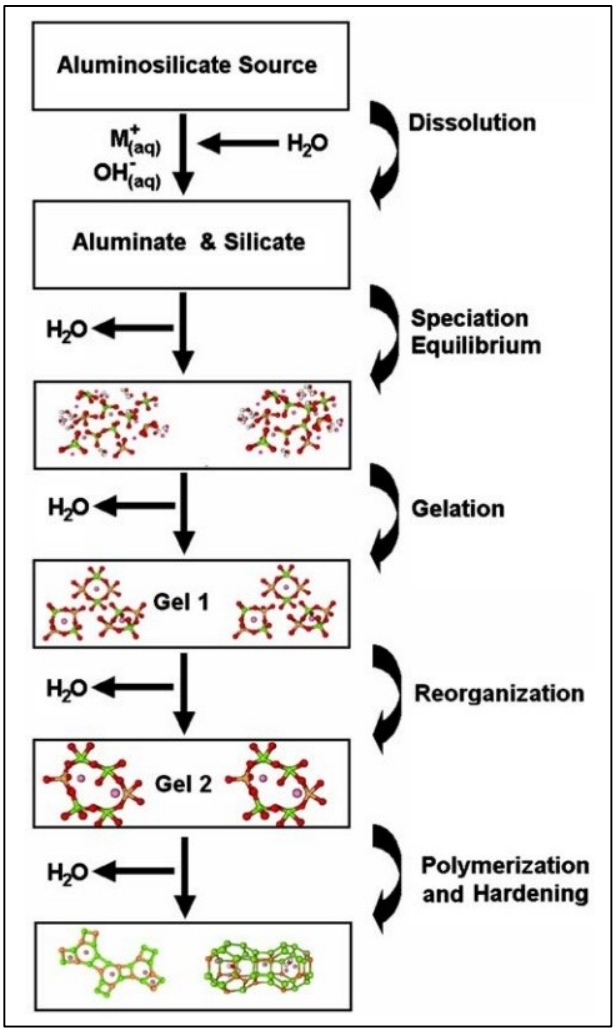

Figure 2.3: Conceptual model for geopolymerization (Duxson et al., 2007)

Unlike OPC, geopolymers do not form calcium silicate hydrates (CSH), but utilize the polycondensation of SiO_2 and Al_2O_3 precursors and a high alkali content to get structural strength (Wallah & Rangan, 2006). According to Davidovits (1999), the atomic ratio of silica (SiO_2) and alumina (Al_2O_3) in the poly(sialate) structure governs the properties and application fields if geopolymers, which a low ratio (1, 2 or 3) initiates a very rigid 3D-network and a high ratio (more than 15) provides polymeric character to the geopolymeric materials (Figure 2.4).

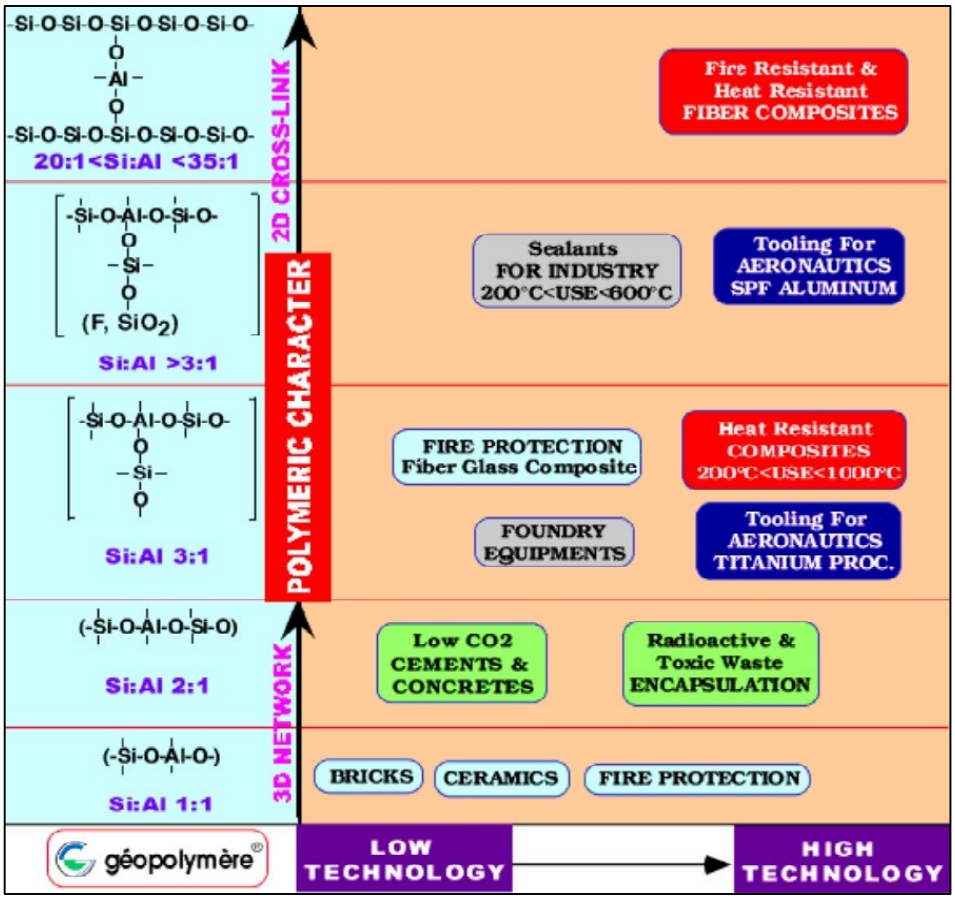

Figure 2.4: Chemical structure and applications (Davidovits, 1999)

The by-product source materials that are rich in SiO_2 and Al_2O_3 include FA, silica fume (SF), RHA, GGBS, MK and POFA. The selection of the source materials for geopolymerization is subject to the material properties, local availability and cost. Although there are many types of CM available for geopolymerization, the use of FA is more prevailing in the manufacture of geopolymer concrete (Hardjito et al., 2004; Hardjito & Rangan, 2005).

2.4.2. Use of fly ash in geopolymer concrete

Class-F FA is more favoured over class-C FA as source material in geopolymerization due to the potentiality of high volume of calcium may obstruct with the polymerization process and alter the microstructure (Gourley, 2003). Moreover, the usage of FA as source

material is advantageous due its finer particle size than slag, which has higher reactivity (Hardjito & Rangan, 2005).

On the basis of ASTM C618 (2012) specification, the class-F FA shall conform to the requirements such as prescribed in Table 2.1. The class-F FA used by Fernandez Jiminez et al. (2004) and Hardjito et al. (2004) in their research of geopolymer concrete conform to the requirements as presented in Table 2.1. Other than the chemical composition, the other characteristics such as particle size, amorphous content, morphology and the origin of the FA influence its suitability as source material (Hardjito & Rangan, 2005).

Table 2.1: Chemical composition of class-F FA

Chemical composition (%)	ASTM C618 (2012)	Fernandez Jiminez et al. (2004)	Hardjito et al. (2004)
Silica (SiO_2)	-	51.51	53.36
Alumina (Al_2O_3)	-	27.47	26.49
Ferric oxide (Fe_2O_3)	-	7.23	10.86
Calcium oxide (CaO)	-	4.39	1.34
Sulphuric anhydride (SO_3)	≤ 4.0	0.15	1.70
Loss on ignition (LOI)	≤ 10.0	1.80	1.39
$SiO_2 + Al_2O_3 + Fe_2O_3$	≥ 70.0	86.21	90.71

Note. Adapted from ASTM C618 (2012), Fernandez Jiminez et al. (2004) and Hardjito et al. (2004).

A higher sum of SiO_2, Al_2O and Fe_2O_3 ensures that adequate reactive glassy constituent is present in FA, whereas the LOI measures the unburnt carbon in FA that affect the quality by reducing the fineness and pozzolanic activity as well as increasing the water demand. While the high amount of SO_3 will lead to a loss of durability due to the volume instability caused by the formation of ettringite. The use of the industrial waste, FA in producing geopolymer concrete has definitely created a greener development by

reducing the emission of CO_2 associated with the manufacture of OPC and concrete. In addition, it improves the environmental sustainability through the reduction in land pollution and natural resource consumption.

2.4.3. Factors affecting the geopolymer concrete properties

In comparison with the normal concrete, the geopolymer concrete has more factors that affect its properties due to the incorporation of alkaline activator. The manufacture of geopolymer concrete requires alkaline solution to stimulate the dissolution of solid aluminosilicate and produce an amorphous to semi-crystalline aluminosilicate materials (Sun, 2005). Hence, the properties of geopolymer concrete can be tailored by the alteration of the ratio of SiO_2 to Al_2O_3 and its binder ratio of the source material.

In alkaline solution, the factors such as the types of alkali, the molar ratio of SiO_2 to Al_2O_3 and the ratio of solution to CM had a significant correlation with the mechanical properties of geopolymer concrete. Also, the types of curing system and curing hours that affect the properties of geopolymer concrete will be mentioned after that.

2.4.3.1. Alkaline solution

Among many types of alkaline solution, the mixture of sodium hydroxide (NaOH) and sodium silicate (Na_2SiO_3); or potassium hydroxide (KOH) and potassium silicate (K_2SiO_3) are most favoured alkaline solution (Davidovits, 1999; Palomo et al., 1999; Xu & van Deventer, 2000; Hardjito & Rangan, 2005; Wallah & Rangan, 2006). It is evident that when the alkaline solution contains soluble silicates and hydroxides as activator, the geopolymerization of source material occurred at a higher rate (Palomo et al., 1999).

Moreover, Xu and van Deventer (2000) reported that the NaOH solution has a higher rate of dissolution compared to the KOH solution.

According to Hardjito and Rangan (2005), a higher concentration (molarity) of NaOH solution increases the mechanical strength of FA-based geopolymer concrete (Table 2.2). Similarly, it appeared that a higher reactivity in geopolymerization occurred at higher concentration of the alkaline solution (Katz, 1998). However, Palomo et al. (1999) reported that an excess of the hydroxide concentration (18M) in the geopolymer system resulted in decrease of its compressive strength, while the 12M alkaline solution yields higher compressive.

Table 2.2: Effect of alkaline solutions

Mixture	NaOH solution (in Molars)	Ratio of Na_2SiO_3 to NaOH (by mass)	7-day compressive strength (MPa)
1	8M	0.4	17
2	8M	2.5	57
3	14M	0.4	48
4	14M	2.5	67

Note. Adapted from Hardjito and Rangan (2005).

Furthermore, Hardjito and Rangan (2005) reported that the higher ratio (by mass) of the Na_2SiO_3 to NaOH produced a higher 7-day compressive strength of the geopolymer concrete (Table 2.2). Abdullah et al. (2011) indicated that the optimum ratio of Na_2SiO_3 to NaOH of 2.5 produced the highest strength among the geopolymer concretes with the ratio between 0.5 and 3. In addition, the test results of geopolymer concrete were consistent with the ratio of 2.5 and the cost of Na_2SiO_3 is rather cheaper than NaOH (Hardjito & Rangan, 2005).

2.4.3.2. Curing methods and temperatures

Unlike conventional OPC concrete that cures with water to aid the hydration, there are many curing methods for geopolymer concrete. Riahi et al. (2012) reported that the strength gain of the water-cured geopolymer concrete is higher than the oven-cured, however the oven-cured geopolymer concrete achieved higher compressive strength at 90˚C than the water-cured. Similarly, the Figure 2.5 showed that the oven-cured geopolymer concrete at 65˚C has superior mechanical properties over the curing methods of ambient and external exposure (Kusbiantoro et al., 2012). Furthermore, oven-cured geopolymer concrete experienced a very low shrinkage of about 100 micro strains over a year (Wallah & Rangan, 2006).

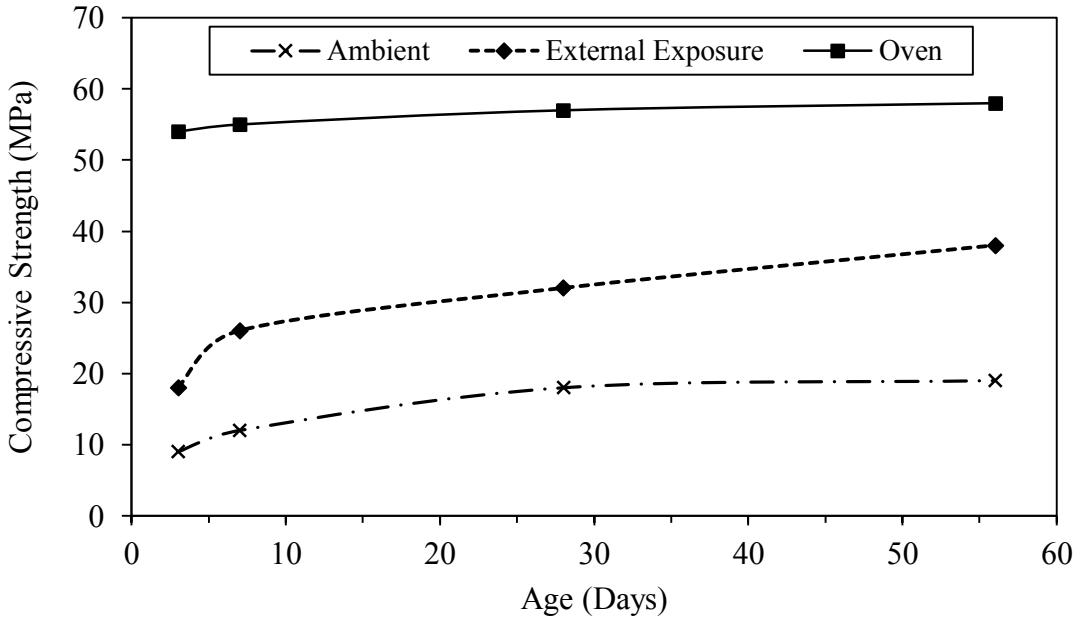

Figure 2.5: Compressive strength of the geopolymer concrete (Kusbiantoro et al., 2012)

The curing temperature acts as a catalyst for the geopolymerization of aluminosilicates, which would affect the mechanical properties of the geopolymer concrete. The Figure 2.6 showed that the increase of the oven curing temperature leads to

the enhancement of the compressive strength; however, the temperature beyond 60˚C did not show a significant growth of compressive strength (Hardjito & Rangan, 2005). Palomo et al. (1999) also reported that increasing of curing temperature give rise to the compressive strength. However, the oven curing at intense heat will cause an adverse effect on physical properties due to the crack existence (van Jaarsveld et al., 2002).

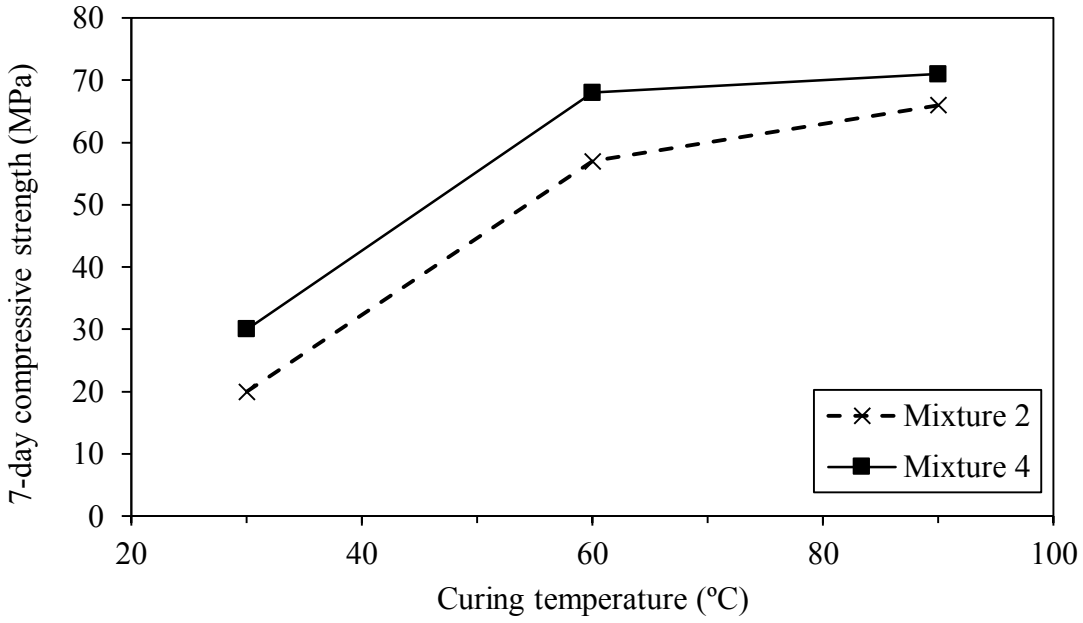

Figure 2.6: Effect of curing temperature on the compressive strength

(Hardjito & Rangan, 2005)

2.4.4. Properties of geopolymer concrete

2.4.4.1. Density and strength

Similar with the conventional OPC concrete, the geopolymer concrete using normal-weight aggregates achieved a density of about 2400 kg/m^3 (Lloyd & Rangan, 2010). In contrast to the well-established strength development of OPC concrete in which the hydration process takes place over a period along with strength gain, the geopolymer concrete does not gain strength exponentially over the time (Hardjito et al., 2004).

Geopolymer concrete is able to achieve high early strength due to the polymerization process that takes place during the oven curing. The Figure 2.7 presents that the 1-day strength improvement of the geopolymer concrete is about 80% of the 28-day strength when oven-cured for 24 hours (Lloyd & Rangan, 2010). Furthermore, Olivia and Nikraz (2012) reported that the flexural strength of geopolymer concrete was 1.4 times higher than the OPC concrete.

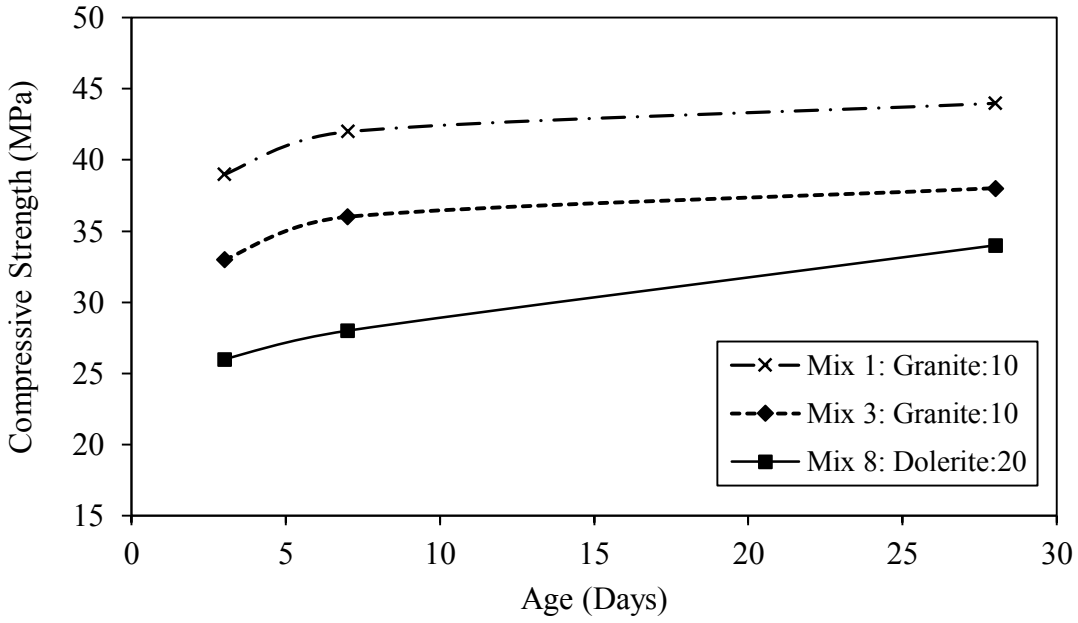

Figure 2.7: The relationship of strength gain with age (Lloyd & Rangan, 2010)

2.4.4.2. Transport properties

The transport properties play an important role in determine the durability of concrete due to the possibility of aggressive chemical agents, which includes CO_2 penetrates into the material structure. Therefore, an increase of porosity weakens the mechanical strength of geopolymer concrete. The strength of the FA-based geopolymer concrete increases with the increase of the alkali modulus up to 1, however further increment of alkali modulus have only minimal impact on its strength (Adam, 2009).

Table 2.3 tabulated that the sorptivity of geopolymer concrete has an inverse relationship with its strength and showed a lower sorptivity compared to the OPC concrete (Olivia & Nikraz, 2012). Tasdemir (2003) reported similar findings as the capillary sorptivity coefficient of concrete decreased with the increase in the compressive strength. Further, Polat et al. (2010) showed a strong correlation on the inverse proportion of the sorptivity against the density of concrete.

Table 2.3: Properties of OPC and geopolymer concrete mixes at 28 and 91 days

Mixtures	28-day		91-day	
	Strength (MPa)	S ($mm/min^{1/2}$)	Strength (MPa)	S ($mm/min^{1/2}$)
OPC	56.22	0.1888	65.15	0.2027
T7	54.04	0.1060	56.51	0.1624
T4	55.27	0.0813	58.85	0.1029
T10	59.08	0.1354	63.29	0.1264

Note. Adapted from Olivia and Nikraz (2012).

2.4.5. Microstructural behaviour of geopolymer concrete

The alkali activation of aluminosilicate is acknowledged for the formation of amorphous aluminosilicate gel and geopolymer and that leads to excellent mechanical and chemical properties (Davidovits, 1994b; Palomo et al., 1999). Therefore, it is essential to study the microstructural characteristics of the geopolymer concrete, especially with the addition of new CM or aggregates.

Ahmari et al. (2012) reported that the geopolymerization has two main effects on the X-ray diffraction (XRD) patterns; a broad amorphous hump from 20˚ to 40˚ is the characteristic of the geopolymeric gel and the reduction of the crystalline peaks that indicate the partial dissolution of the source materials in crystalline phase. The Fourier transform infrared spectroscopy (FTIR) analysis is useful for identification of the reaction

products in geopolymer systems. In FTIR analysis, every major band represents a reaction, such as water molecule (H-O-H) bending vibrations at around 1650 cm^{-1}, stretching vibration of carbon dioxide (O-C-O) near 1430 cm^{-1}, asymmetric stretching vibrations of aluminosilicate or silicon oxide (Si-O-Al or Si-O-Si) appeared at 960–1100 cm^{-1} and among others. Mužek et al. (2012) suggested that the amorphous aluminosilicate gel formed at 960–1100 cm^{-1} is due to the depolymerisation and structural reorganisation of the amorphous phases in geopolymer materials.

Different mineral particles do not act as filler in the matrix but rather bonded with alkaline solution to produce complex reaction that enhance the strength of the matrix with curing age (Xu & van Deventer, 2000). Figure 2.8 showed the development of denser geopolymer matrix over the period of 20 hours to 60 days, which indicated that the curing period has a significant effect in the acquisition of the mechanical dependability (Criado et al., 2010).

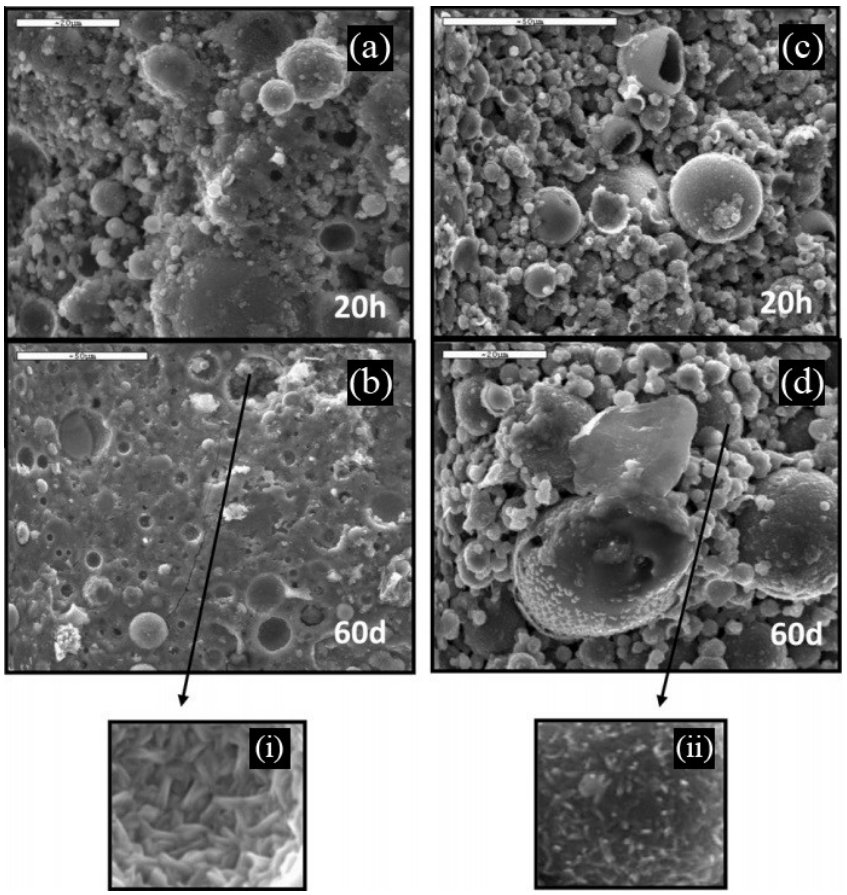

Figure 2.8: Microstructures of two systems studied at 20 hours and 60 days (Criado et al., 2010)

2.5 Utilization of palm oil wastes

Being the second largest palm oil producer in the world, the oil palm has become the most important commodity crop in Malaysia (PORIM, 1998). By contributing millions of tonnes of agricultural wastes, Malaysia faced environmental issues, which the land and air pollution caused by the waste disposal (Figure 2.9) and operation of palm oil factories, respectively. Many researchers have taken initiative to utilize some of these palm oil industry wastes such as OPS and POFA to develop sustainable construction materials (Mannan & Ganapathy, 2004; Tangchirapat et al., 2007; Ahmad et al., 2008; Alengaram et al., 2011b; Shafigh et al., 2011a; Yap et al., 2013). Further reviews on the utilization of palm oil wastes in construction industry will be discussed in the following subsections.

Figure 2.9: The wastes disposal of the OPS and POFA

2.5.1. Oil palm shell as lightweight aggregate

OPS is the hard endocarp, which obtained by breaking the surrounds of the palm kernel. By possessing lightweight and naturally sized aggregate, the use of OPS as LWA in manufacture of LWC is ideal. In addition, the use of OPS will not pollute to produce lethal substances when bonding with cement paste (Basri et al., 1999).

According to Mannan et al. (2006), OPS is likely to decay over time and under vigorous environment which is similar to other biodegradable materials. They investigated that higher compressive strength of oil palm shell concrete (OPSC) could be achieved by pre-treatment the OPS with 20% of polyvinyl alcohol (PVA) solution, which formed a thin film on OPS to reduce its water absorption and enhance the bonding between the OPS and cement paste.

In recent research, Shafigh et al. (2011a) reported that by crushing the larger original OPS aggregate, a high 28-day compressive strength of 53 MPa of OPSC can be obtained. They also showed that there is a linear relationship of early and 28-day compressive strength of the OPSC. Moreover, the grading of OPS as LWA is in accordance to the BS EN 13055-1 (2002), which the size ranged from 5 to 14 mm. The physical and mechanical properties of OPS and granite are presented in Table 2.4.

Table 2.4: The physical and mechanical properties of OPS and granite

Physical and mechanical properties	(Mannan & Ganapathy, 2004)		(Mannan et al., 2006)	(Alengaram et al., 2011a)	(Shafigh et al., 2011a)
	Granite	OPS	PVA-treated OPS	OPS	Crushed OPS
Maximum size (mm)	12.5	12.5	-	12.5	8.0
Specific gravity (saturated surface dry)	2.61	1.17	-	1.27	1.22
Water absorption (24 h) (%)	0.76	23.30	4.25	24.5	18.73
Los Angeles abrasion value (%)	24.0	4.8	-	-	-
Bulk density (compacted) (kg/m^3)	1470	590	-	620	683
Fineness modulus	6.33	6.24	-	-	5.72
Flakiness index (%)	24.9	65.2	-	-	-
Elongation index (%)	33.4	12.4	-	-	-
Aggregate impact value (AIV) (%)	17.29	7.86	1.04	3.91	-

Note. Adapted from Mannan and Ganapathy (2004), Mannan et al. (2006), Alengaram et al. (2011a) and Shafigh et al. (2011a).

2.5.1.1. Use of oil palm shell in concrete

The use of OPS can produce a LWAC, which fulfilled BS EN 206-1 (2000) by acquiring a density of lower than 2000 kg/m^3. The manufacture of the OPSC in the previous research works done by Basri et al. (1999), Mannan and Ganapathy (2004), and Alengaram et al. (2011b) have exhibited a LWAC characteristic with a density of below 2000 kg/m^3. The use of OPS as LWA not only improves environmental sustainability, but also produces a more economical construction material.

Moreover, it is proven in previous research works that the properties of the OPSC are comparable to other structural LWC. According to Teo et al. (2007), the OPSC can easily satisfy the compressive strength requirement for structural LWC. Other than comparable water absorption and water permeability, they also investigated that the OPSC demonstrated a similar bond strength to the structural LWAC. Furthermore, Alengaram et al. (2008) reported that the deflection at service loads and ultimate moment of the OPSC beams were parallel with the NWC beams. Yet, the OPSC beams revealed a stronger bond between the steel reinforcement and the concrete.

By adding fibres, the properties of the OPSC such as ductility and high impact resistance can be enhanced. Shafigh et al. (2011b) acclaimed that adding steel fibres in OPSC improved its properties significantly with respect to the ductility, splitting tensile strength and flexural strength. According to Yap et al. (2013), the addition of the polypropylene and nylon fibres developed a better post-failure compressive strength and toughness of the OPSC. They also investigated that the UPV of the OPSC and OPS fibre-reinforced concrete (OPSFRC) falls under 'good' category. Even with the addition of foam, the OPSC of densities 1500 and 1600 kg/m^3 are considered as structural and

insulating concrete, exhibiting 37 to 39% of reduced thermal conductivity compared to the conventional brick (Alengaram et al., 2013). Additionally, the OPSC beams showed a good aggregate interlock, thus improved its shear behaviour (Jumaat et al., 2009).

2.5.1.2. Use of oil palm shell in geopolymer concrete

Up to now, there are very limited literatures available on the incorporation of OPS in geopolymer concrete (OPSGC). Kupaei et al. (2013) produced 50-mm OPSGC of structural grade 30 where the optimum mix design can be obtained with 14M of alkaline solution, 480 kg/m^3 FA and water to FA ratio of 0.34. Due to the insignificant of strength increase, he recommended the use of 14M over the 16M of alkaline solution. In addition, OPS as coarse aggregate in saturated surface dry (SSD) condition is preferred over air-dry condition for optimum strength development of OPSGC.

2.5.2. Palm oil fuel ash as pozzolanic material

POFA is retained by 5% of solid wastes, which the solid wastes (palm oil raw materials) are amounted as 2.1 million tonnes that undergoes combustion (Sata et al., 2004). Instead of compromise the environmental sustainability, the pozzolanic properties of POFA enabled it to be utilized as replacement in concrete industry. Despite the high alkali content, the reduction of the concrete expansion was found to be effective with the POFA as cement replacement due to the sulphate attack (Awal & Hussin, 1997).

The chemical composition of POFA was found to be comparable to the class-F FA, which satisfy the requirements for Class F pozzolanic materials in accordance to ASTM C618 (2012). The chemical composition of POFA reported in previous research

works is presented in Table 2.5. Further, Chindaprasirt et al. (2008) suggests that the fineness of POFA is higher than OPC, resulted in lower permeability and higher resistance towards chloride attack.

Table 2.5: The chemical composition of POFA

Chemical composition (%)	(ASTM C618, 2012)	(Altwair et al., 2011)	(Tangchirapat et al., 2012)
Silica (SiO_2)	-	66.9	55.5
Ferric oxide (Fe_2O_3)	-	5.7	5.6
Calcium oxide (CaO)	-	5.6	12.4
Magnesium oxide (MgO)	-	3.1	4.6
Potassium oxide (K_2O)	-	5.2	0.0
Sulphuric anhydride (SO_3)	≤ 4.0	0.3	2.3
Alumina (Al_2O_3)	-	6.4	9.2
Loss of ignition (LOI)	≤ 10.0	0.9	7.9
$SiO_2 + Al_2O_3 + Fe_2O_3$	≥ 70.0	79.0	70.3

Note. Adapted from ASTM C618 (2012), Altwair et al. (2011) and Tangchirapat et al. (2012).

2.5.2.1. Use of palm oil fuel ash in concrete

The use of POFA as cement replacement materials has benefited the manufacturing of concrete, in terms of engineering properties and economy aspects. High strength concrete of about 89 MPa can be produced with the 20% cement replacement of POFA by improving its fineness to enhance its reactivity (Sata et al., 2004). Moreover, Altwair et al. (2011) reported that the strength of the POFA increased over curing period because of the consumption of the calcium hydroxide ($Ca(OH)_2$) by the POFA via the pozzolanic reaction. In addition, they also found that the later-strength gain of POFA is higher than that of OPC, as presented in Figure 2.10.

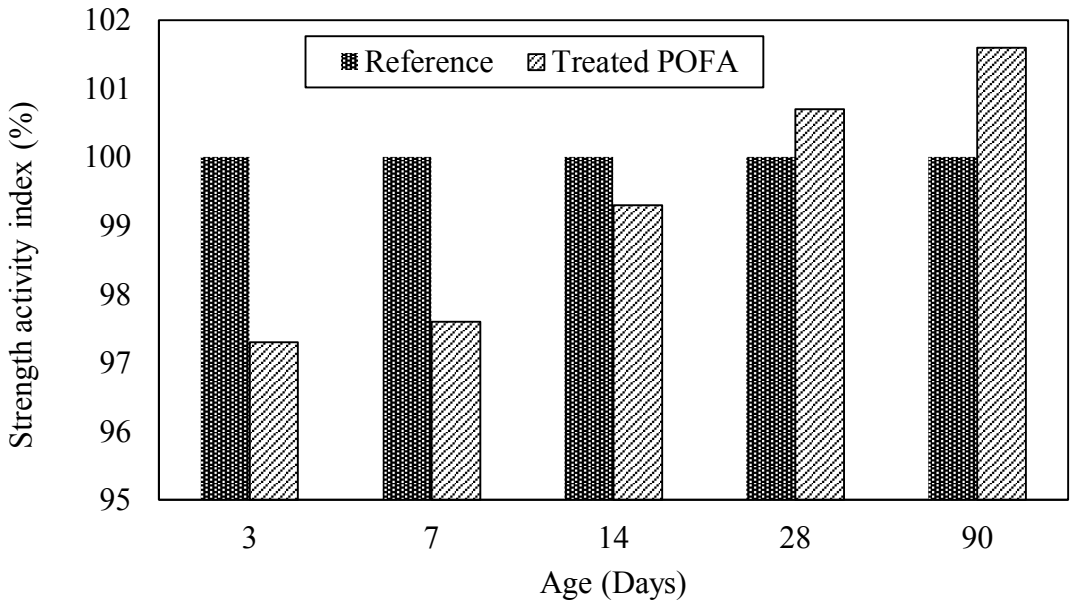

Figure 2.10: Strength activity index against ages of POFA mortar (Altwair et al., 2011)

The increase of POFA as cement replacement in concrete, is however decreases its compressive strength. Figure 2.11 showed that the optimum replacement of POFA was 20% by weight of binder for the manufacture of the recycled aggregate (RCA) concrete (Tangchirapat et al., 2012). The compressive strength gained by the RCA concrete was more than 90% of the OPC concrete. Moreover, the use of POFA enhances the concrete durability by reducing the sulphate attack compared to the OPC concrete. Awal and Hussin (1999) reported that by replacing OPC partially with POFA, the thermal cracking due to the excessive heat release is well controlled.

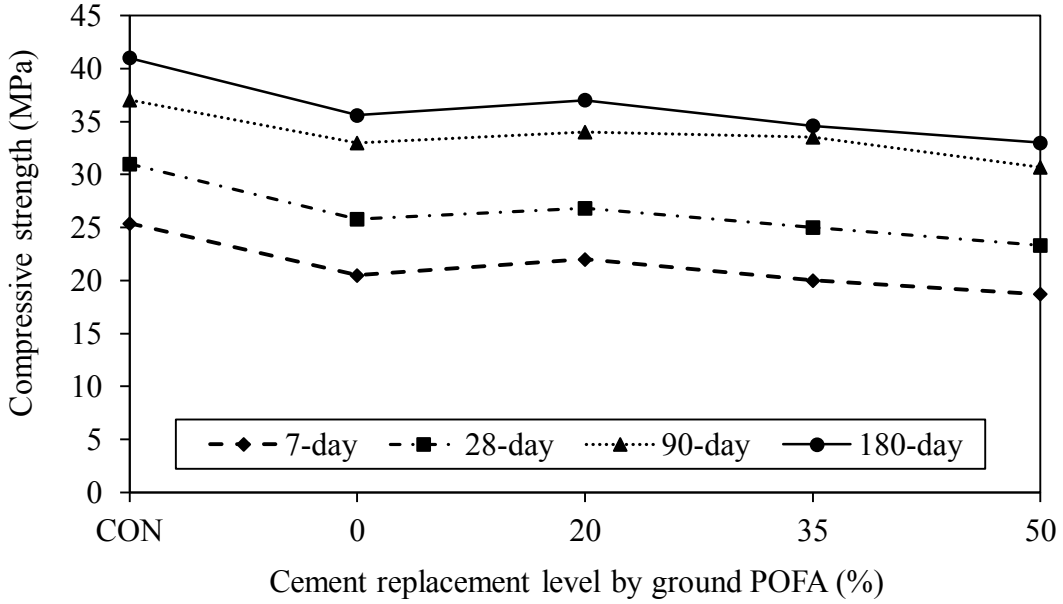

Figure 2.11: Relationship between the compressive strength and POFA replacement level of the RCA concrete (Tangchirapat et al., 2012)

2.5.2.2. Use of palm oil fuel ash in geopolymer concrete

To date, there is only limited literatures available on the replacement of POFA in the production of geopolymer concrete. By replacing 30% of FA with POFA, Ariffin et al. (2011) established the blended ash geopolymer concrete that achieved the 28-day compressive strength of 25 MPa. Moreover, the reinforced geopolymer concrete beam showed a comparable behaviour and failure mode with the OPC reinforced concrete beam (Ariffin et al., 2012). Figure 2.12 shows that the blended ash geopolymer concrete is more durable when exposed to the sulphuric acid, compared to the OPC concrete (Ariffin et al., 2013).

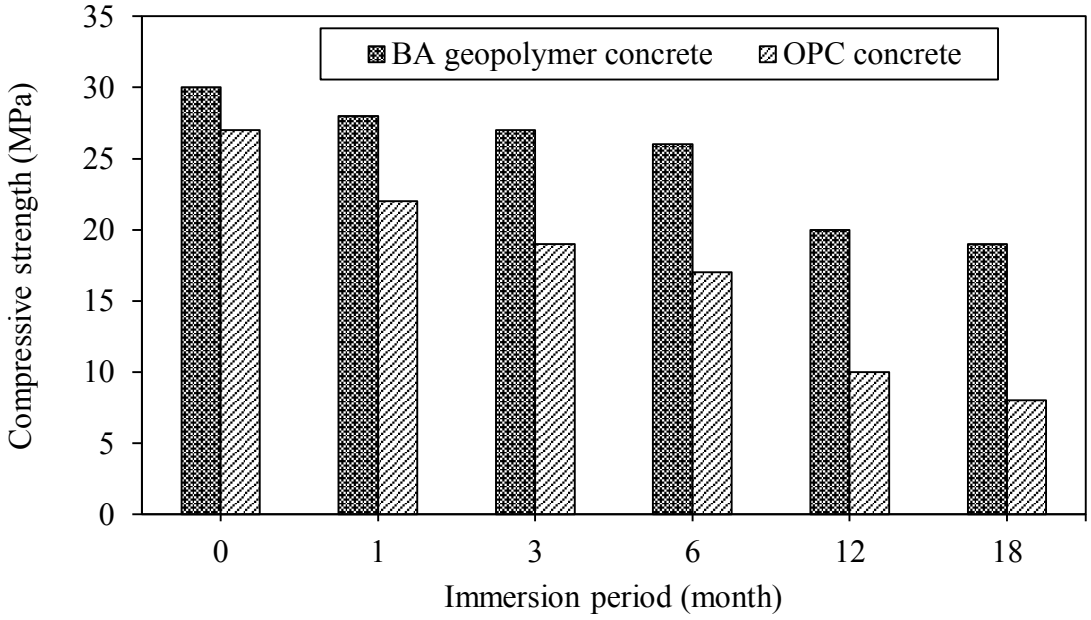

Figure 2.12: Compressive strength of concrete specimens exposed to sulphuric acid for 18 months (Ariffin et al., 2013)

2.6 Significance of previous studies

Table 2.6 presents the significance of previous research works done, which may correlate to the current research work. However, there is no literature available of the current work, where the incorporation of foam and OPS in geopolymer concrete, and utilization of wastes materials such as POFA and FA as binders.

Table 2.6: Significance of previous researches

Authors	Significance of research works
Sata et al. (2004); Ng and Low (2010);	- concrete with 20% replacement of POFA acquired optimum strength.
Abdullah et al. (2012); Kusbiantoro et al. (2012);	- oven-cured geopolymer concrete obtained higher compressive strength, in comparison with the external exposure and ambient curing.
Raden and Hamidah (2012);	- incorporation of preformed foam in FA-based geopolymer concrete with density about 1650 kg/m^3.
Alengaram et al. (2013); Kupaei et al. (2013)	- use of waste paper sludge ash as CM in foamed geopolymer concrete. - use of OPS attained grade 30 50-mm geopolymer concrete. - thermal insulation characteristic of FC focus on the energy efficiency in construction of buildings. - utilization of OPS in the conventional FC, which reduced 56% of thermal conductivity compared with conventional brick.

Note. Adapted from Sata et al. (2004), Ng and Low (2010), Abdullah et al. (2012), Kusbiantoro et al. (2012), Raden and Hamidah (2012), Alengaram et al. (2013) and Kupaei et al. (2013).

CHAPTER THREE

MATERIALS AND METHODS

3.1. Introduction

The experimental methods were designed to determine the material properties of OPS and the effect of foam volume on the properties of fresh and hardened geopolymer concrete. The properties of hardened concrete consists of physical, mechanical, transport and functional behaviours. Additionally, the microstructure analysis of the geopolymer paste and concrete are included such as XRD, FESEM, EDX and FTIR.

Same batches of raw materials were collected from local factories and the equipment for preparations of the specimens such as mixer, steel moulds and curing chamber were maintained. This is to ensure uniformity of the quality of all mixtures. The chapter will describe the procedure of the specimen preparations and tests in detail.

3.2. Materials

3.2.1. Fly ash

The main constituent in the binder of the geopolymer concrete is class-F FA. The FA used in this study was supplied by LaFarge Cements, Malaysia. X-ray fluorescence (XRF) analysis was performed to determine the chemical composition of the FA, is given in Table 3.1.

Table 3.1: Chemical composition of class-F FA and POFA

Chemical composition (%)	Class-F FA	POFA
Silica (SiO_2)	57.6	63.4
Ferric oxide (Fe_2O_3)	5.8	4.2
Calcium oxide (CaO)	0.2	4.3
Magnesium oxide (MgO)	0.9	3.7
Potassium oxide (K_2O)	0.9	6.3
Sulphuric anhydride (SO_3)	0.2	0.9
Alumina (Al_2O_3)	28.9	5.5
Loss of ignition (LOI)	3.6	6.0
$SiO_2 + Al_2O_3 + Fe_2O_3$	92.3	73.1

3.2.2. Palm oil fuel ash

POFA is the waste material produced prior to the combustion of palm fibres, OPS and empty fruit branches at a temperature range of 700–1000 ˚C. The raw POFA was collected from the local palm oil mill, Jugra Palm Oil Mill Sdn Bhd, Banting (Figure 3.1). The POFA collected from the mill was dried in an oven at 105 ± 5 ˚C for 24 hours, followed by sieving through 300 μm to remove foreign particles, which were coarser. Then, the POFA was ground in Los Angeles abrasion machine (Figure D2) for 30,000 cycles to a mean particle size of 45 μm to improve reactivity. The XRF analysis was also done on POFA samples, which the results are presented in Table 3.1. Throughout the research study, the POFA was used to replace 20% of the binder for all mixtures.

Figure 3.1: Solid waste (POFA) from palm oil industry

3.2.3. Alkaline solution

A combined mix of NaOH in pellet form and Na_2SiO_3 solution was used as the alkaline activator. The Na_2SiO_3 solution (12% Na_2O and 30% SiO_2 by mass) was obtained from Vonjun Sdn Bhd and the NaOH pellets was acquired from Merck in bulk quantity. The solution was prepared at least 1 day prior to its use to allow the exothermically heated liquid to cool to ambient temperature.

The NaOH pellets were dissolved in water to produce a molarity of 14M. The mass of NaOH per kilogram (kg) of the solution was measured at 404 grams (g) was dissolved in 1 litre (L). The NaOH solution was then mixed together with Na_2SiO_3 and stirred well by using a glass rod to prepare the alkaline solution in a plastic beaker. The solution was stored in plastic container overnight. Throughout the research study, the ratios of the Na_2SiO_3 solution to NaOH solution and the alkaline solution to binder were kept at 2.5 and 0.55 by mass, respectively.

3.2.4. Water

Potable water, which is used to prepare the alkaline solution and mixing purposes. The provided water from the laboratory is ensured to be free from deleterious material and chemical contaminants. The water to binder ratio for foamed and non-foamed geopolymer concrete (OPSFGC and OPSNFGC) was kept at 0.1.

3.2.5. Superplasticizer

The SP, which was a polycarboxylate ether (PCE) based solution (Glenium Ace 388 RM), was used in all the concrete mixtures. The SP was supplied by BASF (Malaysia) Sdn Bhd. The use of the SP was to improve the workability and strength of the concrete by allowing a low water to binder ratio. The dosage of the SP was 1.5% by mass of binder for all the concrete mixtures.

3.2.6. Foaming agent

The synthetic foaming agent used was SikaAER-50/50, which was a high concentrated liquid foaming admixture for LWAC. The foaming agent was provided by Sika Kimia Sdn Bhd. The chemical base of SikaAER-50/50 was a blend of synthetic surfactants and polymer. The specific gravity of SikaAER-50/50 given by the company was 1.01. According to SikaAER-50/50 technical data sheet, the addition rate was recommended at 0.3–0.6% by weight of binder (0.15–0.18 L per 50 kg of binder). In order to produce a stable foam, the foaming agent was fed into the foaming generator (Figure 3.2) and the air pressure was stipulated at 75 psi or 517 kN/mm^2. The quantity of foam which was

added during the mixing of OPSFGC to achieve the target density was calculated based on the foam density.

Figure 3.2: Foaming generator and stable foam

3.2.7. Aggregates

The OPS obtained from a local crude palm oil producing mill were sieved and those retained at 9.5 mm were then crushed with a stone crushing machine. The crushed OPS of sizes between 2.36 and 9.5 mm was used as the coarse LWA in this study, as presented in Figure 3.5. The OPS were washed with detergent to remove thin oil layer on the surface and air-dried one day before the casting of geopolymer concrete to prepare saturated surface dry (SSD) condition of OPS.

Figure 3.3: Crushed OPS

Mining sand passing through 2.36 mm mesh size and retained at 300 μm sieve was used as fine aggregates for the OPSFGC. On the other hand, mining sand passing through 5 mm and retained on 300 μm was used as fine aggregate for OPSNFGC.

3.3. Mixture proportion

In this research study, there were two types of mixture where geopolymer concrete consisted of foamed and non-foamed specimens that incorporated with OPS as LWA, mining sand as fine aggregates, binder, alkaline solution, SP and water to achieve good workability. Another type of mixture is the geopolymer paste, which contain only the binder and alkaline solution. The following subsections of the chapter give the mixture proportions of both types of mixture.

3.3.1. Geopolymer paste

The material and mix proportion for POFA-FA geopolymer (PFG) paste is presented in Table 3.2. An allowance of about 15% of the mix proportion was provided.

Table 3.2: Mix proportion and quantities of materials for geopolymer paste

Materials proportion				
POFA/binder		=	0.20	
AK/binder		=	0.55	
12 cube specimens (50 mm)		=	0.0015 m^3	
Materials	Mass (kg)	Specific gravity	Density (kg/m^3)	Total mass (kg)
FA	80.00	2.10	996	1.49
POFA	20.00	2.78	249	0.37
AK	55.00	1.57	685	1.03

3.3.2. Foamed and non-foamed OPSGC

The material and mix proportion shown in Table 3.3 is for the OPSFGC of density 1300 kg/m^3, with an allowance of 15%. Similar material and mix proportions was used for the OPSFGC of target densities 1500 and 1700 kg/m^3 are be shown in appendix. The mix proportion for OPSNFGC was without foam, hence the target density is omitted.

Table 3.3: The materials and mix proportion for OPSFGC of target density 1300 kg/m^3

Materials and mix proportion for OPSGC/OPSFGC		
Target density (kg/m^3)	=	1300
Materials proportion		
POFA/FA	=	0.20
Sand/binder	=	1.70
Aggregate/binder	=	0.60
AK/binder	=	0.55
Water/binder	=	0.15
SP/binder	=	0.015

Table 3.3, continued

To prepare specimens of: 20 cubes (100 mm), 3 prisms (100 x 100 x 500 mm), 2 panels (300 x 300 x 50 mm), 2 cylinders (150 ϕ x 300 mm) and 6 cylinders (100 ϕ x 200 mm)			=	0.064 m^3
To prepare 1300 kg/m^3 of OPSFGC, Concrete required Foam required Mass of foam required			= = =	 0.042 m^3 0.022 m^3 2.03 kg
Materials	Mass (kg)	Specific gravity	Density (kg/m^3)	Total mass (kg)
FA	80.0	2.10	392	25.07
POFA	20.0	2.78	98	6.27
Sand	170.0	2.67	832	53.26
OPS	60.0	1.36	294	18.80
AK	55.0	1.57	269	4.70
Water	15.0	1.00	73	0.47
SP	1.5	1.20	7	17.23

3.4. Mixing, casting and curing

The OPS and mining sand were first mixed together in a rotary concrete mixer (Figure D4) for about 2 minutes; this was followed by the addition of binder (FA and POFA) with a further mixing of about 3 minutes. The alkaline solution, water and SP were then gradually added, and mixed for another 5 minutes. The measured mass of foam was then added to achieve the target density of OPSFGC. The fresh density of the OPSFGC was weighed and additional foam was added if target density is not attained due to the collapse and disintegrated of existing foam.

Next, the concrete was poured into the steel moulds and vibrated from a second to avoid the pre-formed foam to collapse. The specimens were protected with plastic layer to prevent evaporation of surface water. Whilst, the slump test was immediately conducted with a fraction of the fresh concrete. The specimens were then transferred to the curing chamber (Figure D5) and cured at a temperature of 65 ˚C for 48 hours before

being de-moulded and tested. The concrete specimens were cast in 100-mm cubes for the compressive test, which was carried out at the ages of 3-, 7-, 14- and 28-days; the same size specimens were used for the UPV and sorptivity tests. Specimens of 100 mm ϕ x 200 mm height cylinders were prepared for the splitting tensile strength and porosity. The tests on the flexural strength and the modulus of elasticity (MOE) were carried out on prism specimens of size 100 x 100 x 500 mm and on 150 ϕ x 300 mm cylinders, respectively. For thermal conductivity test, panels of size 300 x 300 x 55 mm were used.

For the preparation of geopolymer paste, the mixing process excluded inclusion of aggregates. Yet, the binder and alkaline activator were mixed together without any extra water with a stand-type mixer (Figure D6). The paste was then cast in 50-mm cube moulds and cured in oven at a temperature of 65 ˚C for 48 hours. Similar to the geopolymer concrete, moulds were removed from the oven after the curing period and were left to cool down at room temperature before de-moulding to be tested on strength for 3, 7, 14 and 28 days after casting as well as for microstructure analysis on 3 and 28 days after casting.

3.5. Testing procedures

3.5.1. Material properties

Investigation on material properties is essential to ensure that the quality on the properties of the research material so that they possess consistent quality, especially if there is any new batch of material being used. Moreover, the material properties is crucial upon the design of mix proportions, particularly the bulk density, water absorption and specific gravity. In this study, the grading of coarse and fine aggregates were determined using sieve analysis, in accordance to BS 812-103.1 (1985).

Bulk density of the coarse aggregates (OPS) was measured in accordance to BS EN 933-1 (1997). Equation (3.1) and (3.2) are used to calculate the bulk density of OPS of both loose and compacted condition of the material, accordingly.

For loose condition,

$$Bulk\ density\ (kg/m^3) = \frac{weight\ of\ loose\ OPS\ measure - weight\ of\ empty\ measure}{volume\ of\ cylindrical\ measure} \quad (3.1)$$

For compacted condition,

$$Bulk\ density\ (kg/m^3) = \frac{weight\ of\ compacted\ OPS\ measure - weight\ of\ empty\ measure}{volume\ of\ cylindrical\ measure} \quad (3.2)$$

Specific gravity (SG) and water absorption tests for OPS and mining sand were carried out according to ASTM C127 (2012) and ASTM C128 (2012), respectively. The calculations (3.3–3.6) for SG and water absorption of both OPS and mining sand in SSD condition are shown as follows.

For coarse aggregate (OPS),

$$SG_{S1} = \frac{B1}{B1 - C1} \quad (3.3)$$

$$Water\ absorption\ (\%) = \frac{B1 - A1}{A1} \quad (3.4)$$

where *A1* is the mass of OD OPS in air (g); *B1* is the mass of SSD OPS in air (g); and *C1* is the apparent mass of the saturated OPS in water (g).

For fine aggregate (mining sand),

$$SG_{S2} = \frac{S2}{B2+S2-C2} \tag{3.5}$$

$$Water\ absorption\ (\%) = (\frac{S2-A2}{A2}) \times 100 \tag{3.6}$$

where *A2* is the mass of OD mining sand (g); *B2* is the mass of pycnometer filled with water, to calibration mark (g); *C2* is the mass of pycnometer filled with mining sand and water to calibration mark (g); and *S2* is the mass of SSD mining sand (g).

3.5.2. Fresh state properties

The workability of fresh geopolymer concrete was determined using slump test in accordance to BS EN 12350-2 (2009). The crushed OPS was of sizes of 2.36 to 9.5 mm, hence was applicable for this method, which specified that coarse aggregate used should not be larger than 37.5 mm. During the test, sample of fresh geopolymer concrete was filled into the slump cone in three layers and each layer was tamped for 25 times with a stamping rod. The slump was measured immediately after the uplifting of cone (Figure 3.4). The slump values of OPSGC were classified in accordance to BS EN 206-1 (2000).

Figure 3.4: Slump measurement of fresh geopolymer concrete

Fresh density of concrete is an early indicator that decide the type of the hardened concrete (Mannan & Ganapathy, 2004). The measurement of the fresh density was in accordance with BS EN 12350-6 (2009). The fresh geopolymer concrete is filled and compacted into a 1L rigid container with known mass and the difference of the weight was recorded and calculated using equation (3.7) to determine its fresh density.

$$D = \frac{m_2 - m_1}{V} \tag{3.7}$$

where D is the density of the fresh specimen; m_1 is the mass of empty container; m_2 is the container completely filled with compacted fresh specimen; and V is the volume of the container.

In addition, the fresh densities of OPSGC were used to review the consistency and stability of the mixture prior to the target and oven-dry densities. Nambiar and Ramamurthy (2008) stated that without any segregation and bleeding, the stability of foamed concrete (FC) is the consistency where the density ratio is closer to unity. Equations (3.8) and (3.9) were used to determine the consistency and stability of FC.

Consistency = (Fresh density) / (Target density) (3.8)

Stability = (Fresh density) / (Hardened density) (3.9)

3.5.3. Mechanical properties

3.5.3.1. Compressive strength

The compressive strength test of both geopolymer paste and concrete were in accordance to the test procedures given in BS EN 12390-3 (2002). The sizes of cube specimens for geopolymer paste and concrete were 50 and 100 mm, respectively. For each series of paste and concrete, three cubes were tested for compressive strength at 3-, 7-, 14- and 28-days at the pace rate of 0.5 kN/s and 3 kN/s, correspondingly. All the compression tests were carried out using the ADR-Auto 2000 standard compression machine (Figure D7), which comply with the standard. The equation (3.10) was used to calculate the compressive strength.

$$f_c = F/A \tag{3.10}$$

where f_c is the compressive strength of the test specimen; F is the maximum load at failure; and A is the cross-sectional area of the test specimen.

3.5.3.2. Splitting tensile strength

Splitting tensile test is one of the indirect tests, which is used to determine the tensile strength of concrete. Similar testing machine (ADR-Auto 2000) was used and the test specimen was 28-day cylindrical concrete of 100 mm ϕ x 200 mm height (Figure D8), which comply to ASTM C496 (2011). The mean value was obtained from three cylindrical specimens for each series with the pace rate of 0.94 kN/s. The following equation (3.11) was used to calculate the splitting tensile strength.

$$f_t = 2P/\pi ld \quad (3.11)$$

where f_t is the splitting tensile strength of the test specimen; P is the maximum applied load indicated by the testing machine; l is the length of the test specimen; and d is the diameter of the test specimen.

3.5.3.3. Flexural strength

The flexural test method, which is in accordance to ASTM C78 (2010) was adopted to determine the flexural strength of the 28-day prism specimen of size 100 x 100 x 500 mm. Three prism specimens were tested for each series with ADR-Auto EL37-6135 standard flexural machine (Figure D9) at a pace of 0.2 kN/s. Equation (3.12) was then used to calculate the splitting tensile strength.

$$f_r = Pl/bd^2 \quad (3.12)$$

where f_r is the flexural strength of the test specimen; P is the maximum load indicated by the testing machine; l is the span length; b is the average width of the test specimen; and d is the average depth of the test specimen.

3.5.3.4. Modulus of elasticity

The MOE test that comply with ASTM C469 (2010) provides the stress to strain ratio that describe the stiffness of concrete. The test specimen used were of 150 ϕ x 300 mm cylinders. The test set up using ADR-Auto 2000 as given in Figure D10, was adopted with a pace of 5.3 kN/s is as shown in Figure D11. The equation (3.13) was used to determine the MOE.

$$E_s = \Delta\sigma/\Delta\varepsilon \quad (3.13)$$

where E_s is the static MOE of the test specimen; $\Delta\sigma$ is the difference in stresses; and $\Delta\varepsilon$ is the difference in strains.

3.5.4. Transport properties

3.5.4.1. Ultrasonic pulse velocity

The UPV test was carried out to check the uniformity of concrete by measuring the travelling time for pulse between the ends of specimens (Figure D11). The test was in accordance with ASTM C597 (2009) using a portable ultrasonic non-destructive digital indicating tester (PUNDIT) at the ages of 3-, 7-, 14- and 28-days on 100-mm cube specimens. The data obtained from the UPV test can establish the quality of the concrete, where the data can be calculated from the equation (3.14) below.

$$V = L/T \quad (3.14)$$

where V is the pulse velocity; L is the distance between centres of the transducer faces; and T is the transit time.

3.5.4.2. Porosity test

The porosity test was done using disc specimens of size 100 ϕ x 50 mm at the age of 28 days for the geopolymer concrete, which the 100 ϕ x 200 mm cylinder was cut into four disc specimens. The test was carried out to predict the durability and serviceability of concrete. The vacuum saturation technique (Figure D12) was applied for this test, which is based on ASTM C1202 (2012), and has been proven to be the most efficient (Safiuddin

& Hearn, 2005). The specimens were oven-dried for 48 hours at 105 ± 5˚C before testing in order to achieve constant weight. The equation (3.15) below was used to determine the porosity of the geopolymer concrete.

$$Permeable\ porosity\ (\%) = \frac{W_s - W_d}{W_s - W_b} \times 100 \quad (3.15)$$

where W_s is the SSD mass of the test specimen in air (g); W_d is the OD mass of the test specimen in air (g); and W_b is the buoyant mass of the saturated specimen in water (g).

3.5.4.3. Sorptivity test

The sorptivity test was carried out to measure the rate of water absorption. The test specimens (100-mm cube) were cured for 28 days before being oven-dried at 105 ± 5 ˚C for 48 hours until a constant weight was achieved. Then the specimen was lightly greased and covered with cling film on its sides and placed in a container to absorb water vertically from its base (Figure 3.5). The weight of the specimen was observed at intervals of time of 1, 4, 9, 16, 25, 36, 49 and 64 minutes. The sorptivity of specimen was then calculated using the equation (3.16).

$$i = A + St^{1/2} \quad (3.16)$$

where i is the cumulative volume of water absorbed at time t (mm^3/mm^2); A is the surface area of the test specimen (mm^2); S is the sorptivity coefficient ($mm/min^{1/2}$); and t = recorded time (min).

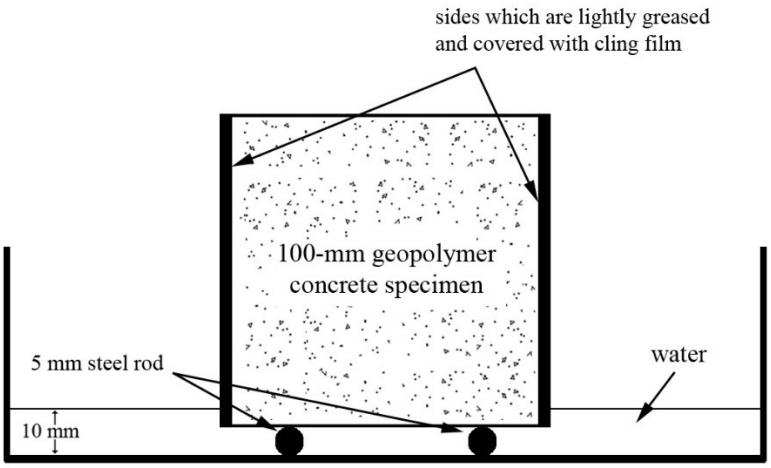

Figure 3.5: Test set-up for the sorptivity test of geopolymer concrete

3.5.4.4. Water absorption test

The water absorption test was carried out to measure the water permeable pores. Similar to the porosity test, the test specimens are of size 100 ϕ x 50 mm. The test was performed with 28-day OPSGC specimen, in accordance with ASTM C642 (2013). The specimen was first oven-dried at 105 ± 5 ˚C for 48 hours to remove any moisture content. After that, the weight of the specimen was measured soon after immersion in water for 30 minutes. The water absorption was calculated using equation (3.17).

$$Water\ absorption\ (\%) = \frac{W_s - W_d}{W_d} \times 100 \qquad (3.17)$$

where W_s is the SSD mass of the test specimen in air after immersion (g); W_d is the OD mass of the test specimen in air (g)

3.5.5. Thermal conductivity

The thermal conductivity test was performed to measure the quantity of heat transmitted through the concrete. The specimens were tested at the age of 28 days, in accordance with BS EN 12664 (2001). The panels were oven-dried for 24 hours at a temperature of 105 ± 5 ˚C to remove any moisture present. Besides that, the rough surface of the panel was cut and grind into smooth surface to avoid any gap formation between the plates (hot or cold) and the surface panel. Type-T thermocouples (copper – constantan) were used to measure the temperatures. Figure D13 showed the model of the current transformer and multiplexer used in thermal conductivity equipment are CS10-L and Campbell Scientific AM25T, respectively.

Figures 3.6 and 3.7 show the testing arrangement and schematic diagram of the apparatus. The panel was placed between a hot and cold plate with a temperature of 40 ˚C and 18 ˚C, respectively to stimulate the exterior and interior temperature. Then, it was stacked with foam insulation sheets and covered as shown in Figure 3.7 so that the heat could be transmitted through the specimen vertically instead of dispersing to the side.

The temperatures on the hot and the cold plates were recorded every 10 minutes for 24 hours and the data recorded. The data was collected via Campbell Scientific CR800 data logger and analysed with the LoggerNet program. The mean values of the recorded temperatures were used in the calculation of the thermal conductivity. The thermal conductivity of the concrete specimen was calculated using Fourier's law as given below in equation (3.18). For a comparison purposes, the clay brick was obtained from the Claybricks and Tiles Sdn Bhd, which is in accordance with BS EN 771-1 (2011); whereas, the concrete block was acquired from Rawang Concrete Factory.

$$k = (\Phi \times t_k) / (A \times \Delta T) \quad (3.18)$$

where k is the thermal conductivity; Φ is the heat flow; t_k is the thickness of the test specimen; A is the area of specimen; and ΔT is the temperature difference between hot and cold plates.

Figure 3.6: Thermal conductivity test equipment

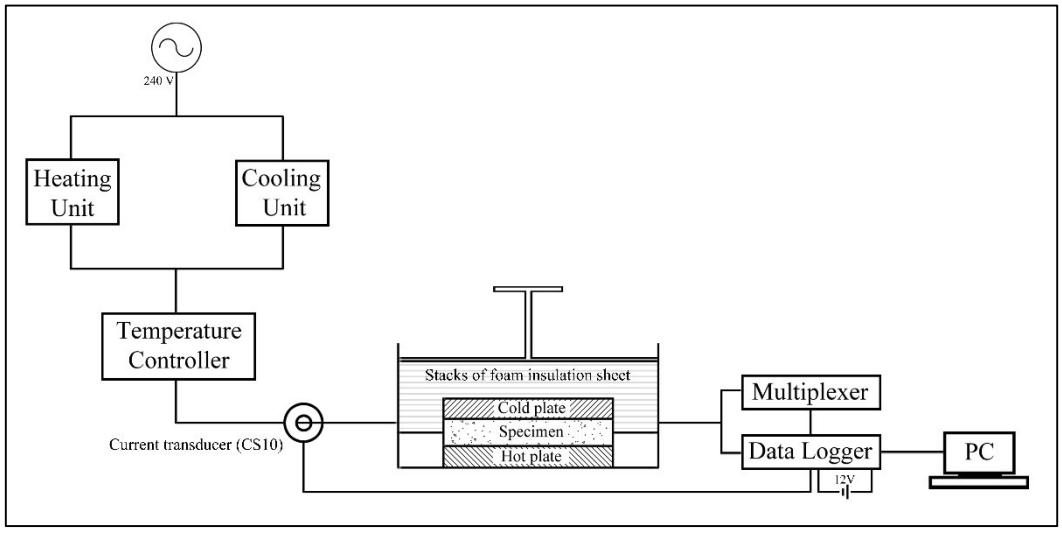

Figure 3.7: The schematic diagram of the thermal conductivity test

3.5.6. Microstructure behaviour

The OPSFGC with densities of 1300 and 1500 kg/m^3 and OPSNFGC were characterized by the FESEM and EDX analysis whereas the PFG paste specimens were characterized by the XRD and FTIR analysis. Both types of specimens were tested at the concrete age of 3 and 28 days to analyse the change in microstructure with development of strength over the curing period.

3.5.6.1. FESEM/EDX analysis

The microstructure study on concrete samples through FESEM/EDX was performed using the Quanta FEG 450 and EDX system from Oxford (Figure D14). The analysis was done in low vacuum mode at an accelerating voltage of 5 kV for FESEM and 10 kV for EDX. This FESEM analysis was performed for all OPSGC specimens at the age of 3 days and 28 days, to characterize their structures such as porosity, cracks and interfacial transition zone (ITZ) while the EDX analysis is performed to investigate their compositions. The sample for investigation was obtained by crushing the OPSGC into smaller pieces and followed by placing it on stub with a carbon tape for further analysis as shown in Figure D15.

3.5.6.2. XRD analysis

The XRD analysis was performed by using the PANalytical Empyrean diffractometer (Figure D16) with a Cu-Kα radiation (45 kV, 30 mA). This test was done to characterize the crystallinity of the 3- and 28-days PFG paste specimens. The PFG paste specimens were crushed and ground into powder form with steel ball grinding machine (Figure D17),

and sieved through a 45 μm mesh. The powder sample was then mounted on a specimen holder as shown in Figure D18. Geopolymer paste was used instead of geopolymer concrete in order to minimize the disruption by aggregate particles on the validity of geopolymer framework analysis (Kusbiantoro et al., 2012). XRD analysis was performed with scanning in a 2θ range from 5˚ to 65˚ at a step size of 0.026˚ and 150 seconds/step.

3.5.6.3. FTIR analysis

Similar to the XRD analysis, the powder from PFG paste specimens was subjected to FTIR analysis. The FTIR spectra was recorded with the Perkin Elmer Spectrum 400 spectrometer in mid-IR mode (Figure D19). Before starting the analysis, rubbing alcohol was used to clean the sample platform. Without any preparations, approximately 5 milligram (mg) of the powder specimen was decanted onto the platform for further analysis. The spectrum was obtained over a range between 4000 to 400 cm^{-1}.

3.6. Summary of tests and analyses

The details of all types of test specimens, which are tested and analysed using different methods were summarized in Table 3.4. Also, the purposes of the tests and analyses were included as well.

Table 3.4 Summary of tests and analyses

Tests and analysis	Purposes	Types of test specimens
Compressive strength test	- to test compressive strength	Cubes (100 mm)
Ultrasonic pulse velocity	- to check the uniformity of concrete	
Sorptivity test	- to measure the rate of water absorption	

Table 3.4, continued

Tests and analysis	Purposes	Types of test specimens
Splitting tensile strength test	- to test the splitting tensile strength	Cylinders (100 ϕ x 200 mm)
Porosity test	- to predict the durability and serviceability of concrete	Cylinders disc (100 ϕ x 50 mm)
Water absorption test	- to measure the water permeable pores	
Modulus of elasticity test	- to determine the stiffness of concrete	Cylinders disc (150 ϕ x 300 mm)
Thermal conductivity	- to measure the quantity of heat transmitted through the concrete	Panels (300 x 300 x 50 mm)
FESEM/EDX analysis	- to characterize the concrete structures	Crushed pieces of about 5 mm
XRD analysis	- to characterize the crystallinity of paste specimens	Fine powder form of paste specimen (sieved through 45 μm)
FTIR analysis	- to determine precise material composition	

CHAPTER FOUR

RESULTS AND DISCUSSION

4.1. Introduction

This chapter presents and discusses the experimental results pertaining to the material properties of the constituent materials; density, mechanical, transport and functional properties of OPSGC; and the morphology and mineralogy of the OPSGC and PFG paste. The investigated properties include compressive strength, splitting tensile strength, flexural strength, MOE, UPV, sorptivity, porosity and thermal conductivity. Three OPSFGC mixtures with densities of 1300, 1500 and 1700 kg/m^3 were prepared using an artificial foaming agent; a control mix without foam and conventional materials – block and brick – were used for comparison of the thermal conductivity.

The interpretation and correlations of the results were established in the form of figures, graphs and tables whereas the given micrographs showed the microstructure of the OPSGC. The calculations and additional data are shown in Appendix. The experimental results are summarised into six different groups as outlined below:

i. Material properties of OPS and mining sand
ii. Fresh state properties of OPSGC
iii. Mechanical properties of OPSGC
iv. Transport properties of OPSGC
v. Thermal conductivity of OPSGC and conventional materials, and
vi. Microstructure behaviour of OPSGC and PFG paste

4.2. Material properties

4.2.1. Oil palm shell

The thickness of the OPS as LWA in this research varies from 1.5 to 2.5 mm. The OPS were crushed and exhibited irregular shapes. The surface texture of OPS was smooth for both curved and rounded faces (Figure 3.3). Properties of OPS such as specific gravity, water absorption and bulk density are shown in Table 4.1.

Table 4.1: Physical properties of OPS

Physical property	OPS
Specific gravity (oven-dry)	1.09
Specific gravity (SSD)	1.36
Apparent specific gravity	1.49
Bulk density (loose) (kg/m^3)	589
Bulk density (compacted) (kg/m^3)	652
Fineness modulus	5.79
Water absorption (24 h) (%)	24.39

Unlike the normal aggregate, OPS exhibited higher water absorption, which was attributed to the large number of pores available inside the LWA. From Figure 4.1, the grading of the crushed OPS was within the range of 2.36 to 9.5 mm, which is suggested by Shafigh et al. (2011a) to improve the workability and compressive strength. The quantity of OPS retained on smaller than 4.75 mm sieve did not exceed 7 kg/m^2, which conform with the ASTM C136 (2001).

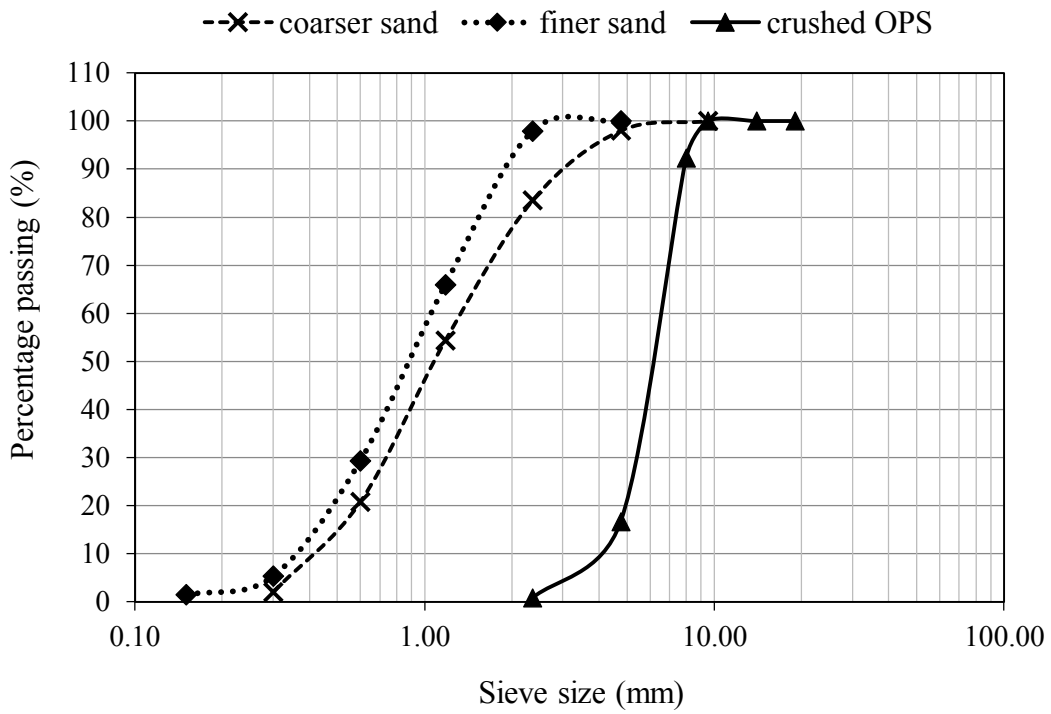

Figure 4.1: The grading of OPS, coarser and finer mining sand

4.2.2. Mining sand

As mentioned in the earlier chapter, the coarser (0.3 to 5 mm) mining sand was used for the manufacture of OPSNFGC whereas the finer (0.3 to 2.36 mm) mining sand was used for the production of the OPSFGC, which the grading of both types of mining sand were presented in Figure 4.1. The specific gravity of the mining sand used in this research study is 2.67. The fineness modulus of the coarser and finer mining sands are 2.6 and 2, respectively.

4.2.3. Fly ash and palm oil fuel ash

The binders used for the manufacture of OPSGC consist of class-F FA and POFA. Conforming to the ASTM C618 (2012), both FA and POFA showed similar chemical characteristics as suggested by results in Table 4.2. The percentages of SO_3 and LOI of

both binders are lower than 4% and 10%, correspondingly. Moreover, the summation percentage of SiO_2, Al_2O_3 and Fe_2O_3 for both binders are more than 70%. Hence, both binders can be classified as Class F pozzolanic material.

Table 4.2: Chemical composition (%) of FA and POFA conforming to ASTM C618 (2012)

	SiO_2	Al_2O_3	Fe_2O_3	CaO	MgO	K_2O	SO_3	LOI
Class-F FA	57.6	28.9	5.8	0.2	0.9	0.9	0.2	3.6
POFA	63.4	5.5	4.2	4.3	3.7	6.3	0.9	6.0
ASTM C618 (2012)	-	-	-	-	-	-	≤ 4.0	≤ 10.0

4.3. Fresh state properties

The workability of the OPSGC was determined by using the slump test, in accordance with BS EN 12350-2 (2009). The slump was immediately measured from the difference between the upper slump cone and the uppermost surface of the fresh OPSGC. Table 4.3 presents the experimental results of the slump test.

Table 4.3: Densities and slump value of fresh OPSGC

Specimen	Target density	Fresh density	28-day ODD	Slump (mm)	Foam volume (%)	Consistency (fresh/target)	Stability (fresh/ODD)
	(kg/m^3)						
OPSFGC13	1300	1404	1291	250	33.8	1.08	1.08
OPSFGC15	1500	1564	1467	240	23.7	1.04	1.07
OPSFGC17	1700	1822	1721	200	13.5	1.07	1.06
OPSNFGC	-	1968	1791	130	-	-	-

Based on the BS EN 206-1 (2000), the OPSNFGC and OPSFGC17 could be classified as S4; whereas OPSFGC13 and OPSFGC15 could be classified as S5. All the experimental slump values were in the permitted range of 5 to 260 mm. The slump values indicated that all the OPSGC specimens exhibited high workability. When the foam was

added, the viscosity of the geopolymer concrete tends to decrease, which increased the workability. Moreover, the addition of foam could lessens the friction between aggregates, thus increasing the workability (Chia & Zhang, 2007). The use of OPS as LWA also contributed to the workability due to smooth surface of the LWA (Basri et al., 1999).

From Table 4.3, the consistency and stability showed results close to unity, indicating the production of consistent, stable and workable foamed concrete (FC) mixture. A theoretical equation to determine the fresh density of FC may not be applicable attributed to the factors such as destroyed of foam during mixing and extended of foam expansion after discharged (Regan & Arasteh, 1990). The difference of the fresh and oven-dry densities of the OPSFGC were ranged from 97 to 113 kg/m^3, which is within the range (100–200 kg/m^3) suggested by Clarke (2002).

4.4. Hardened state properties

4.4.1. Density

The ODD for the development of OPSFGC and OPSNFGC over curing period, ranged from 1291–1794 kg/m^3 as summarized in Table 4.4. The difference between the target and actual densities was within the range of ± 35 kg/m^3, which was well within the range of ± 50 kg/m^3 stipulated for FC. Moreover, the ODD of the OPSFGC and OPSNFGC exhibited the density of LWC in accordance with BS EN 206-1 (2000). The pores introduced in the concrete due to the addition of foam played an important role in the density reduction. It has been reported that the foam volume governs the strength instead of the material properties when the concrete density is at lower range (Nambiar & Ramamurthy, 2006). Figure 4.2 shows that the ODD of geopolymer concrete has a linear relationship with both the compressive strength and the UPV.

In addition, as a porous aggregate, OPS exhibited a voluminous of micro pores which varied in sizes between 16 and 24 μm that could entrap air (Kupaei et al., 2013). It is understood from Table 4.4 that the maximum density difference between the OPSFGC17 and OPSNFGC was only about 70 kg/m^3, which might be attributed to the low quantity of foam added in the former. In addition, it can be observed from Table 4.4 that the ODD of 3-, 7-, 14- and 28-day specimens showed consistency. The stability of the foam also played an important role in maintaining the density as some of the foam might be destroyed during the mixing process.

Table 4.4: ODD and compressive strength of OPSFGC and OPSNFGC

Specimen	Target density (kg/m^3)	Age (days)	ODD (kg/m^3)	Compressive strength (MPa)	Strength/density ratio (N/mm^2 kg/m^3) x 1000
OPSFGC13	1300	3	1331	7.3 (0.2)	5.5
		7	1309	7.8 (0.6)	6.0
		14	1327	8.1 (0.9)	6.1
		28	1291	8.3 (0.7)	6.4
OPSFGC15	1500	3	1469	9.8 (1.2)	6.7
		7	1466	11.5 (0.9)	7.8
		14	1465	12.9 (0.6)	8.8
		28	1467	13.5 (1.1)	9.2
OPSFGC17	1700	3	1730	23.5 (1.3)	13.6
		7	1735	24.7 (0.6)	14.2
		14	1723	24.9 (1.8)	14.4
		28	1721	25.8 (0.5)	15.0
OPSNFGC	-	3	1762	22.4 (1.7)	13.4
		7	1783	25.7 (0.8)	14.4
		14	1794	25.8 (1.5)	14.4
		28	1791	30.1 (1.30)	16.8

Note: The standard deviations (in MPa) of the corresponding compressive strengths are shown in the brackets.

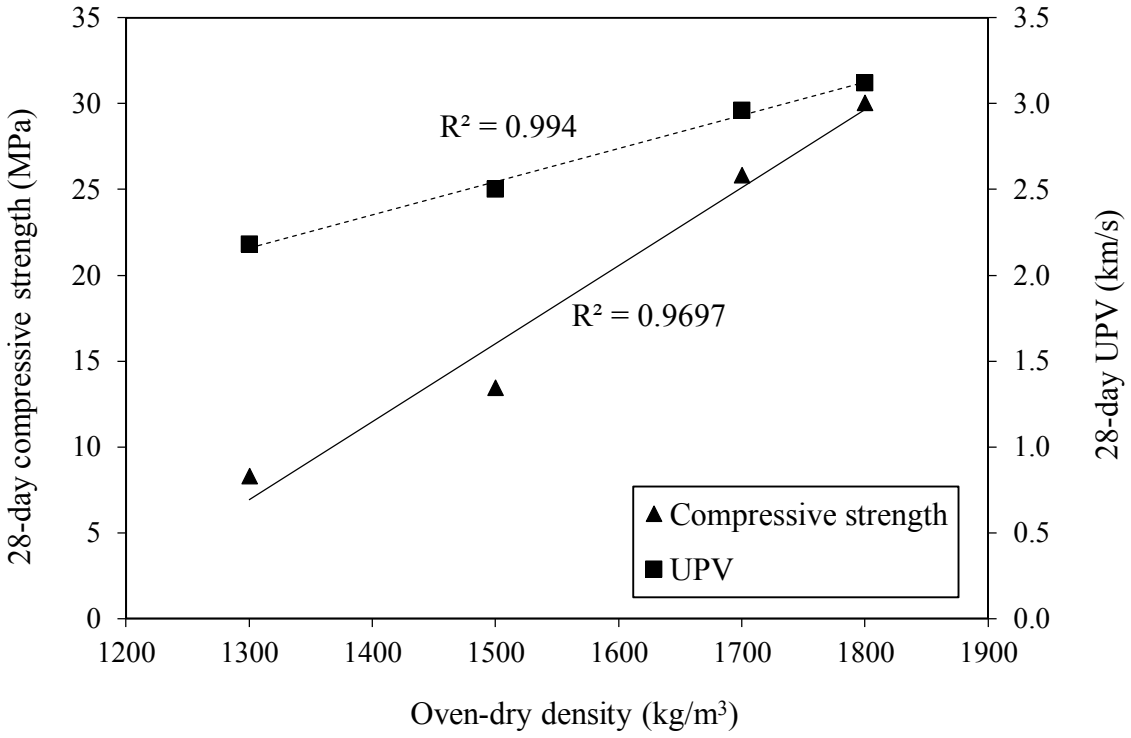

Figure 4.2: Relationship between the compressive strength, ODD and UPV

4.4.2. Ultrasonic pulse velocity

A common technique, the UPV test was employed for analysing the consistency and relative quality of concrete to indicate the existence of defects such as voids and cracks and to assess the cracks' depth (Yap et al., 2013). The measured 3-, 7-, 14- and 28-day UPV values for all geopolymer concrete specimens are presented in Figure 4.3. It is observed that the UPV values of OPSFGC increased with the increase of density as well as the age of the geopolymer concrete. The presence of voids has been recognized to have an influence on the UPV transmission (Neville, 1997). The earlier research done by Karakurt et al. (2010) showed that the increase of UPV values indicates a more compacted form of the concrete. As suggested by Browne et al. (1983), both the OPSFGC17 and OPSNFGC are considered as fair quality concrete as the UPV values fall between 3 and 4 km/s.

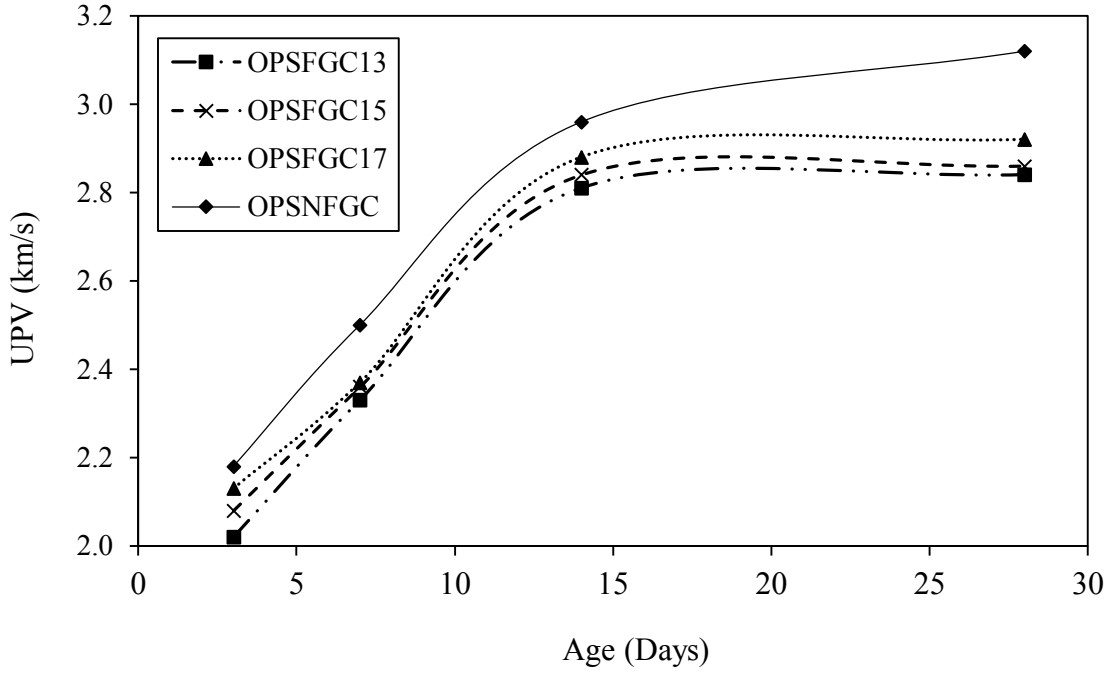

Figure 4.3: Ultrasonic pulse velocity (UPV) of OPSFGC and OPSNFGC

4.4.3. Compressive strength

Figure 4.4 shows the development of the compressive strength for the geopolymer concrete specimens. As known, the increase in the compressive strength over the period of 28 days is not high. In contrast to the well-established strength development of OPC concrete in which the hydration process takes place over a period of time along with strength gain, the geopolymer concrete does not gain strength exponentially over time (Hardjito et al., 2004). The geopolymerization depends on the aluminosilicate contents in the source material, molarity and type of alkaline activator, curing condition and period as well as the ratio of solution to binder among others. Xu and van Deventer (2000) reported that silicon (Si) and aluminium (Al) appeared to be synchro-dissolving from the surface of the materials and yet, there is a higher extent of dissolution in concentrated NaOH alkaline solution.

The compressive strength of OPSFGC and OPSNFGC specimens achieved high early strength due to the polymerization process that takes place during the first 48 hours of heat curing; as expected, the rate of strength gain decreased after 7-day and the strength gain between 7 and 28 days was about 11.3%. This denotes that the elevated curing temperature has accelerated the rate of geopolymerization at early stage, which agreed by Swanepoel and Strydom (2002).

It is evident from Figures 4.2 and 4.4 that the compressive strength is proportional to the density of the specimens, which is in agreement with the earlier findings reported by Alengaram et al. (2013) for FC. The OPSFGC13 appeared as weakest amongst the OPSFGC with 28-day compressive strength of 8.3 MPa compared to 25.8 MPa for OPSFGC17. The non-foamed concrete, OPSNFGC presented as highest 28-day compressive strength of around 30 MPa. The inclusion of different foam contents in the OPSFGC specimens produced tiny air-voids that lead to a lower strength in foamed specimens compared to the non-foamed specimen. At a higher volume of foam, the inclusion of bubbles seemed to produce larger voids that result in widespread of void size and lower mechanical strength (Nambiar & Ramamurthy, 2007a).

Alengaram et al. (2013) described that the OPSC and oil palm shell foamed concrete (OPSFC) achieved the 28-day compressive strength of 28 MPa and 20.2 MPa, respectively. In this investigation, the OPSFGC with an ODD of 1700 kg/m^3 was able to achieve about 26 MPa at the age of 3 days. Thus, with its ability to achieve as high as 90% of its 28-day compressive strength in 3 days, OPSFGC could be considered for the development of precast lightweight concrete. Moreover, by replacing highly siliceous POFA as binder in the geopolymer concrete, the polymerization of the aluminosilicates might be attributed to the high compressive strength in the OPSFGC and OPSNFGC. The

effect of POFA in conventional concrete has shown that 20% of cement replacement produced higher 90-day compressive strength compared to conventional concrete (Chindaprasirt et al., 2007).

The OPSFGC17 with an ODD of 1700 kg/m^3 is categorized as structural grade concrete. Another important factor is the strength to density ratio of the OPSFGC. The OPSFGC17 gives a strength to density ratio of 17, which is about 54% higher than the corresponding NWC (Newman, 1993). The density reduction of about 29% of OPSFGC17 compared to NWC is advantageous, as the structural elements with OPSFGC would reduce the overall cost of the structure. Both the OPSFGC17 and OPSNFGC achieved a 28-day compressive strength of about 26 MPa and 30 MPa, respectively, and hence could be categorized as lightweight structural concrete in accordance with ACI 213R (2003).

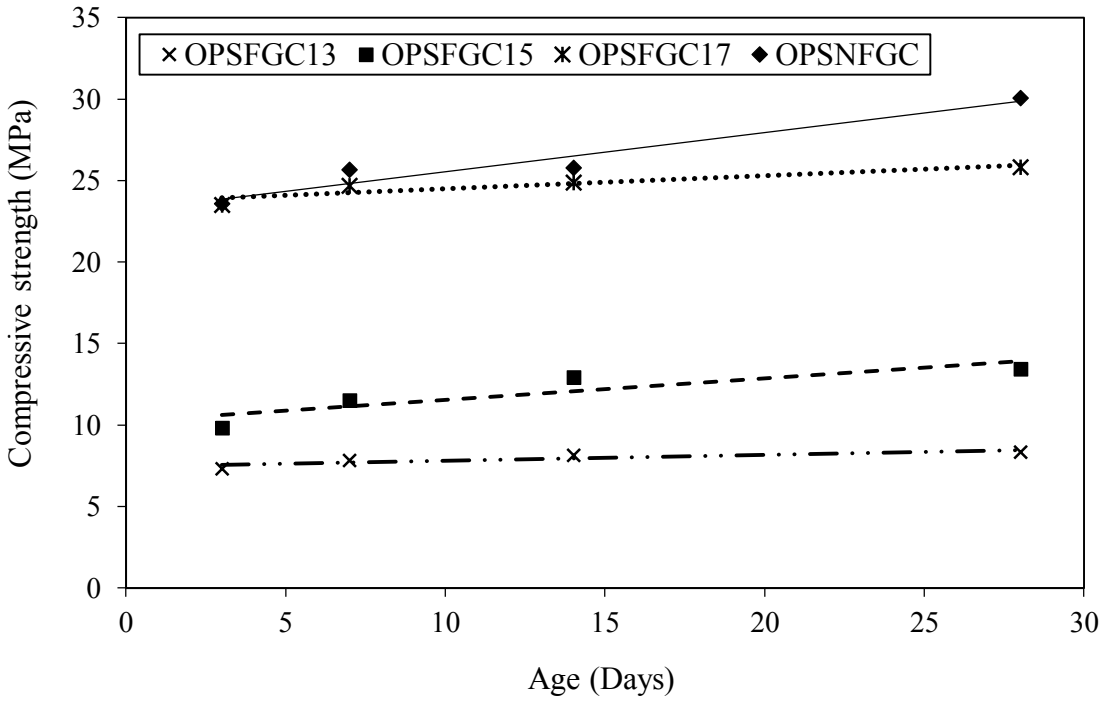

Figure 4.4: Development of compressive strength of OPSFGC and OPSNFGC

4.4.4. Splitting tensile and flexural strengths

The results for the mechanical properties of geopolymer concrete specimens are presented in Table 4.5. Jumaat et al. (2009) revealed that the OPSFC with a density range of 1653 to 1683 kg/m^3 exhibited 28-day splitting tensile strength of 1.46 to 1.68 MPa. However, it can be comprehended from the results for the splitting tensile strength in Table 4.5 that the OPSFGC17 produced a higher 28-day splitting tensile strength of 1.79 MPa compared to the OPSFC of similar density, this might be attributed to the geopolymerization of OPSFGC. Nambiar and Ramamurthy (2007a) reported that the incorporation of FA benefits the concrete strength by layering each bubble to prevent merging bubbles and allowed uniform distribution of air-voids. Furthermore, it can be seen from Table 4.5 that as the density decreased, there was a slight decrease in the tensile strength and MOE, which might be attributed to the amount of pore volume in the OPSFGC. The ratio of the 28-day splitting tensile strength to the corresponding compressive strength of the OPSFGC was about 7.2%; this is comparable to the OPS concrete (6.7 – 8.1 %) reported by Shafigh et al. (2012). Furthermore, the equation (4.1) proposed by Shafigh et al. (2010) to estimate the splitting tensile strength can be used to predict the strength of OPSFGC as it gives close results.

$$f_t = 0.20\sqrt[3]{f_{cu}{}^2} \tag{4.1}$$

where f_t is the 28-day splitting tensile strength (MPa) and f_{cu} is the 28-day compressive strength (MPa).

Table 4.5: Mechanical properties (as of 28-day)

Specimen	Compressive strength	Splitting tensile strength	Flexural strength	Modulus of elasticity (x10^3)
	(MPa)			
OPSFGC13	8.32	0.62	1.48	3.53
OPSFGC15	13.46	0.99	2.16	4.67
OPSFGC17	25.83	1.79	3.23	6.13
OPSNFGC	30.06	2.41	3.74	7.44

Jumaat et al. (2009) showed that the flexural strength of OPSFC varies between 1.76 and 2.15 MPa with a density of about 1700 kg/m^3; however, OPSFGC17 exhibited a higher flexural strength of 50% compared to the OPSFC of similar density. The ratio of 28-day flexural strength of OPSGC to its compressive strength varied between 0.12 and 0.18. Similar to the results in Table 4.5, Yang et al. (2000) stated that for air-entrained concrete, although the flexural strength is reduced with the increase in the air content, this reduction is very low compared to the compressive strength of the concrete. Also, foam concrete with narrower air-void distributions showed higher strength (Nambiar & Ramamurthy, 2007a). The equation (4.2) proposed for OPSC (Shafigh et al., 2010) was found to predict the flexural strength close to the experimental results of the OPSFGC.

$$f_r = 0.58\sqrt{f_{cu}} \tag{4.2}$$

where f_r is the 28-day flexural strength (MPa) and f_{cu} is the 28-day compressive strength (MPa).

4.4.5. Modulus of elasticity

Jones and McCarthy (2005) reported that the MOE of FC is significantly lower than that of NWC and lightweight concrete, typically varying from 1–8 GPa, for dry densities varying between 500 and 1500 kg/m^3, respectively. The results shown in this investigation (Table 4.5) were within the range of 4–5 GPa for similar densities. The pore volume and MOE have a linear relationship, as the increase in the density of the geopolymer concrete enhances the MOE. Besides that, the use of OPS as LWA could contribute to lower MOE due to the stiffness of OPS and the bond between the OPS and the cement matrix (Alengaram et al., 2011b). Due to the low MOE value in OPSC, Teo et al. (2006) suggested that higher load bearing and larger cross section of OPSC beams are required to satisfy the deflection criterion.

4.4.6. Porosity

The relationship between the porosity and the ODD of the specimen at the age of 28-day is shown in Figure 4.5. It can be seen that porosity was mainly influenced by the ODD, which in turn was attributed to the pore volumes. For OPSFGC, the porosity varied between 25% and 40%for densities in the range of 1300–1700 kg/m^3. In addition, the test results shown in Figure 4.5 are consistent with the compressive strength shown in Figure 4.4, where the compressive strength has a linear relationship with the ODD. The strength of concrete is affected by the volume of its overall voids (Neville, 1997). Kearsley and Wainwright (2002) reported that the porosity is largely dependent on dry density and not on the ash type or ash content. They reported a porosity of 40% for FC mixture with a density and ash/cement ratio of 1500 kg/m^3 and 3, which is comparable with the porosity of 34% for the OPSFGC with an ODD of 1500 kg/m^3. In addition, the size, distribution

and tortuosity of pores, the type and distribution of aggregates, and the nature and the thickness of interfacial transition zone also have considerable effects on the permeable porosity of concrete (McCarter et al., 1992).

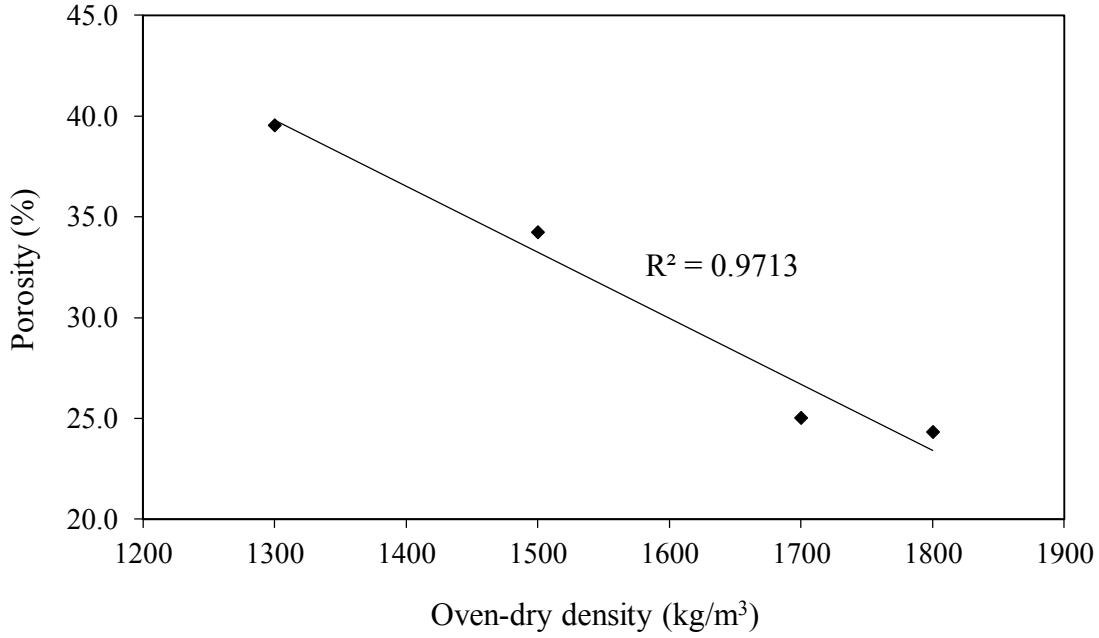

Figure 4.5: Porosity as a function of ODD of OPSFGC and OPSNFGC

4.4.7. Sorptivity

Figure 4.6 shows the result of the sorptivity for the OPSFGC and OPSNFGC specimens and it can be seen from the figure that the correlation coefficients (R^2) exceed 0.97 for all the sorptivity data. An increase in the sorptivity was observed as the density of geopolymer concrete specimens increased, particularly at a density of 1300 kg/m^3 with a sorptivity of 0.208 mm/min$^{1/2}$. The sorptivity for OPSFGC15, OPSFGC17 and OPSNFGC were 0.142, 0.111 and 0.109 mm/min$^{1/2}$, respectively. Hence, the sorptivity increased with an increase in foam volume for OPSFGC; this was similar to the findings reported by Panesar (2013) . A higher volume of foam may induce more pores and pores connectivity that result in higher sorptivity. It can be observed from Figures 4.4 and 4.6,

as the sorptivity of geopolymer concrete increases, the compressive strength decreases. Tasdemir (2003) reported similar findings as the capillary sorptivity coefficient of concrete decreased with the increase in the compressive strength. Further, Polat et al. (2010) showed a strong correlation between the inverse proportion of the sorptivity and the density of the concrete.

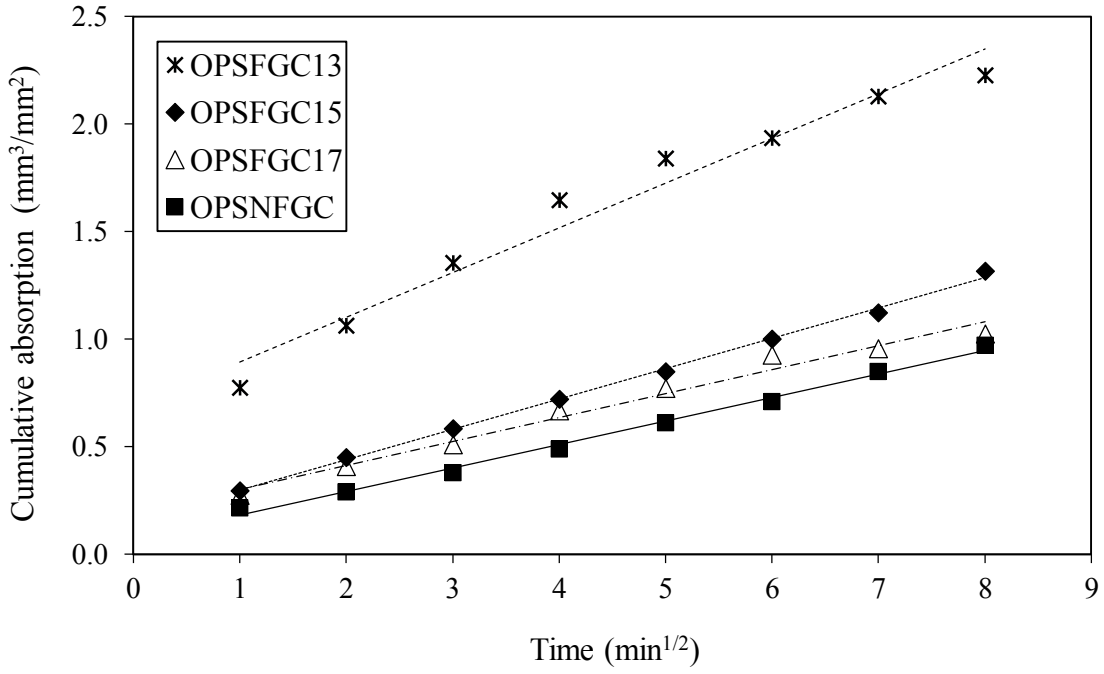

Figure 4.6: Sorptivity of geopolymer concrete specimens at 28 days

4.4.8. Water absorption

According to CEB-FIP (1989), the water absorption values for concrete that are less than 3%, in between 3 to 5% and more than 5% can be categorized as good, average and poor, correspondingly. From Figure 4.7, it is seen that the addition of foam increased the water absorption of OPSGC. It is also observed that the water absorption of OPSFGC was further increased with the increase of foam volume, which agreed with Nambiar and Ramamurthy (2007b) that the water absorption increases with the reduction in density of

FC. Moreover, Lamond and Pielert (2006) mentioned that FC has higher water absorption when compared with the NWC due to its lower density. They also reasoned that the interconnected cell structure of the FC resulted formation of channels for high water absorption. Come to an agreement with the UPV results, the water absorption of OPSFGC17 and OPSNFGC could also be categorized as 'average' quality of concrete by CEB-FIP (1989).

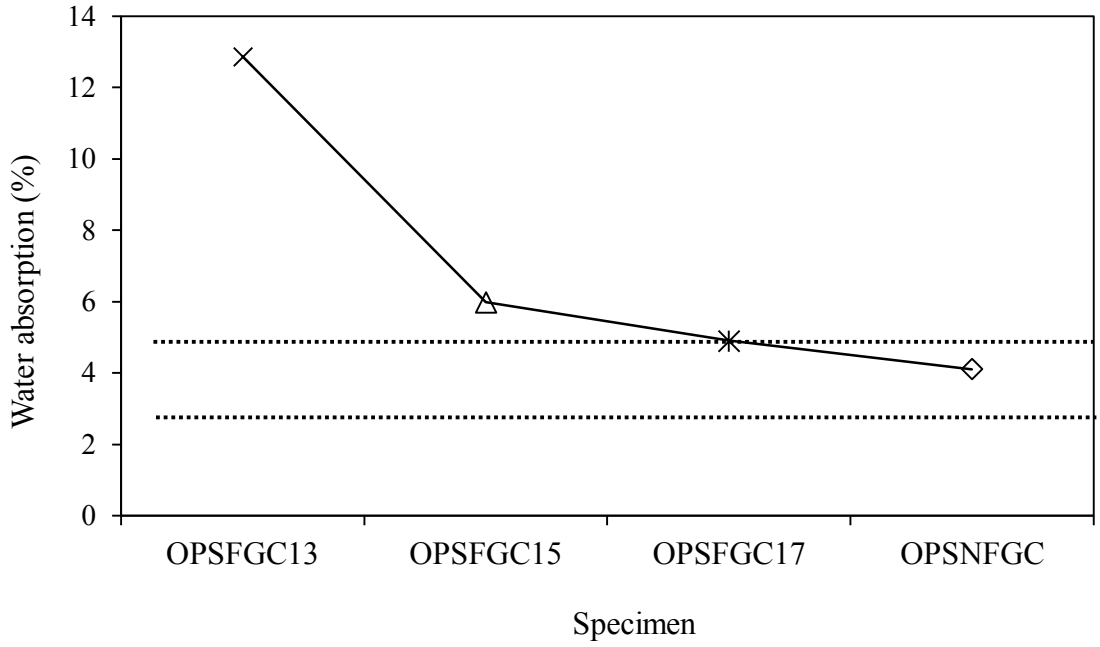

Figure 4.7: Water absorption of the 28-day OPSGC specimen

4.4.9. Thermal conductivity

The thermal conductivity of a material is the quantity of heat transmitted through a unit thickness in a direction perpendicular to a surface of unit area, due to a unit temperature gradient under given conditions (Sengul et al., 2011). The thermal conductivity of the four specimens of OPSFGC and OPSNFGC was compared with the conventional materials – block and brick. As seen from Figure 4.8, the OPSFGC and OPSNFGC exhibited lower thermal conductivity compared to the conventional materials, block and

brick. As for OPSGC, its lower density resulted in lower conductivity, which is comparable to the results reported by other researchers (Ng & Low, 2010; Saygılı & Baykal, 2011; Sengul et al., 2011).

The results proved that the OPSFGC and OPSNFGC is superior in thermal resistivity compared to the conventional materials used such as block and brick. The reduction in the conductivity was about 22%, 17%, 10% and 3% for OPSFGC13, OPSFGC15, OPSFGC17 and OPSNFGC, respectively compared to the block. However, higher resistivity was found for OPSFGC and OPSNFGC compared to brick; the reduction in percentage was 48%, 44%, 40% and 36% for OPSFGC13, OPSFGC15, OPSFGC17 and OPSNFGC specimens, respectively. The fine capillary pores present in clay bricks are responsible for transporting the moisture content through the brick, which increases the conductivity (Alengaram et al., 2013).

Saygılı and Baykal (2011) reported that the decrease in the thermal conductivity is due to the increase of void ratio that decreased the unit weight of concrete. Since air is the poorest conductor compared to the solid and liquid due to its molecular structure (Ng & Low, 2010), it contributes to the lower thermal conductivity in porous concrete. Also, Ramamurthy et al. (2009) reported that FC has excellent thermal insulating properties due to its cellular microstructure. Another parallel is also drawn between the thermal conductivity and UPV; the thermal conductivity is directly proportional to UPV, as the concrete with low UPV value possesses a high air content.

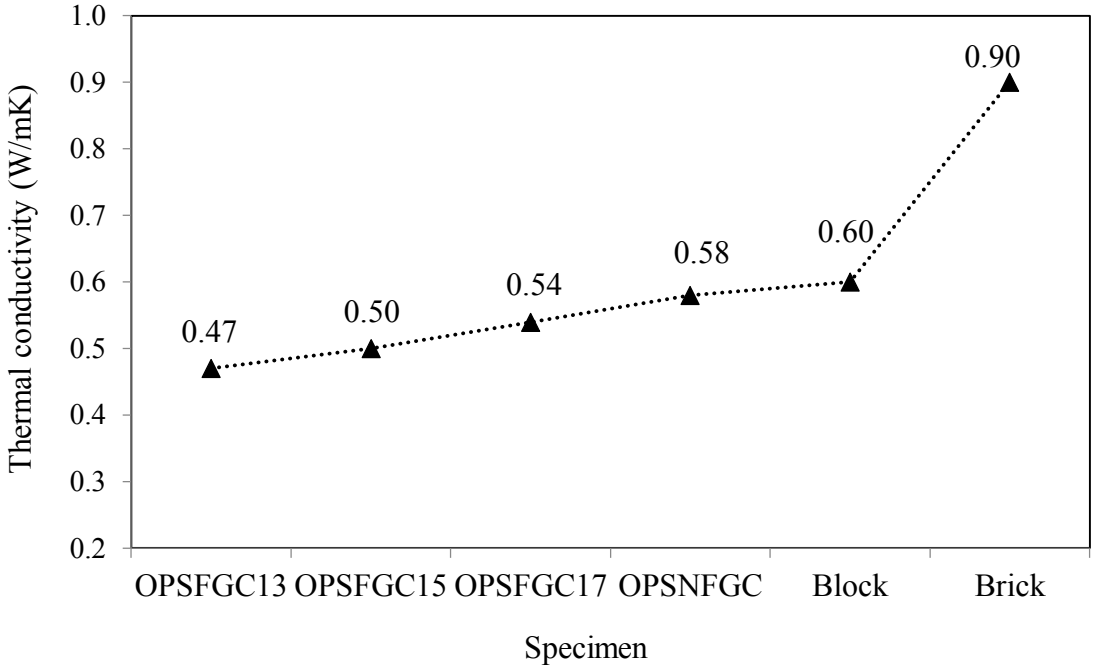

Figure 4.8: Thermal conductivity of specimens

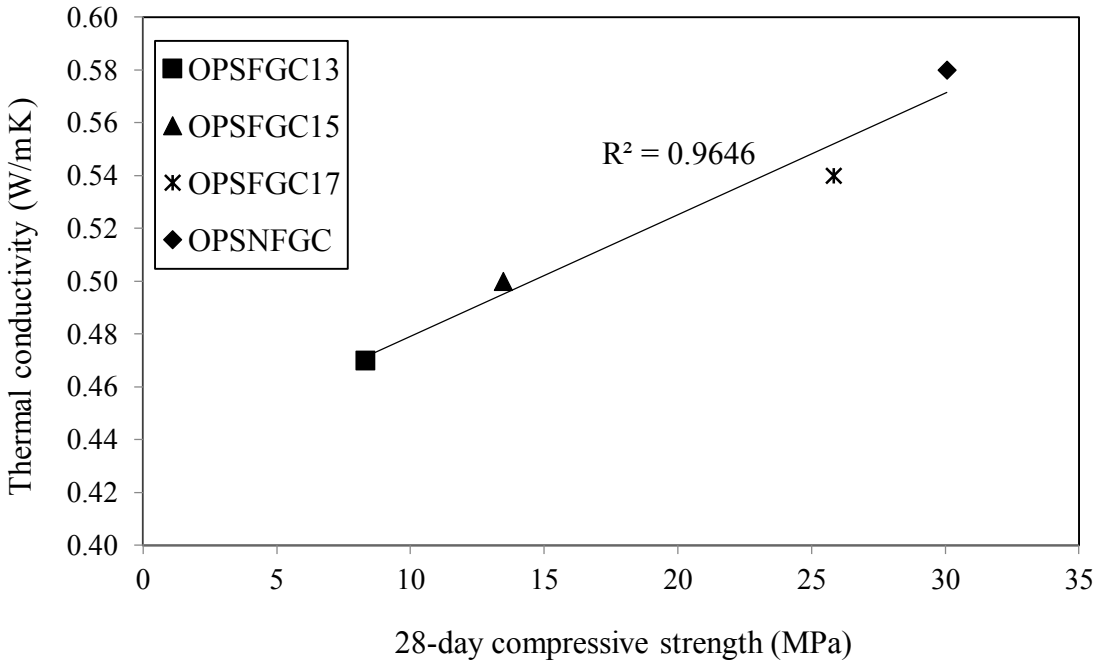

Figure 4.9: Relationship between thermal conductivity and compressive strength of specimens

The superior thermal resistivity of the OPSFGC compared to conventional materials would enable foamed geopolymer concrete (FGC) to be a viable material for energy efficiency. The comparison of the thermal conductivity and its trend with the compressive strength is shown in Figure 4.9. The compressive strength and the thermal conductivity were found to reduce with a decrease in the density of the concrete (Albayrak et al., 2007). Alengaram et al. (2013) have shown that the low density specimen has high air content inside due to the high quantity of foam, thus reducing the rate of heat transferred through the specimen. According to RILEM (1983), OPSFGC17 and OPSNFGC can be categorized as structural grade concrete – Class-I with a compressive strength of more than 15 MPa; OPSFGC13 and OPSFGC15 fall under the category of structural and insulating concrete – Class-II (compressive strength between 3.5 and 15 MPa and the thermal conductivity is less than 0.75 W/mK).

4.5. Microstructure behaviours

The microstructure study was carried out to observe the structure of the PFG paste, OPSFGC and OPSNFGC that include the effect of foam volume on the microstructure, characteristics of the geopolymer paste/matrix with FA and POFA as binders, development in ITZ, presence of pores and micro-cracks (if any). The microstructure study explained the behaviours and development of the concrete over the curing period and varied with the foam volume. In addition, the microstructure study played an important role to support the earlier discussion on the mechanical and transport properties of the concrete. The development of compressive strength of the PFG paste follows a comparable trend with the OPSNFGC, which is shown in Figure 4.10. The FESEM and EDX analyses were carried out on the OPSGC specimens to study their pore structure, ITZ and geopolymerization that varies with the foam volume and curing age. In order to minimize the disruption of aggregate particles on the validity of geopolymer framework

analysis (Kusbiantoro et al., 2012), the PFG paste specimen was used in the XRD and FTIR analysis.

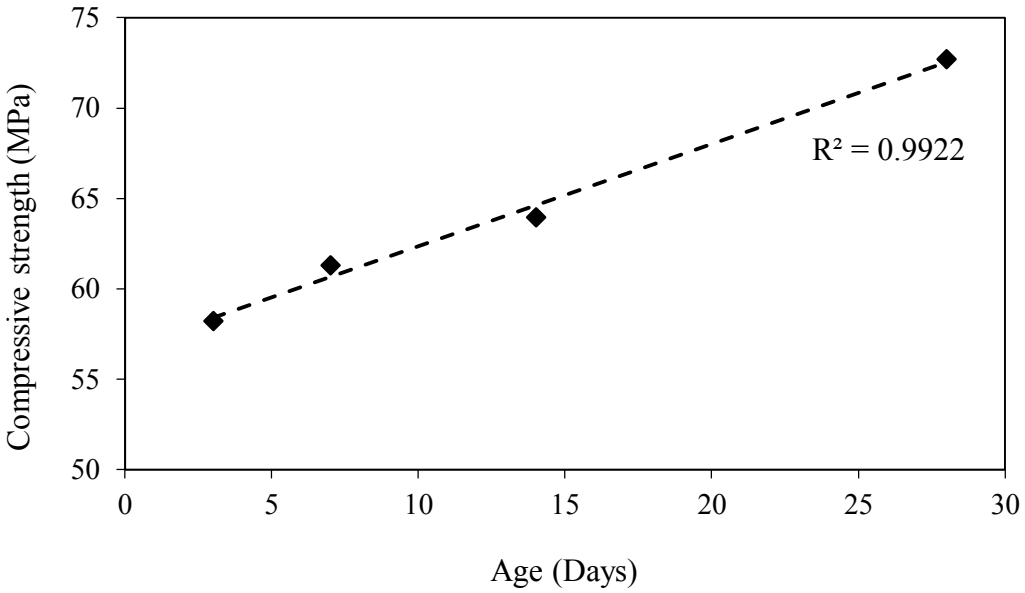

Figure 4.10: Development of compressive strength of PFG paste

4.5.1. FESEM analysis

4.5.1.1. Geopolymerization over curing period

The FESEM analysis was conducted on the OPSFGC and OPSNFGC specimens as presented in Figure 4.11, which depicts morphology features of the specimens at the age of 3- and 28-days.

As clearly seen in each micrograph, there were the glassy phase (aluminosilicate gel) and a number of sphere particles, which were the unreacted FA that are embedded in the glassy gel. Although POFA particles were hardly seen in these micrographs due to their irregular shape (Chindaprasirt et al., 2008), a closer examination of the marked area in Figures 4.11a and 4.11d revealed that they were embedded in the glassy gel. Compared with the 3-day OPSGC in Figures 4.11a, 4.11c and 4.11e, the 28-day OPSGC

micrographs showed a more dense and homogeneous phases in Figures 4.11b, 4.11d and 4.11f. These changes were possibly due to higher degree of gel formation, which resulted in a higher compressive strength in OPSGC at the age of 28-day. In addition, Xu and van Deventer (2000) reported that different mineral particles did not act as fillers in the matrix but rather bonded with alkaline solution to produce complex reaction products that enhance the strength of the matrix with age.

While having a high early strength of at least 73% of 28-day compressive strength, alteration of the SiO_2/Al_2O_3 of source material by partially replacing FA with other binder (in this case is POFA) in geopolymer concrete was not followed by rapid production of the amorphous aluminosilicate gel owing to the inadequacy in the dissolution and polycondensation process (Kusbiantoro et al., 2012). The FESEM micrographs validated that the compressive strength of OPSGC develops with the curing age by exhibiting a more compact and dense matrix at later age, which corresponds the finding where the curing period is an important factor in the acquisition of stronger matrix that lead to higher mechanical strength (Criado et al., 2010). Even so, an adequate water is another important factor, which is required as reaction medium so that the aluminosilicate dissolves via alkaline hydrolysis (Criado et al., 2010).

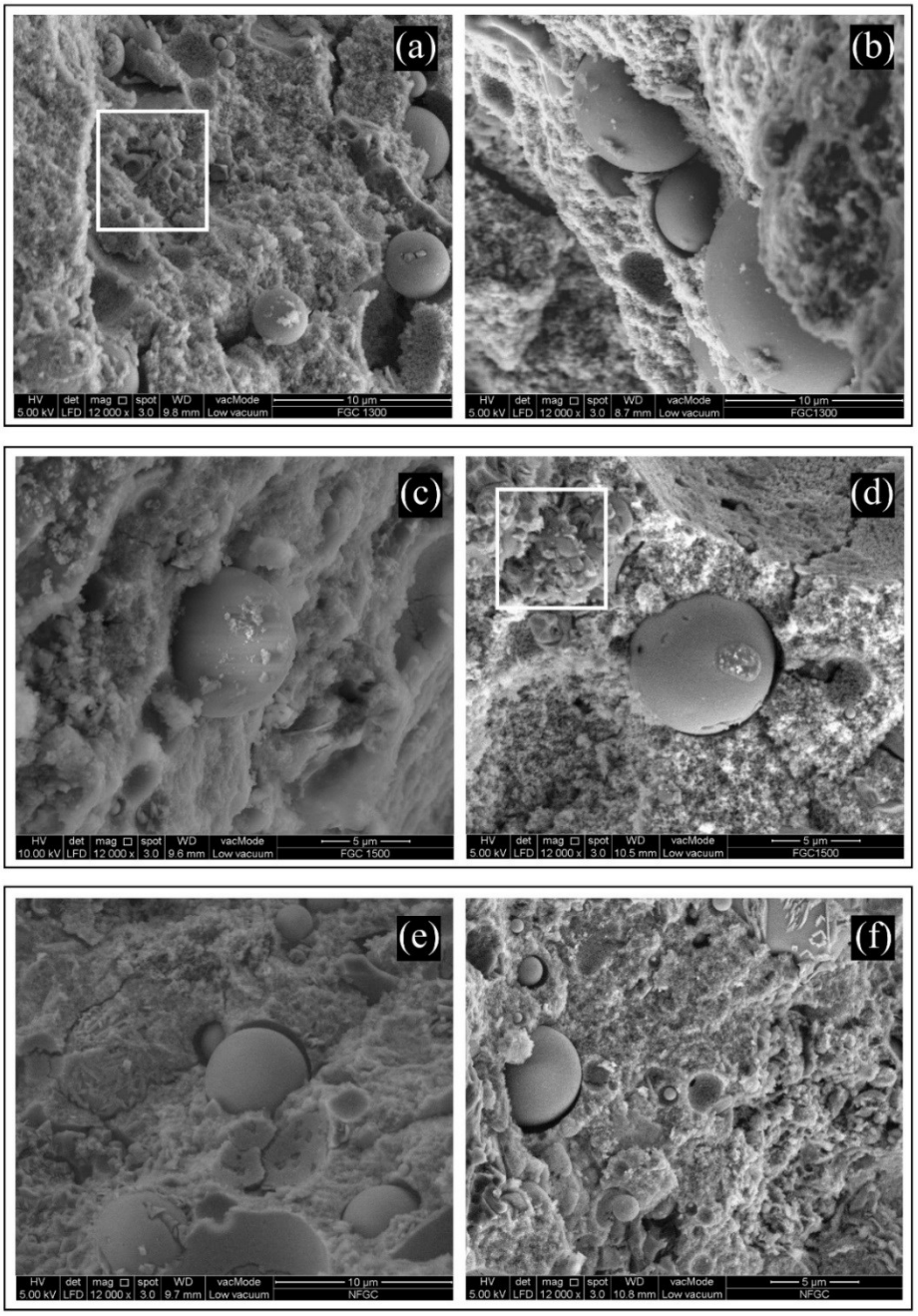

Figure 4.11: FESEM micrographs (magnification of 12000x) of OPSGC at the age of 3- (left) and 28-days (right): (a–b) showing OPSFGC13 at 3- and 28-days; followed by OPSFGC15 (c–d); and OPSNFGC (e–f)

4.5.1.2. Pore structures and micro-cracks

The pore structures and micro-cracks of the OPSFGC and OPSNFGC (Figure 4.12) were studied. The pore structure of the specimens varied over the curing period, effect of foam volume on the concrete strength and formation of micro-cracks on the geopolymer matrix were discussed into three subsections as followings.

i. Pore structure over curing period

The micrographs of the OPSGC specimens at magnification of 100x are presented in Figure 4.12. The pores are apparent for both the OPSFGC13 and OPSFGC15 at the age of 3- and 28-days as shown in Figures 4.12a–4.12d. The FESEM micrographs give a qualitative estimate to the pores size, pores distribution and the material structure after the geopolymerization of the aluminosilicates.

The pore structures in Figures 4.12a–4.12d were attributed to the inclusion of foam during the production of geopolymer concrete, in order to achieve the target density of 1300 and 1500 kg/m^3 for OPSFGC13 and OPSFGC, respectively. The material structure of FC is characterized by its solid microporous matrix and macropores, where the macropores are generally of diameter of more than 60 μm due to the mass expansion triggered by the aeration and the micropores appear in the walls between the macropores (Alexanderson, 1979; Petrov & Schlegel, 1994).

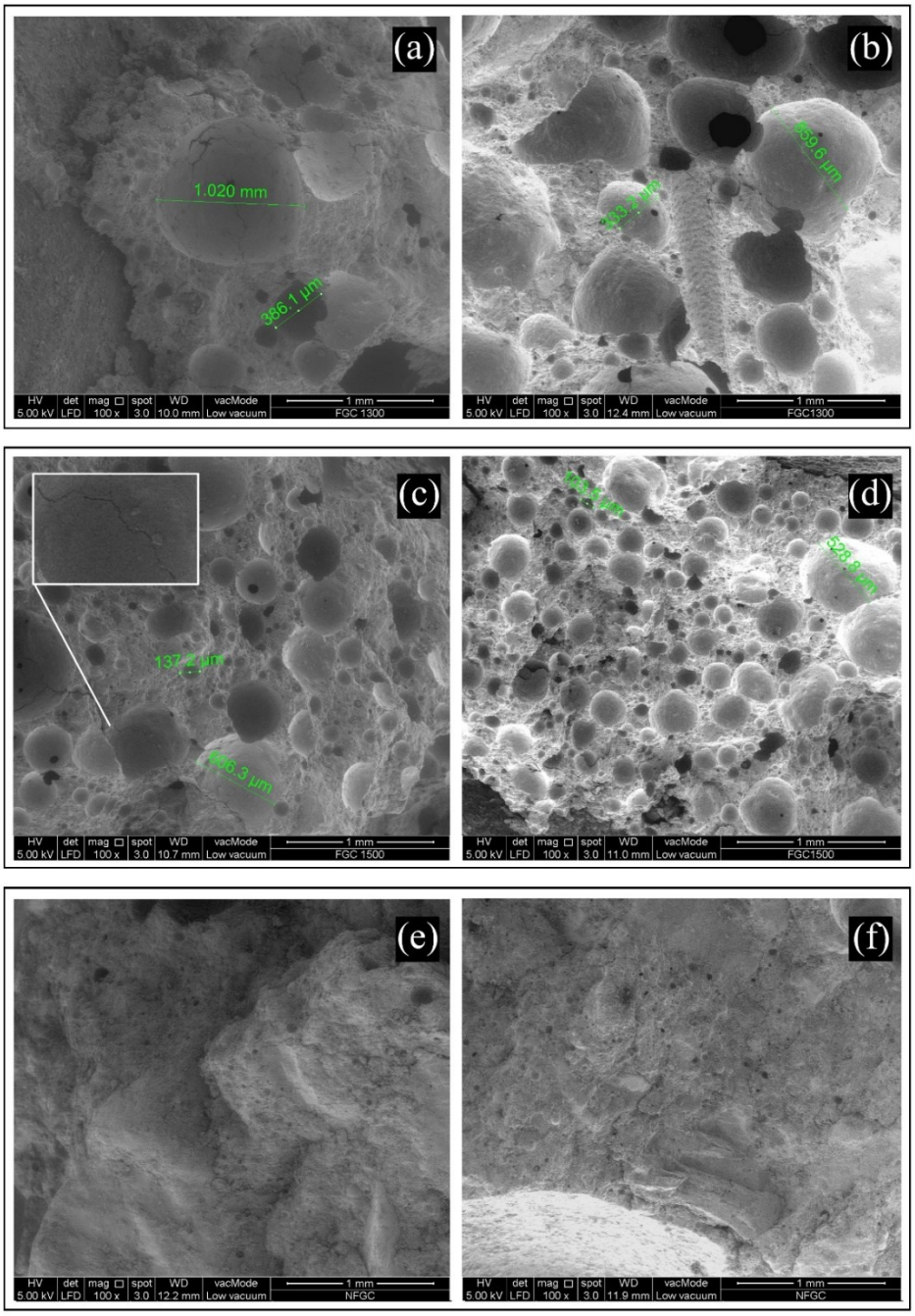

Figure 4.12: Pores structure of OPSFGC and OPSNFGC at the age of 3- (left) and 28-days (right): (a–b) showing OPSFGC13 at 3- and 28-days; followed by OPSFGC15 (c–d); and OPSNFGC (e–f)

The pores in both the OPSFGC13 and OPSFGC15 can be considered as macropores with sizes varying from about 100 µm to 1 mm in diameter. It is indisputable that the pore sizes were reduced with an increase in curing period as shown in the Figures 4.12a–4.12d, which agreed with the finding by Martys and Ferraris (1997) that the

additional curing period reduces the pores size and sorptivity of concrete. The pores of the 3-day OPSFGC13 (approximately 0.386–1 mm) are seen to be decreased to the size of about 333–860 μm at the age of 28-day, whereas pores in the 3-day OPSFGC15 (approximately 137–606 μm) have decreased to the size of about 104–529 μm at the age of 28-day. This confirms that the decrease of the pore size in FGC has led to the improvement in its strength over the curing period.

ii. Effect of foam volume on concrete strength

The compressive strength of FC was shown to be a function of porosity and age (Figures 4.4 and 4.5), where the porosity is largely dependent on the density instead of the ash type or content (Kearsley & Wainwright, 2002). As seen in Figure 4.12, the increase of foam volume increases the pore size, which result in the decrease of the ODD of the OPSGC. It has been reported that at a lower density range, the foam volume controls the strength rather than the material properties (Nambiar & Ramamurthy, 2006).

It is clearly seen that the OPSNFGC (Figures 4.12e–4.12f) has a dense and compact matrix compared to the OPSFGC13 and OPSFGC15 (Figures 4.12a–4.12d), which have porous structures. The density reduction by the formation of macropores is found to be the significant reason for strength drop (Pospisil et al., 1992). Therefore, the 28-day compressive strength of the OPSNFGC is greater than OPSFGC15 by 223%, and even more when compared to the OPSFGC13 (by 361%). As seen in Figures 4.12a–4.12d, the foam possesses a stable and spherical cell structure, which was reported to be vital for optimum structural and functional properties (Prim & Wittmann, 1983). It is found that Alengaram et al. (2013) has developed a structural and insulating FC with an ODD of 1594 kg/m^3 that gives a lower thermal conductivity by 37%, when compared to the conventional brick.

iii. Formation of micro-cracks on the geopolymer matrix

While the OPSNFGC presented a compact matrix, some micro-cracks were spotted (Figures 4.12e–4.12f) upon closer observation. Similar but larger micro-cracks are noticeable in the OPSFGC as shown in Figures 4.12a–4.12d. These micro-cracks may be due to the thermal curing as part of the geopolymerization, mechanical damage during the sample preparation or the drying shrinkage during the electron scanning under vacuum condition (Fernandez Jiminez et al., 2004). As a result, these micro-cracks would limit the binding capacity and may exert negative effect on strength of the geopolymer concrete (Chindaprasirt et al., 2009). A refinement in pores or crack paths by denser geopolymer matrix will significantly enhance the strength of the geopolymer concrete (Kusbiantoro et al., 2012), which can be observed in Figure 4.12 that the denser and compact geopolymer matrix (Figures 4.12e–4.12f) with a finer micro-cracks, obtained higher strength than the matrices (Figures 4.12a–4.12d) with a larger micro-cracks.

4.5.1.3. The ITZ between the OPS and geopolymer matrix

The FESEM micrographs of the interfacial transition zone (ITZ) between the OPS and the geopolymer matrix of POFA and FA are shown in the Figure 4.13. From Figure 4.13, it can be seen that the width of the ITZ varies in the range of 8.3–89.8 μm.

Concrete degradation often occurred due to the compressive load, which is caused by the initiation and propagation of micro-crack in ITZ. The stress during the loading tends to concentrate in the weakest region (ITZ region), which is due to its different elastic ratio between aggregates and the matrix (Zhang et al., 2009). In addition, Demie et al. (2013) stated that the ITZ is caused by the incomplete packing of unreacted FA microsphere particles in the transition zone between the geopolymer paste and aggregates

which attributed to the incomplete dissolution of large proportion of FA and other particles. Therefore, it is crucial to investigate the microstructure of the ITZ where the bonding of the aggregate and the matrix is developed. Being a constructive method, microstructure analysis is able to corroborate the strength analysis since the strength of the geopolymer matrix is influenced by the quality of the pores within (Kusbiantoro et al., 2012) especially on the FGC.

As clearly seen in Figure 4.13, the ITZ is narrowing at 28-day for all specimens. It is identified that the geopolymerization of FA and POFA improves the bonding between the OPS and geopolymer paste throughout the curing period. Hence, the matrix of the connectivity is strengthen during the formation of the aluminosilicate gels. Therefore, the strength development of the geopolymer concrete improves with the reduction of the gap in the ITZ over the curing period. Lo et al. (2007) stated that the concrete strength depends only on the bonding of the ITZ at early age since the aggregate strength had not been fully utilized.

Furthermore, it is observed in Figure 4.13 that the width of the ITZ is increasing with the decrease of density due to the addition of foam in the geopolymer concrete. The ITZ microstructure of OPSFGC (Figures 4.13a–4.13d) display a relatively porous and loose interface compared to the OPSNFGC (Figures 4.13e and 4.13f). The presence of a larger gap in the ITZ, which was induced by the foam that created more pores and crack paths and that, prevented the refinement of the ITZ and weakened the bonds between the OPS and geopolymer matrix. Hence, it resulted in a less homogeneous structure that reduced the strength of the geopolymer concrete. Higher porosity of geopolymer concrete matrix will decreased the proficiency of geopolymer concrete to sustain and distribute the external load well (Kusbiantoro et al., 2012).

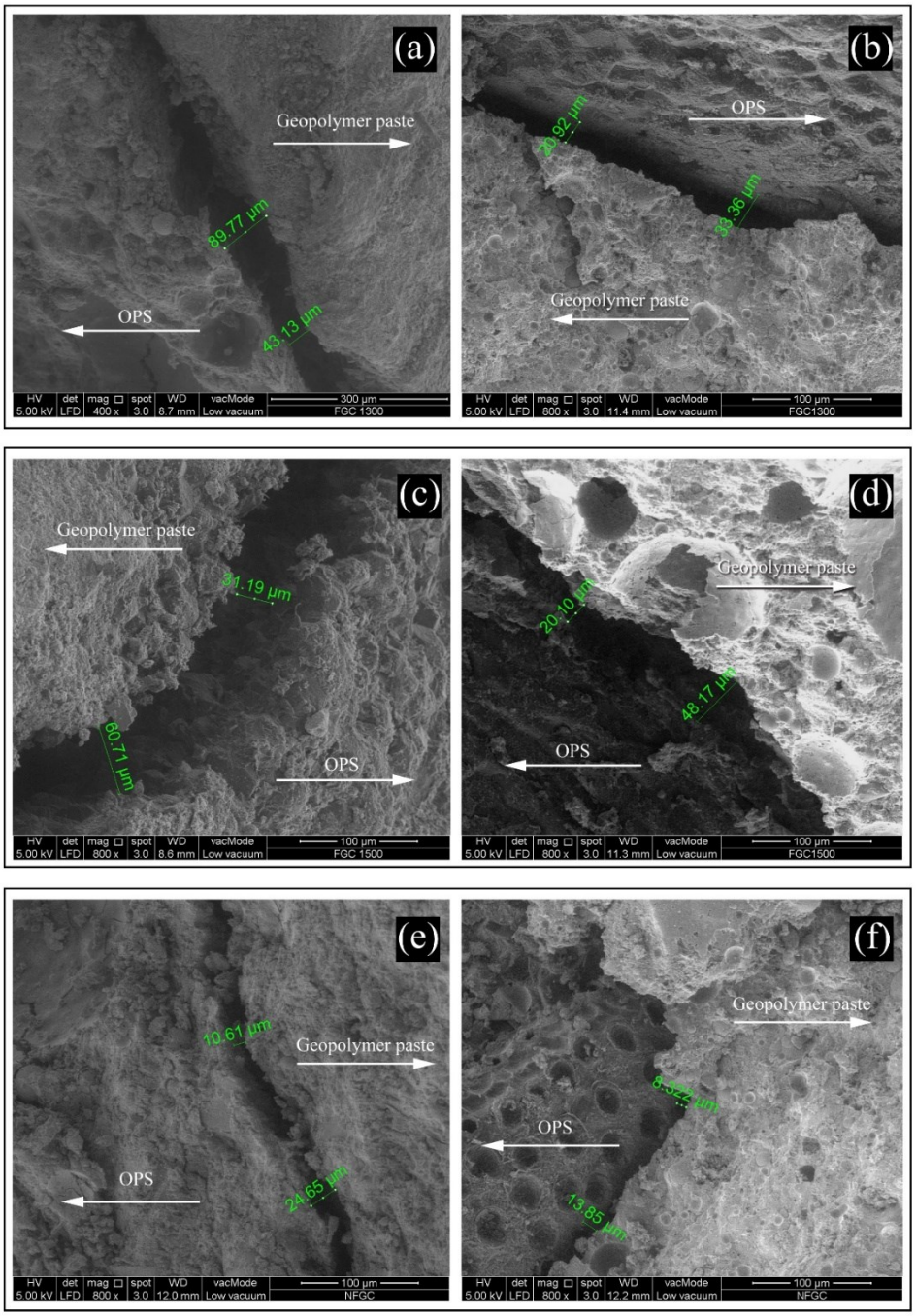

Figure 4.13: Interfacial transition zones of OPSFGC and OPSNFGC at the age of 3- (left) and 28-days (right): (a–b) showing OPSFGC13 at 3- and 28-days; followed by OPSFGC15 (c–d); and OPSNFGC (e–f)

Prior to the measurements shown in the micrographs (Figure 4.13), Figure 4.14 shows correlation of ITZ thickness and compressive strength development of OPSFGC and OPSNFGC. Poon et al. (2004) reported that the strength development of a recycled

aggregate concrete is governed by the ITZ microstructure significantly which is attributed to the higher porosity and absorption of the aggregates. Therefore, the porous OPS might contribute to the reduction of the concrete strength.

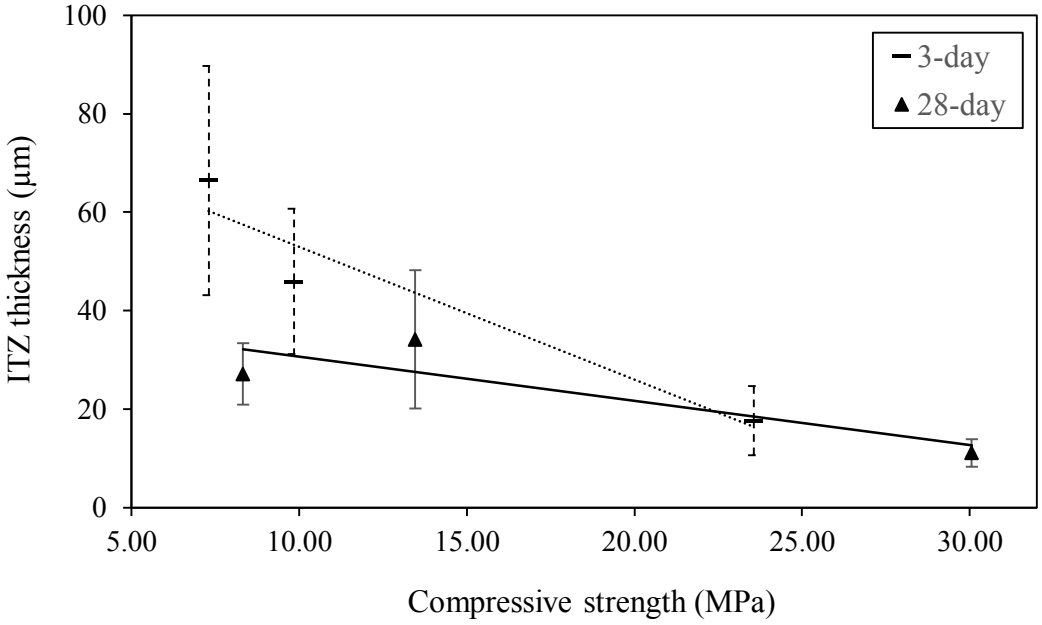

Figure 4.14: Effect of ITZ thickness on 3- and 28-days of compressive strength

Figure 4.14 shows the linear relationship between the ITZ thickness and the compressive strength of the geopolymer concrete at 3- and 28-day. In addition, the range of the ITZ thickness decreased over the curing period, from 3-day to 28-day. These changes over the curing period indicated that the partial dissolution of the crystalline phase over time, which was explained in the XRD results. The OPSNFGC (Figures 4.13e and 4.13f) exhibited higher strength than both the OPSFGC13 and OPSFGC15 (Figures 4.13a–4.13d) for the reason that its ITZ was narrower and less porous which enabled it to have a better load distribution. Nevertheless, the ITZ also governs the transport properties of concrete other than the volume fraction and micro-geometry of the pore structure within the matrix (Wong et al., 2009).

4.5.2. EDX characterization

Table 4.6 presents the weight percentage of the major elements (Si, sodium (Na) and Al) and compares the ratios (Si/Al, Na/Al and Si/Na) obtained from the EDX analysis of the 3- and 28-day OPSGC. The analysis was done at the magnification of 1500x on the geopolymer matrix.

Table 4.6: Weight percentage (%) of the OPSFGC and OPSNFGC by EDX analysis

Element and ratio	OPSFGC13		OPSFGC15		OPSNFGC	
	3-day	28-day	3-day	28-day	3-day	28-day
Si	22.00	25.37	20.23	24.99	22.14	23.68
Na	8.16	5.80	8.27	5.28	8.85	8.04
Al	4.49	4.11	4.81	4.95	6.46	4.28
Si/Al	4.90	6.17	4.21	5.05	3.43	5.53
Na/Al	1.82	1.41	1.72	1.07	1.37	1.88

Alkali metal cation plays an important role in every stage of the geopolymerization of source materials and it is also thought to have an effect on the rate of polycondensation (van Jaarsveld & van Deventer, 1999). He et al. (2012) reported that the Si/Al ratio has a linear relationship with the compressive strength of the geopolymer products, however, the Si/Al ratio may not be the true value of the geopolymers of certain source materials (e.g., red mud) since it is difficult to distinguish the reacted, unreacted and non-reactive silicon and aluminium in geopolymeric composites.

Bondar et al. (2011) suggested that the standard oxide ratio of SiO_2/Al_2O_3 in geopolymer composition ranged between 3.3 and 6.5. The Si/Al ratios in Table 4.6 showed an increasing trend over the curing period for all specimens, varied from 3.43 to 6.17. The increase of the Si/Al ratio over time also leads to a higher strength with denser structure of the matrix (Figure 4.11). Besides the reduction in aluminosilicate compound

strength, the decrease of the Si/Al ratio is accompanied by the increase of crystalline phase in microstructure (Silva et al., 2007). This change denotes that the dissolution rate of Al_2O_3 is higher than the SiO_2, but the rate slows down when the geopolymer system approaches a supersaturated condition (Sindhunata et al., 2006).

The Si/Al ratios displayed a declining trend from 4.90 to 3.43 with an increasing of 3-day compressive strength for the OPSFGC and OPSNFGC specimens. This phenomenon indicates that the aluminium dissolves at higher rate than the silicon during the early stage of geopolymerization, which is similar to the findings by Pietersen et al. (1989). At the age of 28 days, the Si/Al ratio increases with the compressive strength where the rates of dissolution and polycondensation of aluminosilicate gel are enhanced. However, the OPSFGC13 is spotted to have Si/Al ratio of 6.17, which is higher compared to the OPSFGC15 and OPSNFGC with Si/Al ratio of 5.05 and 5.53, respectively. Kusbiantoro et al. (2012) reported that the anomalously high Si/Al ratio is due to the high precipitation of dissolved and unreactive SiO_2 particles in geopolymer framework due to the low geopolymer system reactivity.

The Na/Al ratios of all 3- and 28-day specimens in Table 4.6 exceed 1, indicating that there is a sufficient availability of sodium as cation to form sodium aluminosilicate gels analogous to the CSH in Portland cement systems. Guo et al. (2010) reported that insufficiency of sodium will result in the requirement of another cation to balance the covalent bonding, where there is a possibility of formation of CSH gels in geopolymer system due to the substitution of calcium (Ca) as cation.

4.5.3. XRD analysis

Figure 4.15 represents the XRD patterns of 3- and 28-day PFG paste specimen cured at 65˚C for 48 hours. The main constituents of the PFG paste are quartz (Q, SiO_2), mullite (M, $3Al_2O_3.2SiO_2$) and albite (A, $NaAlSi_3O_8$).

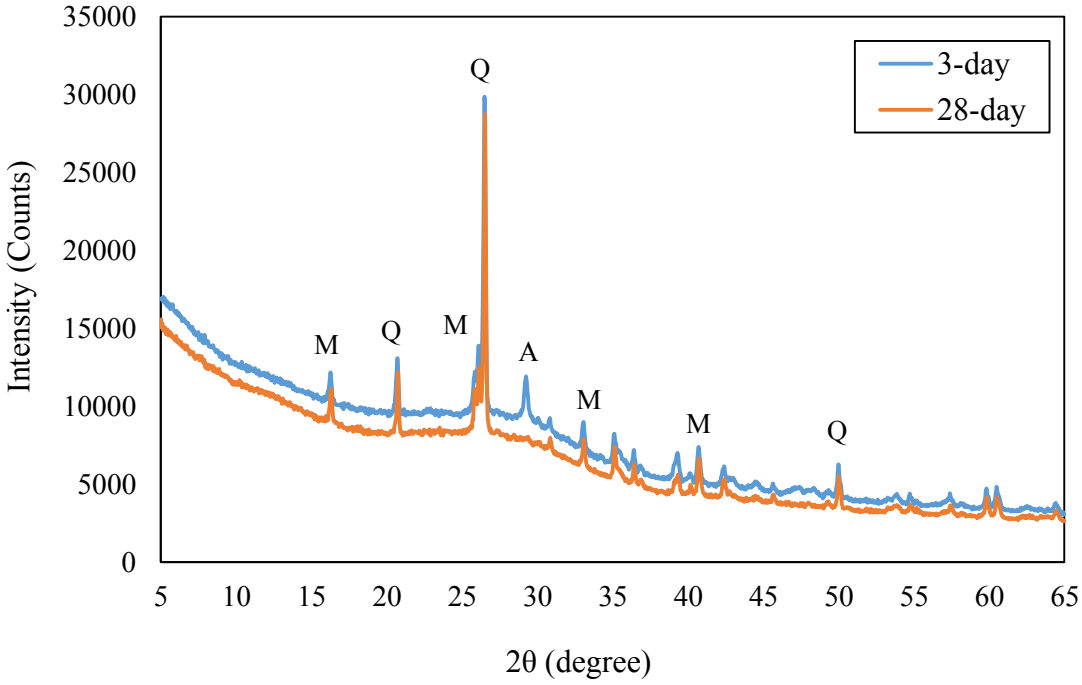

Figure 4.15: XRD patterns of 3- and 28-day of PFG paste

Figure 4.15 shows a similar broad hump between 19˚ and 33˚ (2θ) for both analyses due to the presence of amorphous aluminosilicate gel in the specimen. It is evident that the alkali activation of aluminosilicate leads to the formation of amorphous aluminosilicate gel and geopolymer and that leads to excellent mechanical and chemical properties (Davidovits, 1994a; Palomo et al., 1999). Nevertheless, the formation of the aluminosilicate gel depends on the availability of dissociated silicate $SiO_n(OH)_{4-n}^{n-}$ and aluminate $Al(OH)_4^-$ monomers in the alkaline solution, which is further dependent on the

extent of dissolution of these two species from the original aluminosilicate source (Yip et al., 2008).

Taylor and Matulis (1991) reasoned that for well-defined peaks without significant broadening, the peak areas are still proportional to peak heights. The dissolution of Si and Al from the aluminosilicate source governs the early stage of geopolymerization (Xu & van Deventer, 2000). From the Figure 4.15, it is seen that the decrease of the intensity of the crystalline peaks between 3- and 28-day specimens indicates partial dissolution of the crystalline phase over time. The dissolution increases with the age of the specimen as the compact structure is formed with a longer reaction time (Heah et al., 2012). Both the quartz and mullite phases have been found to be unreactive in 28-day PFG specimen, and this denotes that these peaks are not fully dissolved during the geopolymerization; however, their intensities were lower than the 3-day PFG specimen due to the dilution effect (Lecomte et al., 2003).

The strength development region of the geopolymer matrix can be related to the presence of albite phase (Kupwade-Patil & Allouche, 2013). It is clearly seen from the 28-day PFG specimen (Figure 4.15) that the albite phase is completely dissolved during the geopolymerization. Meanwhile, the quartz and mullite phases present as slightly inactive fillers in the geopolymer binders.

4.5.4. FTIR analysis

Figure 4.16 shows the FTIR spectrum of the PFG paste sample at the age of 28 days and it shows that the major bands are at 3297, 1645, 1429, 989, 796-778 (double band), 566 and 454 cm^{-1}.

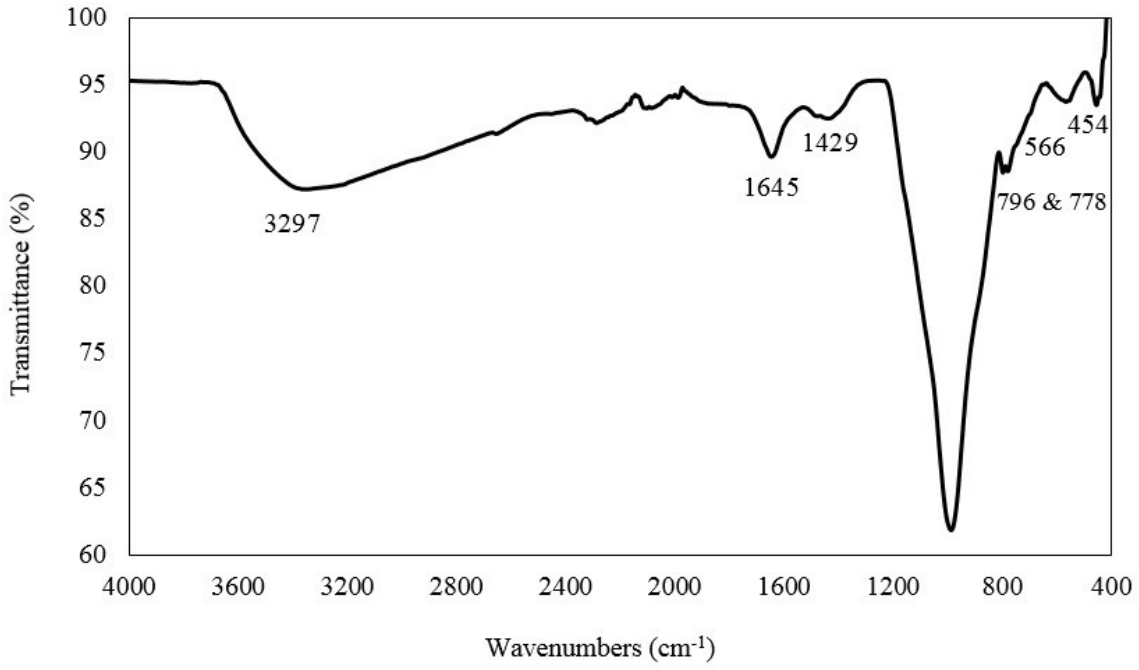

Figure 4.16: Infrared spectrum of 28-day PFG paste

The broad band of PFG specimen at 3297 cm^{-1} and 1646 cm^{-1} characterizes the O-H stretching vibration and H-O-H bending vibration, respectively. These modes of vibration are due to the weakly bound of water molecules that were adsorbed on the surface or trapped in the large cavities (Bakharev, 2005). Water plays an important role in the process of geopolymerization as it associates with the destruction of solid particles and hydrolysis of dissolved Al^{3+} and Si^{4+} ions (Mužek et al., 2012).

The absorption band at 1429 cm^{-1} is attributed to the presence of sodium carbonate (Na_2CO_3); this corresponds to the stretching vibration of the O-C-O bond (Swanepoel & Strydom, 2002). Álvarez-Ayuso et al. (2008) suggested that presence of Na_2CO_3 is due to the atmospheric carbonation of alkaline media.

The strongest band of the PFG specimen at 989 cm^{-1} is corresponded to the asymmetric stretching vibrations of Si-O-T (T = Si or Al). According to Fernández-Jiménez and Palomo (2005), the bond force constant for the mode of Si-O-Al is smaller than the mode of Si-O-Si bond due to the fact that Al-O bond is longer than the Si-O bond. Moreover, the stretching modes are sensitive to the Si-Al composition of the framework and lower frequency is obtained with increasing number of tetrahedral aluminium atoms (Bakharev, 2005). Mužek et al. (2012) suggested that the amorphous aluminosilicate gel formed at this phase is due to the depolymerisation and structural reorganisation of the amorphous phases in geopolymer materials.

The bands in the region between 800 and 500 cm^{-1} are correlated with the tetrahedral vibrations of secondary building unit (SBU) and fragments of the aluminosilicate (Fernández-Jiménez & Palomo, 2005). The double bands at 797 and 778 cm^{-1} observed in Figure 4.16 are assigned to quartz as the crystalline phase in the original FA (Fernández-Jiménez & Palomo, 2005) whereas the band located at 566 cm^{-1} indicates the presence of mullite. Referring to the finding by Mollah et al. (1994), the spectral at 566 cm^{-1} is attributed to the symmetric stretching of Al-O-Si. The T-O bending vibrations can be seen at 455 cm^{-1} where this band provides an indication of the degree of 'amorphisation' of the material, since its intensity does not depend on the degree of crystallization (Mozgawa et al., 1999; Sitarz et al., 2000).

CHAPTER FIVE

CONCLUSIONS AND RECOMMENDATIONS

5.1. Conclusions

Thermal insulating materials play a vital role in reducing the power requirement, and, hence, reducing greenhouse gas emissions. Moreover, the incorporation of waste materials would be an added advantage in environment and economy aspects. Greening the building and construction industry have been practised especially in the developed countries such as United States, Australia, Germany, Japan, etc. Yet, the scientific and government policy has enforced the need to lessen carbon footprint. van Deventer et al. (2012) reported that about 80% of CO_2 can be reduced with the use of geopolymer cement. In Australia, McLellan et al. (2011) estimated that the production cost of geopolymer concrete ranged from 7% lower to 39% higher than OPC concrete, which exhibited similar performance. Differing from the developed countries, the cost of OPSFGC in Malaysia is estimated at approximately 2 times more expensive than the conventional concrete. However, large scale development of geopolymer concrete could lead to lower production cost due to the large order of reagent (McLellan et al., 2011). Hence, when the demand for sustainable buildings and construction is higher, the production cost of geopolymer concrete would be lesser.

This research focuses on the development and microstructure study of the structural and thermal insulating lightweight-foamed geopolymer concrete using locally available waste materials for sustainable development. Three types of foamed and one non-foamed geopolymer were produced using OPS as lightweight aggregate and utilized

POFA and FA as binders; the thermal conductivity of the geopolymer concrete was compared with conventional materials, such as brick and block. From the experimental results, the following conclusions are summarised according to the corresponding research objectives.

Objective i.

To develop structural and non-structural grade of foamed and non-foamed geopolymer concrete using OPS as LWA and utilized FA and POFA as binders

According to BS EN 206-1 (2000), the ODD for the development of OPSFGC and OPSNFGC over the curing period, ranged from 1291–1794 kg/m^3 are characterised as LWC. In this research work, the OPSFGC13 and OPSFGC15 are categorized as the non-structural whereas the OPSFGC17 and OPSNFGC demonstrated as the lightweight structural concrete in accordance with ACI 213R (2003). From the experimental results, the OPSFGC17 and OPSNFGC achieved a 28-day compressive strength of about 26 MPa and 30 MPa, respectively, and hence could be categorized as lightweight structural concrete in accordance with ACI 213R (2003).

In addition, the geopolymer concrete exhibited a high early strength that would allow rapid construction and production of precast lightweight concrete. After cured in oven for 48 hours at the temperature of 65 ˚C, the 3-day compressive strength of the OPSFGC and OPSNFGC could achieved up to 90% when compared with the 28-day compressive strength though the rate of strength gain was decreased about 11.3% after 7-day. Furthermore, the use of OPS as LWA and utilization of FA and POFA have been beneficial towards environmental sustainability and economy aspects.

Objective ii.

To investigate the mechanical and transport properties of the OPSFGC

The addition of foam decreases the density of OPSFGC owing to the increased pore volume. All the ODD of the OPSFGC specimens were within ± 50 kg/m^3 of the target density. The mechanical properties of OPSFGC and OPSNFGC, such as compressive, splitting tensile and flexural strengths, generally reduced with the reduction in the ODD; the MOE also followed a similar trend. From the experimental results, the 28-day compressive strength for the OPSFGC and OPSNFGC specimens ranged from 8.3 to 30.1 MPa; the 28-day splitting tensile strengths are between 0.6 and 2.4 MPa; the 28-day flexural strength varied from 1.5 to 3.7 MPa; and the MOE of the specimens are ranged from 3.5 to 7.4 GPa. The splitting tensile and flexural strengths were found to give close results when applied on the equations (4.1 and 4.2) proposed by Shafigh et al. (2010) to predict the strength of OPSC. The strength to density ratio of 17 for the OPSFGC17 was 54% higher than the corresponding NWC.

The 28-day UPV values (ranged from 2.18 to 3.12 km/s) varied inversely with the density of the OPSGC specimens. Nevertheless, it is found that the OPSFGC17 and OPSNFGC with UPV value of about 3 km/s, fall in the category of 'fair' quality concrete, which is suggested by Browne et al. (1983). Moreover, the porosity varied between 25% and 40% for the OPSFGC of densities in the range of 1300–1700 kg/m^3 and high porosity of concrete lowered the compressive strength. Additionally, the sorptivity is linearly increased with a reduction in compressive strength and density of the OPSFGC and OPSNFGC. A higher volume of foam may induced more pores and pores connectivity that result in higher sorptivity. Other than sorptivity, the water absorption of the specimens also increased with the increasing of foam volume. In agreement with the UPV

results, the water absorption of OPSFGC17 and OPSNFGC also categorized as 'average' quality of concrete by CEB-FIP (1989).

Objective iii.

To determine the thermal conductivity of OPSFGC and OPSNFGC, in comparison with the conventional materials such as block and brick

The thermal conductivity of OPSFGC and OPSNFGC results showed that an increase in the quantity of foam enabled its resistivity. The experimental results were proven that the OPSFGC and OPSNFGC are superior in thermal resistivity compared to the conventional materials used such as block and brick. OPSFGC with higher foam volume formed a more porous structure with higher air content, contributes to its lower density that would attain a higher thermal resistivity. The reduction in the conductivity was about 22%, 17%, 10% and 3% for OPSFGC13, OPSFGC15, OPSFGC17 and OPSNFGC, respectively compared to the block. However, higher resistivity was found for foamed and non-foamed concretes compared to brick; the reduction in percentage was 48%, 44%, 40% and 36% for OPSFGC13, OPSFGC15, OPSFGC17 and OPSNFGC specimens, respectively.

The range of compressive strengths and the thermal conductivity of OPSFGC13 and OPSFGC15 were found to be about 8 and 13 MPa, and 0.47 and 0.50 W/mK, respectively, and hence these could be categorized as structural and insulating concrete – Class-II, as per the RILEM (1983) classification. Whilst, the OPSFGC17 and OPSNFGC produced a higher compressive strength of about 26 and 30 MPa, respectively fall under the structural grade concrete.

Objective iv.

To study the morphology and mineralogy of the geopolymer paste and OPSFGC with respect to the FESEM/EDX, XRD and FTIR spectroscopy.

As shown in the micrographs from the FESEM analysis, it is learnt that the geopolymer matrix of the 28-day OPSGC displayed a more dense and homogeneous phases than the 3-day OPSGC. This change could be attributed to higher degree of gel formation and dissolution of the CM, which validated the compressive strength performance of OPSGC enhanced with the longer curing period. The pores in both the OPSFGC13 and OPSFGC15 were considered as macropores with sizes vary from about 100 μm to 1 mm in diameter, which will be a significant reason of strength drop when compared with OPSNFGC. It is also shown in FESEM micrographs that the additional curing period reduced the pores size, which contributes to the development of the OPSGC.

When comparing with different densities of OPSFGC, the compressive strength is decreasing with lower ODD, which attributed to the addition of higher foam volume that would increases the pores size. Yet, the micrographs of OPSFGC displayed a stable and spherical cell structure that would provide a better thermal resistivity. Larger micro-cracks were noticed at OPSFGC specimens compared to the OPSNFGC that would limit the binding capacity and affect the strength. Furthermore, concrete degradation tend to occur by the propagation of micro-crack in ITZ. The ITZ was narrowed over the curing period due to the geopolymerization of the CM that led to an improvement of the strength. It is also seen that the width of the ITZ is increasing with the decrease of density attributed to the addition of foam in the OPSGC that creates more pores and crack paths; and that prevents the refinement of the ITZ and weakens the bonds between the OPS and geopolymer matrix.

In the EDX analysis, the findings showed that the increase of the Si/Al ratio over time leads to a higher strength and rates of geopolymerization that formed a denser structure of the matrix. The Na/Al ratios of the specimens indicated that there is a sufficient of sodium as cation to form sodium aluminosilicate gels parallel to the calcium silicate hydrates terminology. It is revealed in XRD analysis that the decrease of the intensity of the crystalline peaks between 3- and 28-day specimens indicates partial dissolution of the crystalline phase over time that lead to enhancement of strength. The presence of the amorphous aluminosilicate gel was found in the FTIR analysis, which is the main reaction product formed in the OPSGC.

5.2. Recommendations

Despite the increasing of global environmental issues, the use of geopolymer technology in concrete production could provide a future need in environment sustainability. Yet, a more resource-efficient geopolymer concrete can be produced with the use of waste materials as cementitious materials, coarse and fine aggregates. In addition, the incorporation of foam in geopolymer concrete could provide a more energy-efficient building. In this research work, OPS was utilized as LWA, whereas POFA and FA were used as binder.

To date, there is very limited literatures available on the foamed geopolymer concrete. Besides that, the study on utilization of OPS and POFA in geopolymer concrete is scarce as well. Hence, there are a lot of potentials to explore the geopolymer concrete with the locally available waste. These geopolymer concretes can be further investigated with more detailed properties and behaviours. The scope of this research work is limited and hence, recommendations for future research are outlined as followings:

i. A further investigation on OPSFGC could be explored with target densities of lower than 1000 kg/m^3 and achieved a specific target strength.
ii. The strength development of the foamed and non-foamed OPSGC could be tested on different curing methods, such as external exposure curing that would be a more promising curing method for cast in-situ. However, this type of curing method is subject to local weather condition.
iii. Since the OPSGC exhibited high early strength, a time-dependent analysis such as shrinkage and creep, which affect the stresses and deflection would be an added characteristic.

iv. The manufacture of foamed and non-foamed OPSGC could provide a more energy- and resource- efficient material. However, the energy efficiency and reduction of CO_2 emission should be quantified using appropriate methods or equations.

v. This research work only focused on experimental work, further research can be carried out on computational chemistry to understand and improve the reactivity of the cementitious material, especially on the crystalline nature.

vi. The different ratio of Na_2SiO_3 to NaOH can be further investigated, where the ratio may reacts differently with the blended POFA and FA.

vii. The durability of foamed and non-foamed OPSGC (resistance to chemical attack, weathering action, abrasion and etc.) while sustaining its engineering properties could be studied.

viii. Moreover, the structural behaviours reinforced OPSGC can be further investigated to form an empirical equation for design with respect to flexural, shear, impact and torsion.

ix. Large scale of experimental work could be done by building houses to determine the actual energy efficiency of the commercial building.

x. The PFG paste could be studied as material for finishing option, where it is applied as 'sacrificial layer' towards chemical attacks, fire resistance and many more.

References

Abdullah, M. M. A., Hussin, K., Bnhussain, M., Ismail, K. N., Yahya, Z., & Razak, R. A. (2012). Fly ash-based geopolymer lightweight concrete using foaming agent. *International journal of molecular sciences, 13*(6), 7186-7198.

Abdullah, M. M. A., Kamarudin, H., Bnhussain, M., Nizar, I. K., Rafiza, A. R., & Zarina, Y. (2011). The relationship of NaOH molarity, Na_2SiO_3/NaOH ratio, fly ash/alkaline activator ratio, and curing temperature to the strength of fly ash-based geopolymer. *Advanced Materials Research, 328*, 1475-1482.

ACI 213R. (2003). Guide for structural lightweight aggregate concrete. *American Concrete Institute*, 22-23.

Adam, A. A. (2009). *Strength and durability properties of alkali activated slag and fly ash-based geopolymer concrete.* (PhD), RMIT University Melbourne, Australia.

Ahmad, M. H., Omar, R. C., Malek, M. A., Noor, N., & Thiruselvam, S. (2008). *Compressive strength of palm oil fuel ash concrete.* Paper presented at the Proceedings of the International Conference on Construction and Building Technology, Kuala Lumpur, Malaysia.

Ahmari, S., Ren, X., Toufigh, V., & Zhang, L. (2012). Production of geopolymeric binder from blended waste concrete powder and fly ash. *Construction and Building Materials, 35*, 718-729.

Aïtcin, P. C. (2000). Cements of yesterday and today: Concrete of tomorrow. *Cement and concrete research, 30*(9), 1349-1359.

Albayrak, M., Yörükoğlu, A., Karahan, S., Atlıhan, S., Aruntaş, H. Y., & Girgin, İ. (2007). Influence of zeolite additive on properties of autoclaved aerated concrete. *Building and Environment, 42*(9), 3161-3165.

Aldridge, D. (2000, 23 March). *Foamed concrete for highway bridge works.* Paper presented at the One-day awareness seminar 'Foamed concrete: Properties, applications and potential', University of Dundee, Scotland.

Alengaram, U. J., Al-Muhit, B. A., Jumaat, M. Z., & Liu, M. Y. J. (2013). A comparison of the thermal conductivity of oil palm shell foamed concrete with conventional materials. *Materials & Design, 51*, 522-529.

Alengaram, U. J., Jumaat, M. Z., & Mahmud, H. (2008). Ductility behaviour of reinforced palm kernel shell concrete beams. *European Journal of Scientific Research, 23*(3), 406-420.

Alengaram, U. J., Jumaat, M. Z., Mahmud, H., & Fayyadh, M. M. (2011a). Shear behaviour of reinforced palm kernel shell concrete beams. *Construction and Building Materials, 25*(6), 2918-2927.

Alengaram, U. J., Mahmud, H., & Jumaat, M. Z. (2011b). Enhancement and prediction of modulus of elasticity of palm kernel shell concrete. *Materials & Design, 32*(4), 2143-2148.

Alexanderson, J. (1979). Relations between structure and mechanical properties of autoclaved aerated concrete. *Cement and concrete research, 9*(4), 507-514.

Altwair, N. M., Johari, M. A. M., & Hashim, S. F. S. (2011). Strength activity index and microstructural characteristics of treated palm oil fuel ash. *International Journal of Civil & Environmental Engineering, 11*(5), 100-107.

Álvarez-Ayuso, E., Querol, X., Plana, F., Alastuey, A., Moreno, N., Izquierdo, M., et al. (2008). Environmental, physical and structural characterisation of geopolymer matrixes synthesised from coal (co-)combustion fly ashes. *Journal of Hazardous Materials, 154*(1–3), 175-183.

Ariffin, M. A. M., Bhutta, M. A. R., Hussin, M. W., Tahir, M. M., & Aziah, N. (2013). Sulfuric acid resistance of blended ash geopolymer concrete. *Construction and Building Materials, 43*, 80-86.

Ariffin, M. A. M., Hussin, M. W., & Bhutta, M. A. R. (2011). Mix design and compressive strength of geopolymer concrete containing blended ash from agro-industrial wastes. *Advanced Materials Research, 339*, 452-457.

Ariffin, M. A. M., Hussin, M. W., & Bhutta, M. A. R. A., R. (2012, 12 - 13 June, 2012). *Structural performance of POFA-PFA geopolymer concrete beam.* Paper presented at the 11th International Conference on Concrete Engineering and Technology, Putrajaya, Malaysia.

ASTM C78. (2010). Standard test method for *Flexural strength of concrete (using simple beam with third-point loading)*. West Conshohocken, PA: ASTM International.

ASTM C127. (2012). Standard test method for *Density, relative density (specific gravity), and absorption of coarse aggregate*. West Conshohocken, PA: ASTM International.

ASTM C128. (2012). Standard test method for *Density, relative density (specific gravity), and absorption of fine aggregate*. West Conshohocken, PA: ASTM International.

ASTM C136. (2001). Standard test method for *Sieve analysis of fine and coarse aggregates*. West Conshohocken, PA: ASTM International.

ASTM C469. (2010). Standard test method for *Static modulus of elasticity and Poisson's ratio of concrete in compression*. West Conshohocken, PA: ASTM International.

ASTM C496. (2011). Standard test method for *Splitting tensile strength of cylindrical concrete specimens*. West Conshohocken, PA: ASTM International.

ASTM C597. (2009). Standard test method for *Pulse velocity through concrete*. West Conshohocken, PA: ASTM International.

ASTM C618. (2012). Standard specification for *Coal fly ash and raw or calcined natural pozzolan for use in concrete*. West Conshohocken, PA: ASTM International.

ASTM C642. (2013). Standard test method for *Density, absorption, and voids in hardened concrete*. West Conshohocken, PA: ASTM International.

ASTM C1202. (2012). Standard test method for *Electrical indication of concrete's ability to resist chloride ion penetration*. West Conshohocken, PA: ASTM International.

Awal, A. S. M. A., & Hussin, M. W. (1997). The effectiveness of palm oil fuel ash in preventing expansion due to alkali-silica reaction. *Cement and Concrete Composites, 19*(4), 367-372.

Awal, A. S. M. A., & Hussin, M. W. (1999). *Durability of high performance concrete containing palm oil fuel ash.* Paper presented at the 8th International Conference on Durability of Building Materials and Components, Vancouver, British Columbia, Canada.

Bai, Y., Ibrahim, R., & Basheer, P. A. M. (2004). *Properties of lightweight concrete manufactured with fly ash, furnace bottom ash, and Lytag.* Paper presented at the International Workshop on Sustainable Development and Concrete Technology, Beijing, China.

Bakharev, T. (2005). Resistance of geopolymer materials to acid attack. *Cement and concrete research, 35*(4), 658-670.

Basri, H. B., Mannan, M. A., & Zain, M. F. M. (1999). Concrete using waste oil palm shells as aggregate. *Cement and concrete research, 29*(4), 619-622.

Bondar, D., Lynsdale, C. J., Milestone, N. B., Hassani, N., & Ramezanianpour, A. A. (2011). Effect of adding mineral additives to alkali-activated natural pozzolan paste. *Construction and Building Materials, 25*(6), 2906-2910.

Browne, R. D., Geoghegan, M. P., & Baker, A. F. (1983). Analysis of structural condition from durability results. *Corrosion of Reinforcement in Concrete Construction Proceeding*, 193-222.

BS 812-103.1. (1985). Testing aggregates *Method for determination of particle size distribution*. London: British Standards Institution.

BS EN 206-1. (2000). Concrete *Specification, performance, production and conformity*. London: British Standards Institution.

BS EN 771-1. (2011). Specification for masonry units *Clay masonry units*. London: British Standards Institution.

BS EN 933-1. (1997). Tests for geometrical properties of aggregates *Determination of particle size distribution - sieving method*. London: British Standards Institution.

BS EN 12350-2. (2009). Testing fresh concrete *Slump-test*. London: British Standards Institution.

BS EN 12350-6. (2009). Testing fresh concrete *Desity*. London: British Standards Institution.

BS EN 12390-3. (2002). Testing hardened concrete *Compressive strength of test specimens*. London: British Standards Institution.

BS EN 12664. (2001). Thermal performance of building materials and products *Determination of thermal resistance by means of guarded hot plate and heat flow meter methods. Dry and moist products of medium and low thermal resistance*. London: British Standards Institution.

BS EN 13055-1. (2002). Lightweight aggregates *Lightweight aggregates for concrete, mortar and grout*. London: British Standards Institution.

CEB-FIP. (1989). Diagnosis and assessment of concrete structures - state of art report. *CEB Bulletins, 192*, 83-85.

Chandra, S., & Berntsson, L. (2002). *Lightweight aggregate concrete*: William Andrew.

Chia, K. S., & Zhang, M. H. (2007). Workability of air-entrained lightweight concrete from rheology perspective. *Magazine of Concrete Research, 59*(5), 367-375.

Chindaprasirt, P., Homwuttiwong, S., & Jaturapitakkul, C. (2007). Strength and water permeability of concrete containing palm oil fuel ash and rice husk–bark ash. *Construction and Building Materials, 21*(7), 1492-1499.

Chindaprasirt, P., Jaturapitakkul, C., Chalee, W., & Rattanasak, U. (2009). Comparative study on the characteristics of fly ash and bottom ash geopolymers. *Waste Management, 29*(2), 539-543.

Chindaprasirt, P., Rukzon, S., & Sirivivatnanon, V. (2008). Resistance to chloride penetration of blended Portland cement mortar containing palm oil fuel ash, rice husk ash and fly ash. *Construction and Building Materials, 22*(5), 932-938.

Clarke, J. L. (2002). *Structural lightweight aggregate concrete*: Taylor & Francis.

Criado, M., Fernández-Jiménez, A., & Palomo, A. (2010). Alkali activation of fly ash. Part III: Effect of curing conditions on reaction and its graphical description. *Fuel, 89*(11), 3185-3192.

Davidovits, J. (1994a). Geopolymers: Inorganic polymeric new materials. *Journal of Materials Education, 16*, 91-139.

Davidovits, J. (1994b). *Global warming impact on the cement and aggregates industries*.

Davidovits, J. (1999). *Chemistry of geopolymeric systems, terminology.* Paper presented at the International Conference Geopolymere, Saint-Quentin, France.

Demie, S., Nuruddin, M. F., & Shafiq, N. (2013). Effects of micro-structure characteristics of interfacial transition zone on the compressive strength of self-compacting geopolymer concrete. *Construction and Building Materials, 41*, 91-98.

Duxson, P., Fernández-Jiménez, A., Provis, J. L., Lukey, G. C., Palomo, A., & van Deventer, J. S. J. (2007). Geopolymer technology: the current state of the art. *Journal of Materials Science, 42*(9), 2917-2933.

Fernández-Jiménez, A., & Palomo, A. (2005). Mid-infrared spectroscopic studies of alkali-activated fly ash structure. *Microporous and Mesoporous Materials, 86*(1–3), 207-214.

Fernandez Jiminez, A., Lachowski, E. E., Palomo, A., & Macphee, D. E. (2004). Microstructural characterisation of alkali-activated PFA matrices for waste immobilisation. *Cement and Concrete Composites, 26*(8), 1001-1006.

Gelim, M., & Ali, K. (2011). *Mechanical and physical properties of fly ash foamed concrete.* University Tun Hussein Onn Malaysia, Johor, Malaysia.

Gourley, J. T. (2003). *Geopolymers; opportunities for environmentally friendly construction materials.* Paper presented at the International Conference and Exhibition on Adaptive Materials for a Modern Society, Sydney, Australia.

Guo, X., Shi, H., & Dick, W. A. (2010). Compressive strength and microstructural characteristics of class C fly ash geopolymer. *Cement and Concrete Composites, 32*(2), 142-147.

Hamidah, M. S., Azmi, I., Ruslan, M. R. A., Kartini, K., & Fadhil, N. M. (2005). Optimisation of foamed concrete mix of different sand–cement ratio and curing conditions. *Use of foamed concrete in construction. London: Thomas*.

Hardjito, D., & Rangan, B. V. (2005). Development and properties of low-calcium fly ash-based geopolymer concrete *Research Report GC 1*. Perth, Australia: Curtin University of Technology.

Hardjito, D., Wallah, S. E., Sumajouw, D. M. J., & Rangan, B. V. (2004). Factors influencing the compressive strength of fly ash-based geopolymer concrete. *Civil Engineering Dimension, 6*(2), 88-93.

He, J., Zhang, J., Yu, Y., & Zhang, G. (2012). The strength and microstructure of two geopolymers derived from metakaolin and red mud-fly ash admixture: A comparative study. *Construction and Building Materials, 30*, 80-91.

Heah, C. Y., Kamarudin, H., Al Bakri, A. M. M., Binhussain, M., Luqman, M., Nizar, I. K., et al. (2012). Curing behavior on kaolin-based geopolymers. *Advanced Materials Research, 548*, 42-47.

Jones, M. R., & McCarthy, A. (2005). Preliminary views on the potential of foamed concrete as a structural material. *Magazine of Concrete Research, 57*(1), 21-32.

Jumaat, M. Z., Alengaram, U. J., & Mahmud, H. (2009). Shear strength of oil palm shell foamed concrete beams. *Materials & Design, 30*(6), 2227-2236.

Karakurt, C., Kurama, H., & Topcu, İ. B. (2010). Utilization of natural zeolite in aerated concrete production. *Cement and Concrete Composites, 32*(1), 1-8.

Katz, A. (1998). Microscopic study of alkali-activated fly ash. *Cement and concrete research, 28*(2), 197-208.

Kearsley, E. P., & Wainwright, P. J. (2002). The effect of porosity on the strength of foamed concrete. *Cement and concrete research, 32*(2), 233-239.

Kılıç, A., Atiş, C. D., Yaşar, E., & Özcan, F. (2003). High-strength lightweight concrete made with scoria aggregate containing mineral admixtures. *Cement and concrete research, 33*(10), 1595-1599.

Kupaei, R. H., Alengaram, U. J., Jumaat, M. Z., & Nikraz, H. (2013). Mix design for fly ash based oil palm shell geopolymer lightweight concrete. *Construction and Building Materials, 43*, 490-496.

Kupwade-Patil, K., & Allouche, E. (2013). Impact of alkali silica reaction on fly ash-based geopolymer concrete. *Journal of Materials in Civil Engineering, 25*(1), 131-139.

Kusbiantoro, A., Nuruddin, M. F., Shafiq, N., & Qazi, S. A. (2012). The effect of microwave incinerated rice husk ash on the compressive and bond strength of fly ash based geopolymer concrete. *Construction and Building Materials, 36*, 695-703.

Lamond, J. F., & Pielert, J. H. (2006). *Significance of tests and properties of concrete and concrete-making materials* (Vol. 169). West Conshohocken, PA: ASTM International.

Lecomte, I., Liegeois, M., Rulmont, A., Cloots, R., & Maseri, F. (2003). Synthesis and characterization of new inorganic polymeric composites based on kaolin or white clay and on ground-granulated blast furnace slag. *Journal of materials research, 18*(11), 2571-2579.

Lloyd, N., & Rangan, B. (2010). *Geopolymer concrete: A review of development and opportunities.* Paper presented at the 35th Conference on Our World in Concrete & Structures, Singapore.

Lo, T. Y., Tang, W. C., & Cui, H. Z. (2007). The effects of aggregate properties on lightweight concrete. *Building and Environment, 42*(8), 3025-3029.

Mahlia, T. M. I. (2002). Emissions from electricity generation in Malaysia. *Renewable Energy, 27*(2), 293-300.

Mahlia, T. M. I., Taufiq, B. N., Ismail, & Masjuki, H. H. (2007). Correlation between thermal conductivity and the thickness of selected insulation materials for building wall. *Energy and Buildings, 39*(2), 182-187.

Malhotra, V. M. (1999). *Role of supplementary cementing materials in reducing greenhouse gas emissions.* Paper presented at the International Conference on Infrastructure Regeneration and Rehabilitation Improving the Quality of Life through Better Construction - A vision for the next millenium, Swamy, Sheffield, UK.

Mannan, M. A., Alexander, J., Ganapathy, C., & Teo, D. C. L. (2006). Quality improvement of oil palm shell (OPS) as coarse aggregate in lightweight concrete. *Building and Environment, 41*(9), 1239-1242.

Mannan, M. A., & Ganapathy, C. (2004). Concrete from an agricultural waste-oil palm shell (OPS). *Building and Environment, 39*(4), 441-448.

Martys, N. S., & Ferraris, C. F. (1997). Capillary transport in mortars and concrete. *Cement and concrete research, 27*(5), 747-760.

McCarter, W. J., Ezirim, H., & Emerson, M. (1992). Absorption of water and chloride into concrete. *Magazine of Concrete Research, 44*(158), 31-37.

McLellan, B. C., Williams, R. P., Lay, J., van Riessen, A., & Corder, G. D. (2011). Costs and carbon emissions for geopolymer pastes in comparison to ordinary portland cement. *Journal of Cleaner Production, 19*(9–10), 1080-1090.

Mehta, P. K. (2002). Greening of the concrete industry for sustainable development. *Concrete International, 23*.

Meyer, C. (2009). The greening of the concrete industry. *Cement and Concrete Composites, 31*(8), 601-605.

Mindess, S., Young, J. F., & Darwin, D. (2003). *Concrete*.

Mollah, M. Y. A., Hess, T. R., & Cocke, D. L. (1994). Surface and bulk studies of leached and unleached fly ash using XPS, SEM, EDS and FTIR techniques. *Cement and concrete research, 24*(1), 109-118.

Mozgawa, W., Sitarz, M., & Rokita, M. (1999). Spectroscopic studies of different aluminosilicate structures. *Journal of Molecular Structure, 511–512*(0), 251-257.

Mužek, M. N., Zelić, J., & Jozić, D. (2012). Microstructural characteristics of geopolymers based on alkali-activated fly ash. *Chemical and Biochemical Engineering Quarterly, 26*(2), 89-95.

Naik, T. R. (2008). Sustainability of concrete construction. *Practice Periodical on Structural Design and Construction, 13*(2), 98-103.

Naik, T. R., Ramme, B. W., Kraus, R. N., & Siddique, R. (2003). Long-term performance of high-volume fly ash concrete pavements. *ACI Materials Journal, 100*(2).

Nambiar, E. K. K., & Ramamurthy, K. (2006). Models relating mixture composition to the density and strength of foam concrete using response surface methodology. *Cement and Concrete Composites, 28*(9), 752-760.

Nambiar, E. K. K., & Ramamurthy, K. (2007a). Air-void characterisation of foam concrete. *Cement and concrete research, 37*(2), 221-230.

Nambiar, E. K. K., & Ramamurthy, K. (2007b). Sorption characteristics of foam concrete. *Cement and concrete research, 37*(9), 1341-1347.

Nambiar, E. K. K., & Ramamurthy, K. (2008). Fresh state characteristics of foam concrete. *Journal of Materials in Civil Engineering, 20*(2), 111-117.

Narayanan, N., & Ramamurthy, K. (2000). Structure and properties of aerated concrete: A review. *Cement and Concrete Composites, 22*(5), 321-329.

Neville, A. M. (1997). *Properties of concrete* (4th and final ed.). Harlow, United Kingdom: Pearson Education Limited.

Newman, J. B. (1993). Properties of structural lightweight aggregate concrete. In J. L. Clarke (Ed.), *Structural lightweight aggregate concrete* (pp. 19-44). Glassgow: Blackie Academic and Professional.

Newman, J. B., & Choo, B. S. (2003). *Advanced concrete technology set*: Butterworth-Heinemann.

Ng, S. C., & Low, K. S. (2010). Thermal conductivity of newspaper sandwiched aerated lightweight concrete panel. *Energy and Buildings, 42*(12), 2452-2456.

Olivia, M., & Nikraz, H. (2012). Properties of fly ash geopolymer concrete designed by Taguchi method. *Materials & Design, 36*, 191-198.

Palomo, A., Grutzeck, M. W., & Blanco, M. T. (1999). Alkali-activated fly ashes: A cement for the future. *Cement and concrete research, 29*(8), 1323-1329.

Panesar, D. K. (2013). Cellular concrete properties and the effect of synthetic and protein foaming agents. *Construction and Building Materials, 44*, 575-584.

Papadopoulos, A. M., & Giama, E. (2007). Environmental performance evaluation of thermal insulation materials and its impact on the building. *Building and Environment, 42*(5), 2178-2187.

Petrov, I., & Schlegel, E. (1994). Application of automatic image analysis for the investigation of autoclaved aerated concrete structure. *Cement and concrete research, 24*(5), 830-840.

Pietersen, H. S., Fraay, A. L. A., & Bijen, J. M. (1989). Reactivity of fly ash at high pH. *MRS Online Proceedings Library, 178*, null-null.

Polat, R., Demirboğa, R., Karakoç, M. B., & Türkmen, İ. (2010). The influence of lightweight aggregate on the physico-mechanical properties of concrete exposed to freeze–thaw cycles. *Cold Regions Science and Technology, 60*(1), 51-56.

Poon, C. S., Shui, Z. H., & Lam, L. (2004). Effect of microstructure of ITZ on compressive strength of concrete prepared with recycled aggregates. *Construction and Building Materials, 18*(6), 461-468.

PORIM. (1998). Malaysia palm oil. *Palm Oil Research Institute of Malaysia*.

Pospisil, F., Jambor, J., & Belko, J. (1992). Unit weight reduction of fly ash aerated concrete. In H. Folker & A. A. Balkema (Eds.), *Advances in Autoclaved Aerated Concrete* (pp. 43-52).

Prim, P., & Wittmann, F. H. (1983). Structure and water absorption of aerated concrete. *Autoclaved aerated concrete, moisture and properties. Amsterdam: Elsevier*, 43-53.

Raden, M. A. M. A., & Hamidah, M. S. (2012, 12 - 13 June, 2012). *Strength characteristic of foamed geopolymer concrete.* Paper presented at the 11th International Conference on Concrete Engineering and Technology, Putrajaya, Malaysia.

Ramamurthy, K., Nambiar, E. K. K., & Ranjani, G. I. S. (2009). A classification of studies on properties of foam concrete. *Cement and Concrete Composites, 31*(6), 388-396.

Regan, P. E., & Arasteh, A. R. (1990). Lightweight aggregate foamed concrete. *Structural Engineer, 68*(9), 167-173.

Riahi, S., Nazari, A., Zaarei, D., Khalaj, G., Bohlooli, H., & Kaykha, M. M. (2012). Compressive strength of ash-based geopolymers at early ages designed by Taguchi method. *Materials & Design, 37*, 443-449.

Rickard, W. D. A. (2012). *Assessing the suitability of fly ash geopolymers for high temperature applications.* (PhD), Curtin University of Technology, Perth, Australia.

RILEM. (1983). *FIP Manual of Lightweight Aggregate Concrete* (2nd ed.). London: Surry University Press.

Safiuddin, M., & Hearn, N. (2005). Comparison of ASTM saturation techniques for measuring the permeable porosity of concrete. *Cement and concrete research, 35*(5), 1008-1013.

Sata, V., Jaturapitakkul, C., & Kiattikomol, K. (2004). Utilization of palm oil fuel ash in high-strength concrete. *Journal of Materials in Civil Engineering, 16*(6), 623-628.

Saygılı, A., & Baykal, G. (2011). A new method for improving the thermal insulation properties of fly ash. *Energy and Buildings, 43*(11), 3236-3242.

Sengul, O., Azizi, S., Karaosmanoglu, F., & Tasdemir, M. A. (2011). Effect of expanded perlite on the mechanical properties and thermal conductivity of lightweight concrete. *Energy and Buildings, 43*(2-3), 671-676.

Shafigh, P., Jumaat, M. Z., & Mahmud, H. (2010). Mix design and mechanical properties of oil palm shell lightweight aggregate concrete: A review. *International Journal of Physical Sciences, 5*(14), 2127-2134.

Shafigh, P., Jumaat, M. Z., Mahmud, H., & Alengaram, U. J. (2011a). A new method of producing high strength oil palm shell lightweight concrete. *Materials & Design, 32*(10), 4839-4843.

Shafigh, P., Jumaat, M. Z., Mahmud, H., & Hamid, N. A. A. (2012). Lightweight concrete made from crushed oil palm shell: Tensile strength and effect of initial curing on compressive strength. *Construction and Building Materials, 27*(1), 252-258.

Shafigh, P., Mahmud, H., & Jumaat, M. Z. (2011b). Effect of steel fiber on the mechanical properties of oil palm shell lightweight concrete. *Materials & Design, 32*(7), 3926-3932.

Short, A., & Kinniburgh, W. (1978). *Lightweight concrete* (3rd ed.). London: Applied Science Publishers Ltd.

Silva, P. D., Sagoe-Crenstil, K., & Sirivivatnanon, V. (2007). Kinetics of geopolymerization: Role of Al_2O_3 and SiO_2. *Cement and concrete research, 37*(4), 512-518.

Sindhunata, van Deventer, J. S. J., Lukey, G. C., & Xu, H. (2006). Effect of curing temperature and silicate concentration on fly-ash-based geopolymerization. *Industrial & Engineering Chemistry Research, 45*(10), 3559-3568.

Sitarz, M., Handke, M., & Mozgawa, W. (2000). Identification of silicooxygen rings in SiO_2 based on IR spectra. *Spectrochimica Acta Part A: Molecular and Biomolecular Spectroscopy, 56*(9), 1819-1823.

Sun, P. (2005). *Fly ash based inorganic polymeric building material.* (PhD), Wayne State University, Detroit, Michigan.

Swanepoel, J. C., & Strydom, C. A. (2002). Utilisation of fly ash in a geopolymeric material. *Applied Geochemistry, 17*(8), 1143-1148.

Tangchirapat, W., Khamklai, S., & Jaturapitakkul, C. (2012). Use of ground palm oil fuel ash to improve strength, sulfate resistance, and water permeability of concrete containing high amount of recycled concrete aggregates. *Materials & Design, 41*, 150-157.

Tangchirapat, W., Saeting, T., Jaturapitakkul, C., Kiattikomol, K., & Siripanichgorn, A. (2007). Use of waste ash from palm oil industry in concrete. *Waste Management, 27*(1), 81-88.

Tasdemir, C. (2003). Combined effects of mineral admixtures and curing conditions on the sorptivity coefficient of concrete. *Cement and concrete research, 33*(10), 1637-1642.

Taylor, J. C., & Matulis, C. E. (1991). Absorption contrast effects in the quantitative XRD analysis of powders by full multiphase profile refinement. *Journal of Applied Crystallography, 24*(1), 14-17.

Teo, D. C. L., Mannan, M. A., & Kurian, V. J. (2006). Flexural behaviour of reinforced lightweight concrete beams made with oil palm shell (OPS). *Journal of advanced concrete technology, 4*(3), 459-468.

Teo, D. C. L., Mannan, M. A., Kurian, V. J., & Ganapathy, C. (2007). Lightweight concrete made from oil palm shell (OPS): Structural bond and durability properties. *Building and Environment, 42*(7), 2614-2621.

van Deventer, J. S. J., Provis, J. L., & Duxson, P. (2012). Technical and commercial progress in the adoption of geopolymer cement. *Minerals Engineering, 29*(0), 89-104.

van Jaarsveld, J. G. S., & van Deventer, J. S. J. (1999). Effect of the alkali metal activator on the properties of fly ash-based geopolymers. *Industrial & Engineering Chemistry Research, 38*(10), 3932-3941.

van Jaarsveld, J. G. S., van Deventer, J. S. J., & Lukey, G. C. (2002). The effect of composition and temperature on the properties of fly ash- and kaolinite-based geopolymers. *Chemical Engineering Journal, 89*(1–3), 63-73.

Visagie, M. (2000). *The effect of microstructure on the properties of foamed concrete.* (MEng), University of Pretoria, South Africa.

Wallah, S. E., & Rangan, B. V. (2006). Low calcium fly ash based geopolymer concrete: long term properties *Research Report GC 2* (pp. 76-80). Perth, Australia: Curtin University of Technology.

Wilson, M. A., Hoff, W. D., & Hall, C. (1991). Water movement in porous building materials - absorption from a small cylindrical cavity. *Building and Environment, 26*(2), 143-152.

Wong, H. S., Zobel, M., Buenfeld, N. R., & Zimmerman, R. W. (2009). Influence of the interfacial transition zone and microcracking on the diffusivity, permeability and sorptivity of cement-based materials after drying. *Magazine of Concrete Research, 61*(8), 571-589.

Xu, H., & van Deventer, J. S. J. (2000). The geopolymerisation of alumino-silicate minerals. *International Journal of Mineral Processing, 59*(3), 247-266.

Yang, Q., Zhu, P., Wu, X., & Huang, S. (2000). Properties of concrete with a new type of saponin air-entraining agent. *Cement and concrete research, 30*(8), 1313-1317.

Yap, S. P., Alengaram, U. J., & Jumaat, M. Z. (2013). Enhancement of mechanical properties in polypropylene– and nylon–fibre reinforced oil palm shell concrete. *Materials & Design, 49*, 1034-1041.

Yip, C. K., Lukey, G. C., Provis, J. L., & van Deventer, J. S. J. (2008). Effect of calcium silicate sources on geopolymerisation. *Cement and concrete research, 38*(4), 554-564.

Zhang, J., Sun, H., Wan, J., & Yi, Z. (2009). Study on microstructure and mechanical property of interfacial transition zone between limestone aggregate and Sialite paste. *Construction and Building Materials, 23*(11), 3393-3397.

APPENDICES

APPENDIX A

Material properties of sodium hydroxide and sodium silicate

Table A1: Specification of NaOH pellets

1.06482.1000 Sodium hydroxide pellets suitable for use as excipient EMPROVE® exp Ph Eur,BP,FCC,JP,NF,E 524

Assay (acidimetric,NaOH)	≥ 98.0	%
Assay (total alkalinity calc. as NaOH)	98.0 - 100.5	%
Identity	passes test	
Appearance of solution	passes test	
Insoluble substances and organic matter	passes test	
Carbonate (as Na_2CO_3)	≤ 0.5	%
Chloride (Cl)	≤ 0.005	%
Phosphate (PO_4)	≤ 0.002	%
Silicate (SiO_2)	≤ 0.01	%
Sulphate (SO_4)	≤ 0.003	%
Total nitrogen (N)	≤ 0.0005	%
Heavy metals (as Pb)	≤ 0.0005	%
Al (Aluminium)	≤ 0.001	%
As (Arsenic)	≤ 0.0003	%
Cu (Copper)	≤ 0.0005	%
Fe (Iron)	≤ 0.001	%
Hg (Mercury)	≤ 0.00001	%
K (Potassium)	≤ 0.1	%
Pb (Lead)	≤ 0.00005	%
Zn (Zinc)	≤ 0.0025	%
Residual solvents (Ph. Eur./USP/ICH)	excluded by manufacturing process	

Residues of metal catalysts or metal reagents acc. to EMEA/CHMP/SWP/4446/2000 are not likely to be present.

Conforms to Ph Eur, BP, FCC, JP, NF, E524
Conforms to the purity criteria on food additives according to the current European Commission Regulation.

Dr. Andreas Lang
Responsible laboratory manager quality control

This document has been produced electronically and is valid without a signature.

Merck KGaA, Frankfurter Straße 250, 64293 Darmstadt (Germany): +49 6151 72-0
EMD Millipore Corporation - A division of Merck KGaA, Darmstadt, Germany
290 Concord Road, Billerica, MA 01821, USA, Phone: (781) 533-6000
SALSA 000000000000/ V. 60424 Date: 26.04.2013

Table A2: Specification of Na_2SiO_3

Vonjun Sdn Bhd	PC Laboratory Agent
Sodium silicate, Na_2SiO_3 (Product No.: C0792)	2.5L
Liquid	
Type analysis	
Weight, per ml at 20˚C	About 1.50g
About 12% Na_2O and 30% SiO_2	

Table A3: Preparation of 14M alkaline solution

From periodic table, the total molecular weight of NaOH is 40 g/mol.

Thus, for 14M of NaOH = 14 x 40 = 560 g per litre of the solution.

The mass of NaOH solids was measured as 404 g per kg of the 14M NaOH solution, while the remaining mass of the solution is the weight of water.

The ratio of Na_2SiO_3/NaOH used was 2.5.

Therefore, the details to prepare a 1000 g of 14M alkaline solution are as following:

NaOH solution = 285.7 g of alkaline solution
Na_2SiO_3 solution = 714.3 g of alkaline solution

NaOH solids = ratio of mass of NaOH solids per litre of water x mass of NaOH solution
= (404/1000) x 285.7
= 115.4 g
H_2O = 285.7 – 115.4 = 170.3 g

The final quantities of NaOH pellets, Na_2SiO_3 solution and H_2O to prepare 14M alkaline solution are 115.4, 714.3 and 170.3 g, respectively.

APPENDIX B

Materials and mix proportions of OPSFGC

Table B1: Materials and mix proportion for OPSFGC of target density 1500 kg/m^3

MATERIALS AND MIX PROPORTION FOR OPSFGC		
TARGET DENSITY (kg/m^3)	=	1700
MATERIALS PROPORTION		
POFA/FLY ASH (POFA/FA)	=	0.20
SAND/CEMENT (S/FA)	=	1.70
AGGREGATE/CEMENT (A/FA)	=	0.60
ALKALINE/CEMENT (AK/FA)	=	0.55
WATER/CEMENT (W/FA)	=	0.15
SUPERPLASTICIZER/CEMENT (SP/FA)	=	0.015

MATERIALS	MASS (kg)	SPECIFIC GRAVITY	QUANTITY
FLY ASH	80.00	2.10	38.10
POFA	20.00	2.78	7.19
SAND	170.00	2.67	63.67
OPKS	60.00	1.36	44.12
ALKALINE	55.00	1.57	35.03
WATER	15.00	1.00	15.00
SUPERPLASTICIZER	1.50	1.20	1.25
	TOTAL VOLUME		204.36

DENSITY FOR I m^3 OF CONCRETE- PKSFC		
MATERIALS		**DENSITY (kg/m^3)**
FLY ASH	=	391.47
POFA	=	97.87
SAND	=	831.87
OPKS	=	293.60
ALKALINE SOLUTION	=	269.13
WATER	=	73.40
SUPERPLASTICIZER	=	7.34
TOTAL	=	1964.68

Table B1, continued.

DENSITY AND FOAM		
CONCRETE DENSITY (kg/m^3)	=	1964.68
TARGET DENSITY	=	1500.00
DENSITY OF THE OPSFGC	=	1500.00
FOAM (%)	=	0.24
LWC (%)	=	0.76

SPECIMENS	VOLUME (m^3)	QUANTITY	TOTAL (m^3)
CUBE (100 mm)	0.001	20	0.0200
PRISM (100 x 100 x 500 mm)	0.00500	3	0.0150
PANEL (300 x 300 x 50 mm)	0.00450	2	0.0090
CYLINDER (150 x 300 mm)	0.00530	2	0.0106
CYLINDER (100 x 200 mm)	0.00157	6	0.0094
		TOTAL VOLUME (m^3)	0.06403
		≈	0.0640
	VOLUME OF CONCRETE (m^3)	=	0.0489
	VOLUME OF FOAM (m^3)	=	0.0116

FINAL QUANTITIES OF MATERIALS (kg)			15% increased (kg)
FOAM	=	1.64	1.88
FLY ASH	=	25.07	28.82
POFA	=	6.27	7.21
SAND	=	53.26	61.25
OPKS	=	18.80	21.62
WATER	=	4.70	5.41
SUPERPLASTICIZER	=	0.47	0.54
ALKALINE SOLUTION	=	17.23	19.81

Table B2: Materials and mix proportion for OPSFGC of target density 1700 kg/m^3

MATERIALS AND MIX PROPORTION FOR OPSFGC		
TARGET DENSITY (kg/m^3)	=	1700
MATERIALS PROPORTION		
POFA/FLY ASH (POFA/FA)	=	0.20
SAND/CEMENT (S/FA)	=	1.70
AGGREGATE/CEMENT (A/FA)	=	0.60
ALKALINE/CEMENT (AK/FA)	=	0.55
WATER/CEMENT (W/FA)	=	0.15
SUPERPLASTICIZER/CEMENT (SP/FA)	=	0.015

MATERIALS	MASS (kg)	SPECIFIC GRAVITY	QUANTITY
FLY ASH	80.00	2.10	38.10
POFA	20.00	2.78	7.19
SAND	170.00	2.67	63.67
OPKS	60.00	1.36	44.12
ALKALINE	55.00	1.57	35.03
WATER	15.00	1.00	15.00
SUPERPLASTICIZER	1.50	1.20	1.25
		TOTAL VOLUME	(204.36)

DENSITY FOR I m^3 OF CONCRETE- PKSFC		
MATERIALS		**DENSITY (kg/m^3)**
FLY ASH	=	391.47
POFA	=	97.87
SAND	=	831.87
OPKS	=	293.60
ALKALINE SOLUTION	=	269.13
WATER	=	73.40
SUPERPLASTICIZER	=	7.34
TOTAL	=	1964.68

DENSITY AND FOAM		
CONCRETE DENSITY (kg/m^3)	=	1964.68
TARGET DENSITY	=	1700.00
DENSITY OF THE OPSFGC	=	1700.00
FOAM (%)	=	0.13
LWC (%)	=	0.87

Table B2, continued.

SPECIMENS	VOLUME (m^3)	QUANTITY	TOTAL (m^3)
CUBE (100 mm)	0.001	20	0.0200
PRISM (100 x 100 x 500 mm)	0.00500	3	0.0150
PANEL (300 x 300 x 50 mm)	0.00450	2	0.0090
CYLINDER (150 x 300 mm)	0.00530	2	0.0106
CYLINDER (100 x 200 mm)	0.00157	6	0.0094
		TOTAL VOLUME (m^3)	0.06403
		≈	0.0640
	VOLUME OF CONCRETE (m^3)	=	0.0554
	VOLUME OF FOAM (m^3)	=	0.0075

FINAL QUANTITIES OF MATERIALS (kg)			15% increased (kg)
FOAM	=	1.06	1.22
FLY ASH	=	25.07	28.82
POFA	=	6.27	7.21
SAND	=	53.26	61.25
OPKS	=	18.80	21.62
WATER	=	4.70	5.41
SUPERPLASTICIZER	=	0.47	0.54
ALKALINE SOLUTION	=	17.23	19.81

APPENDIX C

Mechanical, transport and thermal characteristics of foamed and non-foamed OPSGC

Table C1: Compression strength test

Specimen	Day	ODD (kg/m^3)		Compressive strength (MPa)	
		Per specimen	*Average*	*Per specimen*	*Average*
OPSFGC13	3	1324.0	1331.3	7.51	7.3
		1342.0		7.25	
		1328.0		7.15	
	7	1286.0	1309.0	7.29	7.8
		1343.0		7.68	
		1298.0		8.48	
	14	1311.0	1326.7	7.21	8.1
		1342.0		9.06	
		1327.0		8.17	
	28	1267.0	1291.2	7.70	8.3
		1288.7		8.17	
		1317.9		9.10	
OPSFGC15	3	1495.8	1469.4	11.18	9.8
		1453.5		9.18	
		1459.0		9.17	
	7	1482.0	1466.0	12.22	11.5
		1452.0		11.74	
		1464.0		10.53	
	14	1470.0	1465.3	13.24	12.9
		1469.0		12.24	
		1457.0		13.28	
	28	1495.8	1466.6	14.15	13.5
		1453.5		14.04	
		1450.5		12.20	

Table C1, continued.

Specimen	Day	ODD (kg/m^3)		Compressive strength (MPa)	
		Per specimen	*Average*	*Per specimen*	*Average*
OPSFGC17	3	1714.0	1729.7	22.99	23.5
		1732.0		25.02	
		1743.0		22.54	
	7	1748.0	1734.7	25.20	24.7
		1734.0		24.06	
		1722.0		24.73	
	14	1724.0	1723.3	23.49	24.9
		1734.0		26.85	
		1712.0		24.32	
	28	1732.0	1720.9	25.24	25.8
		1731.9		25.98	
		1698.8		26.26	
OPSNFGC	3	1758.0	1762.3	20.43	22.4
		1759.0		23.20	
		1770.0		23.46	
	7	1789.0	1783.3	25.82	25.7
		1777.0		24.80	
		1784.0		26.34	
	14	1787.0	1793.8	26.76	25.8
		1816.3		24.09	
		1778.1		26.42	
	28	1779.1	1791.4	30.62	30.1
		1790.0		30.94	
		1805.0		28.62	

Table C2: Splitting tensile and flexural strengths test

Specimen	28-day splitting tensile strength (MPa)		28-day flexural strength (MPa)	
	Per specimen	*Average*	*Per specimen*	*Average*
OPSFGC13	0.639 0.532 0.678	0.616	1.579 1.411 1.456	1.482
OPSFGC15	1.104 0.900 0.979	0.994	2.055 2.294 2.120	2.156
OPSFGC17	1.675 1.783 1.910	1.789	3.145 3.366 3.169	3.227
OPSNFGC	2.219 2.603 -	2.411	3.595 3.888 -	3.742

Table C3: Sorptivity test

FGC-1300		FGC-1500		FGC-1700		NFGC	
time (mins)	*i* ($x10^3$)	time (mins)	*i* ($x10^3$)	time (mins)	*i* ($x10^3$)	time (mins)	*i* ($x10^3$)
1	0.77	*1*	0.29	*1*	0.27	*1*	0.22
4	1.06	*2*	0.45	*2*	0.41	*2*	0.29
9	1.36	*3*	0.58	*3*	0.51	*3*	0.38
16	1.65	*4*	0.72	*4*	0.67	*4*	0.49
25	1.84	*5*	0.85	*5*	0.77	*5*	0.61
36	1.94	*6*	1.00	*6*	0.93	*6*	0.71
49	2.13	*7*	1.12	*7*	0.96	*7*	0.85
64	2.23	*8*	1.31	*8*	1.03	*8*	0.97

Table C4: Porosity test

Specimen	W_b (g)	W_{SSD} (g)	W_{ODD} (g)	Porosity (%)	
				Per specimen	*Average*
OPSFGC13	234.2	597.7	457.2	38.65	39.54
	238.2	598.1	452.6	40.43	
OPSFGC15	287.7	646.7	527.2	33.29	34.25
	290.4	669.9	536.3	35.20	
OPSFGC17	311.5	666.0	577.4	24.99	25.04
	327.0	696.9	604.1	25.09	
OPSNFGC	325.6	676.4	593.8	25.50	24.35
	317.8	667.3	579.4	25.19	

Table C5: Thermal conductivity test

Specimen	Temperature (˚C)		Current (A)	Thermal conductivity (W/mK)	
	Hot plate	*Cold plate*		*Per specimen*	*Average*
OPSFGC13	44.18	19.33	0.10	0.473	0.47
	44.18	20.36	0.09	0.466	
OPSFGC15	44.10	19.34	0.10	0.479	0.50
	44.02	20.01	0.10	0.524	
OPSFGC17	44.18	21.40	0.09	0.494	0.54
	38.70	16.72	0.11	0.591	
OPSNFGC	44.00	21.87	0.10	0.554	0.58
	43.96	21.62	0.11	0.597	
Block	43.99	20.21	0.12	0.639	0.60
	40.82	17.51	0.11	0.557	
Brick	39.67	17.01	0.17	0.897	0.90

APPENDIX D

Figure D1: Collection of POFA at Jugra Palm Oil Mill Sdn Bhd, Banting

Figure D2: The LA abrasion machine used to ground POFA

Figure D3: FA and POFA as binder of geopolymer concrete

Figure D4: Rotary concrete mixer

Figure D5: Curing chamber for geopolymer specimens

Figure D6: Stand-type mixer

Figure D7: ADR-Auto 2000 standard compression machine by ELE International

Figure D8: Test specimen of splitting tensile strength

Figure D9: ADR-Auto EL37-6135 standard flexural machine by ELE International

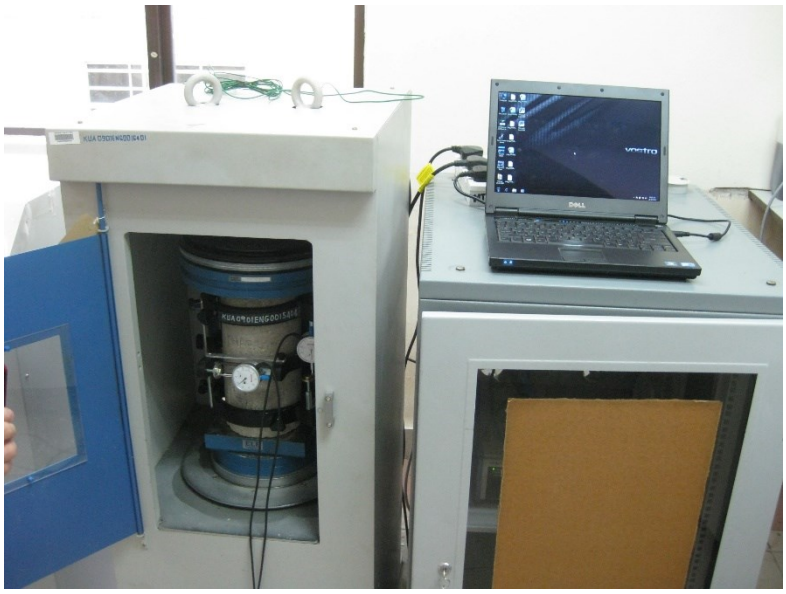

Figure D10: MOE test set up for geopolymer concrete

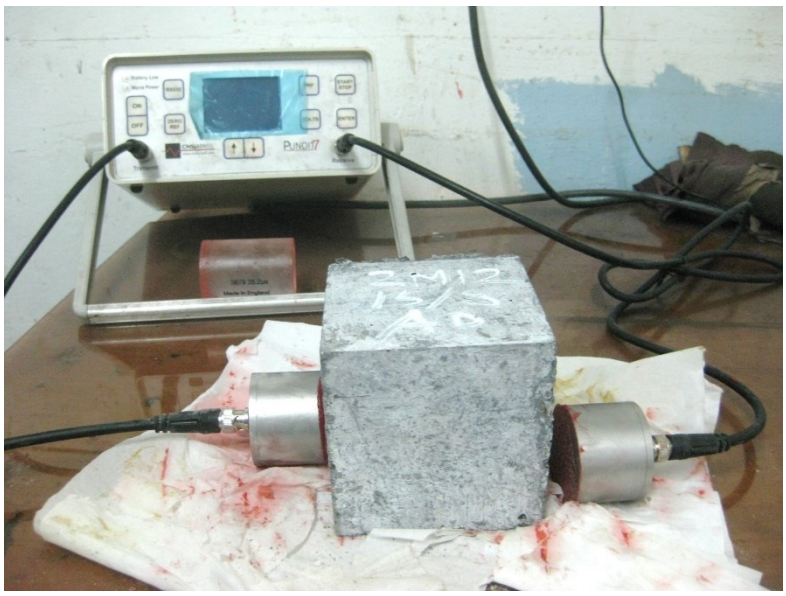

Figure D11: UPV test using the PUNDIT

Figure D12: Test set-up for the porosity of geopolymer concrete

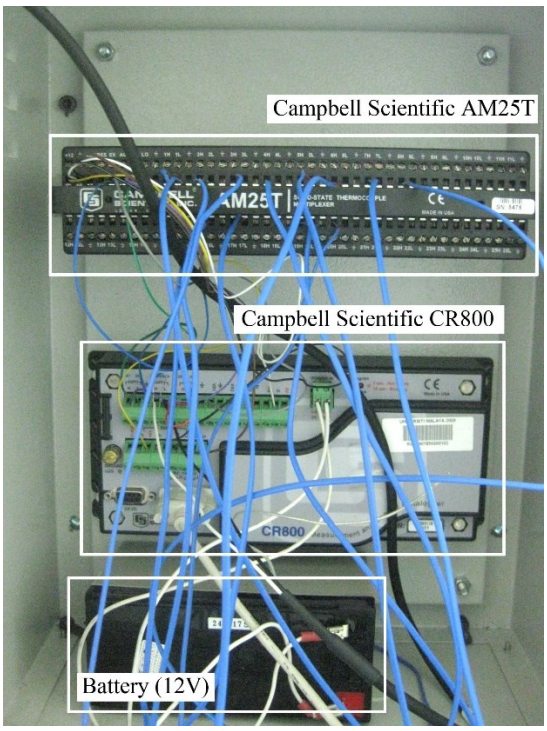

Figure D13: Multiplexer, data logger and battery

Figure D14: The Quanta FEG 450 and EDX system from Oxford

Figure D15: Placement of OPSGC specimens on stub with carbon tape

Figure D16: The PANalytical Empyrean diffractometer

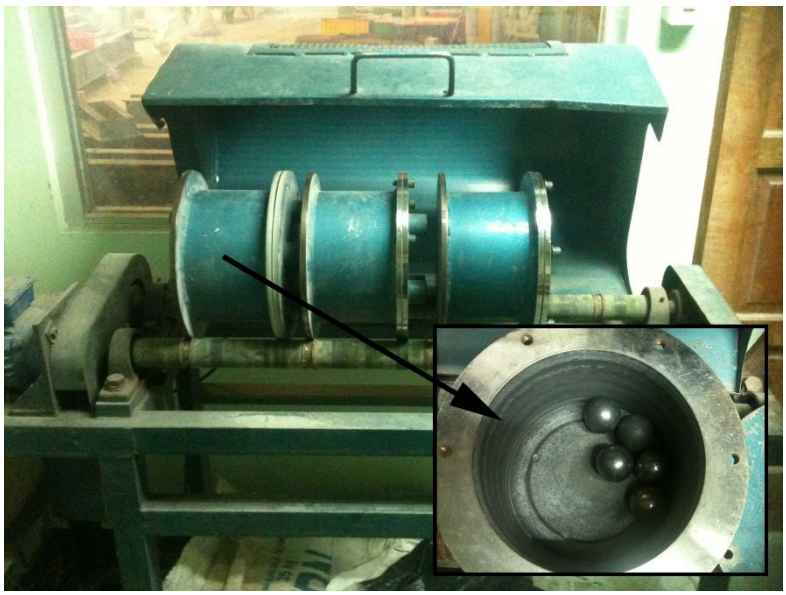

Figure D17: Steel ball grinding machine

Figure D18: Specimen holder for XRD analysis

Figure D19: The Perkin Elmer Spectrum 400 spectrometer

LIST OF PUBLICATIONS

Alengaram, U. J., Al-Muhit, B. A., Jumaat, M. Z., & **Liu, M. Y. J.** (2013). A comparison of the thermal conductivity of oil palm shell foamed concrete with conventional materials. *Materials & Design, 51*, 522-529.

Liu, M. Y. J., Alengaram, U. J., Jumaat, M. Z., & Mo, K. H. (2014). Evaluation of thermal conductivity, mechanical and transport properties of lightweight aggregate foamed geopolymer concrete. *Energy and Buildings, 72*, 238-245.

Liu, M. Y. J., Chua, C. P., Alengaram, U. J., & Jumaat, M. Z. (2014). Utilization of palm oil fuel ash as binder in lightweight oil palm shell geopolymer concrete. *Advances in Materials Science and Engineering, 2014*.

Liu, M. Y. J., Alengaram, U. J., Yap, S. P., & Jumaat, M. Z. (2014). Utilization of oil palm shell as lightweight aggregate in lightweight-foamed concrete. *Journal of Asian Scientific Research*. (Under review).

Mo, K. H., Alegaram, U. J., **Liu, M. Y. J.**, & Jumaat, M. Z. (2014). Permeation properties of lightweight of oil palm shell concrete. *Journal of Asian Scientific Research*. (Under review).

Mo, K. H., Alengaram, U. J., Jumaat, M. Z., **Liu, M. Y. J.**, & Lim, J. (2014). The beneficial effect of ground granulated blast furnace slag on sorption, strength and shrinkage properties of oil palm shell concrete. *The Scientific World Journal*. (Under review).